DISSERTATION

BINDING OF MBNL1 TO CUG REPEATS SLOWS 5'-TO-3' RNA DECAY BY XRN2 IN A CELL CULTURE MODEL OF TYPE I MYOTONIC DYSTROPHY

Submitted by

Junzhen Zhang

Graduate Degree Program in Cell and Molecular Biology

In partial fulfillment of the requirements

For the Degree of Doctor of Philosophy

Colorado State University

Fort Collins, Colorado

Fall 2017

Doctoral Committee:

Advisor: Carol J Wilusz
Co-Advisor: Jeffrey Wilusz

Dawn Duval
Santiago Di Pietro
Tingting Yao

ABSTRACT

BINDING OF MBNL1 TO CUG REPEATS SLOWS 5'-TO-3' RNA DECAY BY XRN2 IN A CELL CULTURE MODEL OF TYPE I MYOTONIC DYSTROPHY

Type I myotonic dystrophy (DM1) is a multi-systemic inherited disease caused by expanded CTG repeats within the 3' UTR of the dystrophia myotonica protein kinase (DMPK) gene. The encoded CUG repeat-containing mRNAs are toxic to the cell and accumulate in nuclear foci, where they sequester cellular RNA-binding proteins such as the splicing factor Muscleblind-1 (MBNL1). This leads to widespread changes in gene expression. Currently, there is no treatment or cure for this disease. Targeting CUG repeat-containing mRNAs for degradation is a promising therapeutic avenue for myotonic dystrophy, but we know little about how and where these mutant mRNAs are naturally decayed.

We established an inducible C2C12 mouse myoblast model to study decay of reporter mRNAs containing the DMPK 3' UTR with 0 (CUG0) or ~700 (CUG700) CUG repeats and showed that the CUG700 cell line exhibits characteristic accumulation of repeat-containing mRNA in nuclear foci. We utilized qRT-PCR and northern blotting to assess the pathway and rate of decay of these reporter mRNAs following depletion of mRNA decay factors by RNA interference.

We have identified four factors that influence decay of the repeat-containing mRNA – the predominantly nuclear 5' → 3' exonuclease XRN2, the nuclear exosome containing

RRP6, the RNA-binding protein MBNL1, and the nonsense-mediated decay factor, UPF1. We have discovered that the 5' end of the repeat-containing transcript is primarily degraded in the nucleus by XRN2, while the 3' end is decayed by the nuclear exosome. Interestingly, we have shown for the first time that the ribonucleoprotein complex formed by the CUG repeats and MBNL1 proteins represents a barrier for XRN2-mediated decay. We suggest that this limitation in XRN2-mediated decay and the resulting delay in degradation of the repeats and 3' region may play a role in DM1 pathogenesis. Additionally, our results support previous studies suggesting that UPF1 plays a role in initiating the degradation of mutant DMPK transcripts.

This work uncovers a new role for MBNL1 in DM1 and other CUG-repeat expansion diseases and identifies the nuclear enzymes involved in decay of the mutant DMPK mRNA. Our model has numerous applications for further dissecting the pathways and factors involved in removing toxic CUG-repeat mRNAs, as well as in identifying and optimizing therapeutics that enhance their turnover.

ACKNOWLEDGEMENTS

I would like to start off by thanking my advisor and co-advisor, Drs. Carol and Jeffrey Wilusz for their training and support. During the process, they have patiently guided me through this fascinating new world of molecular biology. I appreciate greatly your different perspectives which gradually shape me from a graduate student into an independent researcher. I would also like to thank my graduate committee members, Drs. Dawn Duval, Santiago Di Pietro, and Tingting Yao. I am grateful for their advice, guidance and encouragement towards my dissertation project which contributes to my scientific progress.

Over the course of my work and studies, I appreciate so much the countless help I received from many members of the Wilusz lab. The friendship you have shared with me, is one of the most valuable things I have acquired in graduate school. I would like to thank Dr. Mary Schneider for creating the tet-responsive cell lines. Adam M. Heck for performed the 4sU metabolic labeling experiments in the human myoblasts. REU student Megan Helf assisted me with the beginning of the UPF1 protein knockdown experiment. Besides providing me with protocols, reagents and advice, Dr. Aimee L. Jalkanen provided cDNAs from iPS cells and Hela cells for the cytoplasmic/nuclear fractionation experiments. Dr. Stephanie L. Moon taught me several techniques and provided me advice towards research and presentations. Dr. Joe Russo taught me many techniques, shared with me tips of different experiments, and provided valuable advice on interpretation of data and presentations. John Anderson has taught me many techniques, especially ones with radiation. He has also helped track down important

reagents and protocols. Phillida Charley taught me many things related to Northern Blotting. Dr. Stephen Coleman was always so patient with me, and whenever asked, would give detailed explanation of scientific facts. I would like to also thank Dr. Ashley Neff, who so patiently helped me with CM502 when I was completely and utterly overwhelmed at the start of graduate school.

I am also thankful that Dr. Brian Geiss provided me access and training for microscope and luciferase assay machine. I appreciate Dr. Alan Schenkel, Dr, Mercedes Gonzalez-Juarrero, Dr. David G Maranon, Taghreed Alturki and Andrea Sánchez Hidalgo for the training and help with the microscopy work. I appreciate all the effort Dr. Tim Stasevich and Dr. Tatsuya Morisaki put towards our understanding of CUG repeat half-life via live cell imaging.

Finally, I must thank my family for their love and support throughout this. I greatly appreciate my parents who have unconditionally supported me all these years. I would also like to thank Dayi and Ellen who brought a sense of home to me half a globe away. Most importantly, I must thank my husband, Clayton, who is my biggest supporter through this rather challenging time, and continuously providing me the source of energy with love and laughter.

TABLE OF CONTENTS

CHAPTER 1: INTRODUCTION

1.1 Type I Myotonic Dystrophy

Myotonic dystrophy, also known as dystrophia myotonica (DM), is a genetic condition comprising two clinical disorders: type I myotonic dystrophy (DM1), originally known as Steinert's disease, and type II myotonic dystrophy (DM2), also known as proximal myotonic myopathy (PROMM). These two disorders have overlapping phenotypes but distinct molecular defects. DM1 is linked to a CTG-repeat expansion in the 3' untranslated region (UTR) of the dystrophia myotonica protein kinase (DMPK) gene (Brook et al., 1992), while DM2 is linked to a CCTG repeat expansion in an intron of the zinc finger 9 gene (ZNF9; Liquori et al., 2001). The focus of this dissertation is on type I myotonic dystrophy, but DM2 will also be discussed when relevant.

1.1.1 Prevalence and clinical features of type I myotonic dystrophy

Myotonic dystrophy 1 (DM1, [MIM 160900]) is a multi-systemic, autosomal dominant inherited disease that was first described in 1909 by Steinert (Steinert, 1909). It is the most common adult form of muscular dystrophy with a prevalence ranging from 2.1 to 14.3 per 100,000 population worldwide (Mathieu and Prévost, 2012; Meola, 2013).

The DM gene locus maps to chromosome 19q13.3 (Krahe et al., 1995; Renwick et al., 1971; Stallings et al., 1988). DM1 is caused by expansion of a trinucleotide CTG repeat in the 3' UTR of the DMPK gene. The severity and age of onset are strongly correlated with the number of CTG repeats in the 3' UTR of the DMPK gene (Botta et al., 2008; Gourie-Devi et al., 1998; Hunter et al., 1992; Marchini et al., 2000; Melacini et al., 1995; Takahashi et al.; Yoo et al., 2017). Unaffected individuals have 5-37 CTG repeats,

while adult-onset DM1 patients with mild to classic symptoms have from 50 to 1000 such repeats. Individuals with congenital DM (CDM) have more than 1000 repeats (Figure 1; Brook et al., 1992).

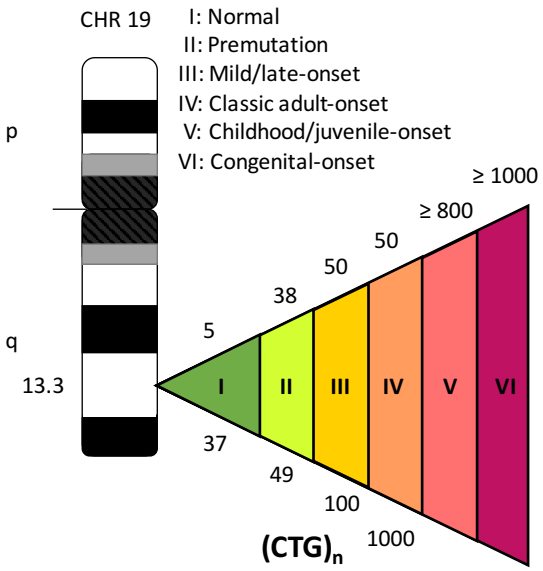

Figure 1: Correlation of CTG-repeats length to age of on-set. DMPK gene is maps to chromosome 19q13.3. Unaffected individuals have 5-37 CTG repeats, individuals with 38-49 repeats are considered having premutation, mild/late-onset individuals have 50-100 repeats, class adult-onset individuals have 50-1000 repeats, childhood/juvenile-onset patients have no less than 800 repeats, while congenital DM1 patients have no less than 1000 repeats.

DM1 is a complex condition that can affect all systems of the human body, making it difficult to diagnose. Affected individuals display considerable variability in symptoms (Ho et al., 2015). Additionally, the extent of repeat expansion varies between tissues and over time within a single individual (Ho et al., 2015).

Common features

1) Skeletal and smooth muscle malfunction in DM1

The signature symptoms of DM1 include myotonia (slowing of muscle relaxation after voluntary or involuntary muscle contraction), muscle weakness, and muscle wasting (Mateos-Aierdi et al., 2015; Udd and Krahe, 2012). Skeletal muscle weakness leads to immobility and respiratory insufficiency, which is the major cause of death at the late stage of adult-onset DM1 (Udd and Krahe, 2012). Smooth muscle dysfunction results in gastrointestinal symptoms ranging from constipation to diarrhea and incontinence (Bellini et al., 2006).

2) Cardiac manifestations in DM1

Cardiac conduction delays resulting in arrhythmia commonly occur in DM1 patients, and often arise before skeletal muscle symptoms (Nigro et al., 2012; Palladino et al., 2016; Udd and Krahe, 2012). Tragically, cardiac involvement represents the second most common cause of death for DM1 patients (Berul et al., 1999; Freyermuth et al., 2016; Kalsotra et al., 2014; Koshelev et al., 2010; Perfetti et al., 2014; Wang et al., 2009). Cardiac muscle weakness leading to dilated cardiomyopathy is rare but can be seen in the final stages of the disease (Palladino et al., 2016).

3) Neurological symptoms in DM1

Brain abnormalities manifest as neurological (sleep apnea, numbness and daytime sleepiness) symptoms in those affected by DM1. DM1 patients also suffer from progressive cognitive impairments. (Astrea et al., 2016; Cabada et al., 2017; Ho et al., 2015; Konzen et al., 2017; Marchini et al., 2000; Rollnik et al., 2013; Udd and Krahe, 2012).

4) Other frequent complaints in DM1

Due to its multi-systemic nature, DM1 can also cause a host of other issues throughout the body of affected individuals. For example, those with adult-onset of DM1 may experience the development of cataracts before the age of 50 as the first symptoms observed (Dogan et al., 2016; Reardon et al., 1993; Rollnik et al., 2013; Schoser and Timchenko, 2010; Udd and Krahe, 2012; Usuki et al., 2000). Further examples include the impairment of endocrine functions. Such patients can suffer from insulin resistance that leads to diabetes, as well as hypothyroidism. Male hypogonadism and infertility as

well as miscarriages in females are also common (Dahlqvist et al., 2015; Dansithong et al., 2005; Marchini et al., 2000).

Symptoms seen in childhood and juvenile-onset patients

In children and adolescents affected with childhood-onset (age 1-10) or juvenile-onset (age 10-20) DM1, symptoms are predominantly displayed through personality and behavior disturbances. The most frequent psychopathology diagnoses are attention deficit with hyperactivity disorder (ADHD) and/or anxiety disorder leading to cognitive dysfunction (Astrea et al., 2016; Baldanzi et al., 2016; Douniol et al., 2012).

Congenital myotonic dystrophy (CDM)

Congenital DM1 patients have severe developmental abnormalities that can be present to a lesser degree in patients with DM1 who become symptomatic during adulthood (Ranum and Day, 2004). They typically suffer from hypotonia, immobility, and respiratory difficulties, as well as cognitive defects and motor developmental delay (Astrea et al., 2016; Ho et al., 2015; Schoser and Timchenko, 2010).

Diagnosis, treatments, and prognosis

As DM1 can affect many, if not all, systems, it is hard for physicians to properly diagnose and refer. Family history, early appearance of cataracts and muscle symptoms generally lead to a presumptive diagnosis. However, the gold standard for diagnosing myotonic dystrophy is genetic testing to determine the number of CTG repeats. This is accomplished through triplet-repeat primed PCR (TP-PCR) and/or Southern blotting (Dryland et al., 2013; Singh et al., 2014; Warner et al., 1996).

Treatments currently available for DM only target specific symptoms, but fail to slow progression. However, early intervention can reduce or avert complications and greatly enhance quality of life (Thornton et al., 2017). The prognosis is hard to predict due to individual patient differences, but in severe cases, respiratory and cardiac complications can be life-threatening at an early age (Ho et al., 2015). There is a 30-40% mortality rate for CDM within the neonatal period, but those who survive have a mean life expectancy of 45 years. For comparison, childhood/juvenile-onset DM1 patients have a life expectancy of approximate 60 years (Ho et al., 2015).

1.1.2 Etiology and pathogenesis

Identification and function of the DMPK gene

As noted above, DM1 is caused by expanded trinucleotide CTG repeats in the 3' UTR of the Dystrophia Myotonica Protein Kinase (DMPK) gene (Brook et al., 1992; Buxton et al., 1992; Fu et al., 1992; Harley et al., 1992; Mahadevan et al., 1992). When transcribed, the mutant transcripts are retained in nuclear foci, while wild type DMPK mRNA can be exported to the cytoplasm and act as templates for translation (Davis et al., 1997; Taneja et al., 1995). The DMPK gene encodes a serine-threonine protein kinase (Shelbourne and Johnson, 1992), which is involved in the Ca^{2+} homeostasis in skeletal muscle cells (Benders et al., 1997).

DM1 is not caused by loss of DMPK function

Although the mutation in the 3' untranslated region (3' UTR) of the mRNA does not directly affect the DMPK protein, the mis-localization of the mutant RNA results in reduced protein levels and haploinsufficiency (Carango et al., 1993; Davis et al., 1997; Fu et al., 1993; Krahe et al., 1995; Maeda et al., 1995; Wang et al., 1995). However,

knocking out the DMPK gene causes only mild myopathy in mice and fails to recapitulate many of the phenotypes of DM1 (Hamshere and Brook, 1996; Jansen et al., 1996; Reddy et al., 1996). Furthermore, simply expressing the DMPK 3' UTR with 960 CTG repeats can recapitulate many DM1 phenotypes in a mouse model (Orengo et al., 2008). Consequently, though reduced DMPK protein expression may contribute to the disease, it is not the primary cause of disease.

Effects of CTG repeat on expression of neighboring genes

One additional aspect to consider in the quest for a molecular explanation of DM1 is that triplet repeat expansion in the DMPK gene locally represses and condenses chromatin conformation, which can affect expression of neighboring genes (Barbé et al., 2017; Boucher et al., 1995; Frisch et al., 2001; Hamshere and Brook, 1996; Lee and Cooper, 2009; Wang et al., 1994). The upstream neighboring gene of DMPK is DMWD (dystrophia myotonica-containing WD repeat motif), and the downstream gene is SIX5 (former DM locus-associated homeodomain protein, DMAHP). However it is controversial whether the expression of DMWD is actually affected by the presence of expanded CTG triplet repeats in the DMPK gene (Alwazzan et al., 1999; Frisch et al., 2001). On the other hand, a decrease in the expression of SIX5 has been reported in DM1 patients (Barbé et al., 2017; Yanovsky-Dagan et al., 2015). Interestingly, mice lacking SIX5 exhibit cataracts, cardiac conduction issues and sterility, all of which are seen in DM1, but not muscle pathology (Klesert et al., 2000; Personius et al., 2005; Sarkar et al., 2000). Hence, the effects of CTG repeat expansion on neighboring genes could indeed contribute to some phenotypes of DM1, but it is unlikely to be the primary cause of the major muscle-associated pathology observed in the disease. The cause of

the major pathologies associated with DM1 is likely to be the variant RNA molecule itself.

RNAs containing CUG repeats are the primary driver of disease

Interestingly, mouse models expressing the expanded CUG repeats within the DMPK 3' UTR on their own can recapitulate many features of DM1 including nuclear RNA foci, sustained myotonia, muscle wasting and loss of muscle function (Orengo et al., 2008; Seznec et al., 2001; Wang et al., 2007), while the DMPK 3' UTR with no repeats is not toxic to the cell at all (Ho et al., 2005a). This strongly suggests that the mutant DMPK mRNA with expanded repeats is the primary cause of disease for DM1. Additionally, mice containing expanded CUG repeats within the 3' UTR of the human skeletal α-actin (hACTA1) gene exhibit myotonia, histological myopathy and splicing defects, similar to those seen in DM1, though lack of non-muscle features (Mankodi et al., 2000, 2002; Wheeler et al., 2009). This further demonstrates that CUG repeats alone are sufficient to induce DM1 phenotypes. Therefore, it is evident that the mutated expanded repeat sequence itself in the RNA is the primary culprit for DM1.

Effects of CUG repeats on processing and localization of DMPK mRNA

CUG repeats in RNA form a hairpin/stem-loop structure with U-U mismatches stabilized by 1-2 hydrogen bonds (Chen et al., 2017; Koch and Leffert, 1998; Mooers et al., 2005; Tian et al., 2000). Considering the large number of the repeats (n=50 to over 1000) in DM1 patients, this complex structure can be very extensive and may have the ability to dramatically impact mRNA processing and export.

While a large portion of the wild type DMPK transcript resides in the nucleus (Gudde et al., 2017a) in a diffuse distribution (Davis et al., 1997), they can be exported out to the

cytoplasm for translation (Davis et al., 1997; Smith et al., 2007). Intriguingly, however, the mutant DMPK RNA with expanded CUG repeats is predominantly retained in the nucleus and forms characteristic foci (Taneja et al., 1995). These mutant RNA foci do not accumulate in an identifiable nuclear domain (Mankodi et al., 2003) – they do not co-localize with nucleoli, the perinucleolar compartment (responsible for RNA transcription, processing and trafficking between nucleus and cytoplasm; Pollock and Huang, 2010), or Cajal bodies (where several types of small nuclear ribonucleoprotein particles (snRNPs) are assembled and recycled; Machyna et al., 2015), or SC-35 domains (a.k.a. nuclear speckles or splicing factor compartments). In order to begin to understand why these mRNAs are retained in nuclear foci, capping, polyadenylation and splicing pattern were compared between the wild type and mutant transcripts.

Both wild type and mutant DMPK transcripts are capped like normal mature mRNA (Davis et al., 1997). Both wild type and mutant DMPK mRNA have longer than usual poly(A) tails (length of ~500 nt compared to ~250 nt normally, Gudde et al., 2017a). It is not clear why wild type DMPK transcripts are hyperadenylated. However, this could simply reflect the fact that any nuclear retained mRNA could subsequently be recognized as aberrant/unwanted and tagged for nuclear decay through hyperadenylation (Bresson and Conrad, 2013; Bresson et al., 2015).

In terms of splicing, repeat-containing DMPK transcripts appear to be either spliced normally as the wild type DMPK mRNA (Davis et al., 1997; Gudde et al., 2017a; Tiscornia and Mahadevan, 2000), or in some cases have exon 15 – which contains the expanded CUG repeats – completely spliced out using a cryptic site located 3’ of the repeats (Tiscornia and Mahadevan, 2000). Thus overall, it is unclear whether standard

nuclear mRNA processing events contribute in a large fashion to the nuclear localization of mutant DMPK transcripts.

Interestingly, although mutant DMPK mRNA does not co-localize with nuclear speckles, it does accumulate at the edge of them, perhaps indicating a block of entry into these domains (Smith et al., 2007). Nuclear speckles appear to serve as a screening point for properly processed, export-ready RNA (Johnson et al., 2000; Molenaar et al., 2004). Thus it seems possible that failure to process or assemble a competent messenger ribonucleoprotein (mRNP) could be responsible for the accumulation of mutant DMPK in foci near splicing speckles. Another aspect to consider is that structure of the mutant DMPK transcripts may be actively contributing to nuclear retention. The giant hairpins formed by CUG repeats in the mutant DMPK RNA may be sterically blocking it from being efficiently exported through nuclear pores (Holt et al., 2007; Koch and Leffert, 1998; Smith et al., 2007), though cytoplasmic mutant DMPK mRNA foci can be detected (Dansithong et al., 2008; Pettersson et al., 2014).

Finally, an important question in the field is whether DMPK mRNA foci represent only a marker of DM1 or if they actively contribute to the pathology associated with the disease. A mouse model expressing only 5 CTG repeats within the DMPK 3’ UTR, does not exhibit accumulation of the reporter RNA in foci, but experiences myotonia and cardiovascular symptoms of DM1 (Mahadevan et al., 2006), suggesting that DMPK nuclear foci are not required for many aspects of the DM1 phenotype. In addition, it is not simply the expansion of any triplet repeat in RNA that can cause disease. Cell lines expressing CAG repeat-containing RNAs, though capable of forming nuclear foci, exhibit no phenotypes of DM1 (Ho et al., 2005b). Additionally, it is putative whether all

the DMPK transcripts are within foci or some of the toxic RNAs adopt a diffusive state as single RNA in the nucleus (Gudde et al., 2016; Jain and Vale, 2017; Pettersson et al., 2015; Querido et al., 2011). Overall, these evidences indicate that it is the CTG repeats, regardless of foci formation, that are responsible for inducing the pathogenic features of DM1.

Sequestration of proteins contributes to pathogenesis

Sequestration of proteins is a natural function of some long noncoding RNAs (lncRNAs) (Hirose et al., 2014; Kino et al., 2010; Lee et al., 2016). For example, the abundant lncRNA *NORAD* (*Noncoding RNA Activated by DNA Damage*) has 17 binding sites for PUM1 and PUM2 RBPs enabling it to act as a sponge or decoy and prevent these proteins from binding other targets (Lee et al., 2016; Tichon et al., 2016). Loss of NORAD results in DNA damage due to down-regulation of DNA replication, mitosis, and DNA repair factors by the excess PUM proteins. Any RNA with repetitive sequence can in principle act as a sponge for RBPs or miRNAs. Thus triplet repeat expansion can turn an mRNA into a sponge with functions similar to lncRNAs. This can result in the sequestered RBPs losing their function. This can lead to cytopathology – and is a leading candidate for the molecular mechanism that underlies disease in DM1.

The best characterized and most abundant protein associated with and sequestered by CUG repeats is muscleblind (MBNL1), which belongs to the muscleblind protein family comprising MBNL1, MBNL2 and MBNL3 in mammalian cells. MBNL1 is an RNA binding protein which serves as a regulator of splicing by binding to the intronic signals in pre-mRNA through conserved tandem zinc finger domains containing three cysteine and one histidine residue (CCCH; Begemann et al., 1997). MBNL1 is expressed ubiquitously

in all tissues, with the highest expression in cardiac and skeletal muscle tissues – precisely the tissues that are most heavily involved in DM1 (Fardaei et al., 2002). Unfortunately for DM1 patients, MBNL1 protein also binds to the stem-loop structured CUG repeats with U-U mismatch in patient cells with high affinity and specificity (Miller et al., 2000; Warf and Berglund, 2007). Thus mutant DMPK RNAs containing expanded CUG repeats bind and sequester MBNL1 protein within the nuclear foci (Mankodi et al., 2001; Miller et al., 2000; Yuan et al., 2007). Once sequestered, MBNL1 can no longer serve its function, causing its natural target pre-mRNAs to be mis-spliced (especially in muscle tissues, see Table 1), which results in reprogramming of gene expression that is toxic to the organism. This toxicity due to MBNL1 loss-of-function contributes tremendously to DM1 phenotypes (see Table 1). Also, MBNL2 (a principal factor dysregulated in the DM central nervous system) and MBNL3 (predominantly expressed in placenta) protein also co-localize with mutant DMPK mRNA foci (Charizanis et al., 2012; Ho et al., 2004) and their sequestration contributes to mis-regulated splicing events (Ho et al., 2004).

The MBNL family of proteins may not be the only nuclear factors which are sequestered in significant amounts by expanded CUG repeat-containing RNAs. Two nuclear transcription factors, Sp1 and RAR$\boldsymbol{\gamma}$, can bind to CUG repeat structures. A decrease in the expression of their targeted genes, for example CLCN1 (chloride voltage-gated channel 1), has been noted in DM1 patient cells and this could further contribute to DM1 pathogenesis (Ebralidze et al., 2004). Finally, there may be other factors bound to the repeats that haven't been investigated, which can also play some role in causing DM1. Currently, however, the field largely remains focused on MBNL1 as the major protein

targeted for sequestration by nuclear retained DMPK mRNAs that contain expanded CUG repeats.

Indirect effects of CUG-repeat containing mutant DMPK RNA on gene expression

Even though MBNL1 loss-of-function is thought to be a primary reason for mutant DMPK mRNA toxicity, a MBNL1 knockout mouse model cannot reproduce all the phenotypes seen in human DM1. Notably, the MBNL1 knockout mouse does not exhibit cardiac conduction problems or muscle wasting. Therefore other factors must contribute to DM1 pathogenesis (Kanadia et al., 2003).

The best characterized factor that is indirectly affected in DM1 is CELF1, which belongs to the CUGBP Elav-like (embryonically lethal abnormal vision-like) family of splicing factors (Ladd et al., 2001). CELF1 is ubiquitously expressed, and present in both the nucleus and cytoplasm (Timchenko et al., 1996a, 1996b). However, unlike MBNL1, CELF1 does not bind to structured CUG repeats in DM1 or co-localize with mutant DMPK mRNA in the nuclear foci (Fardaei et al., 2001; Mankodi et al., 2003). In DM1 patients and animal models, CELF1 is up-regulated possibly through a PKCθ-mediated phosphorylation event which stabilizes the protein (Kim et al., 2016; Kuyumcu-Martinez et al., 2007; Lee and Cooper, 2009; Philips et al., 1998; Timchenko et al., 2001).

CELF1 shares RNA targets with MBNL1 protein, but with antagonist effects. For example, MBNL1 promotes intron 2 exclusion in CLCN1 pre-mRNA splicing, while CELF1 protein favors intron 2 retention (see Table 1). Overexpression of CELF1 protein can recapitulate some phenotypes of DM1, including developmental delay and muscular dystrophy (Ho et al., 2005a; Timchenko et al., 2004; Ward et al., 2010).

Staufen 1 protein (STAU1), a ubiquitously expressed, double-stranded RNA-binding protein falls into the same class as CELF1. It is not seen in mutant DMPK mRNA foci but is increased in DM1 skeletal muscle (Ravel-Chapuis et al., 2012) and influences MBNL1 dependent splicing events contributing to DM1 pathogenesis (Bondy-Chorney et al., 2016).

In addition to affecting RBPs, triplet repeat expansion in DM1 can also lead to abnormal expression of several transcription factors. For instance, NKX2.5 is induced in skeletal and cardiac muscle, which contributes to defects in skeletal myogenesis and cardiotoxicity (Gladman et al., 2015; Yadava et al., 2008). MEF2 transcription factors are decreased which leads to depletion of several miRNAs and has global effects on muscle specific gene expression (Caine et al., 2014; Chau and Kalsotra, 2014; Ikeda et al., 2009; McKinsey et al., 2002).

Finally, mutant DMPK mRNA indirectly affects expression of other genes by serving as a source of siRNAs. CUG/CAG repeats are cleaved by Dicer to trigger downstream silencing effects through the RNA interference (RNAi) pathway (Krol et al., 2007; Provost et al., 2002; Zhang et al., 2002). Interestingly this may actually be beneficial given that endonucleolytic cleavage enhances turnover of the DMPK transcript. However, it is not clear to what extent Dicer targets the mutant transcripts, given that they are primarily nuclear and Dicer is primarily cytoplasmic.

Impact of the mutant mRNA on cell metabolism

Based on current molecular models, DM1 has been largely termed a spliceopathy, a disease caused by aberrant splicing leading to altered gene expression patterns (Botta et al., 2008; Freyermuth et al., 2016; Garcia-Lopez et al., 2008; Ho et al., 2005b). The

altered balance of CELF1 and MBNL1 function in DM1 (excess CELF1 and reduced MBNL1) results in a switch in splicing from adult to embryonic patterns (Dansithong et al., 2005; Ho et al., 2005a; Kim et al., 2014; Ladd et al., 2001). Unfortunately, these embryonic isoforms are not sufficient for proper adult tissue function (Chau and Kalsotra, 2014). Although MBNL1 and CELF1 act antagonistically, they do not compete for the same binding site. For their shared pre-mRNA targets, the CELF1 binding motif is enriched in the upstream intron which favors exon skipping leading to fetal isoforms, while the MBNL1 motif is enriched in the downstream intron promoting exon inclusion (Giudice et al., 2014; Kalsotra et al., 2008). Some major mis-splicing events and their associated phenotypes are listed below in Table 1.

Table 1: Mis-splicing events associated with DM1 phenotypes

Target pre-mRNA	MBNL1 loss-of-function	CELF1 gain-of-function	Phenotype	Reference
Chloride channel subunit 1 (CLCN1)	Intron 2 retention, exon 6 or 7 inclusion (fetal isoform)	Intron 2 retention, exon 7 inclusion (fetal isoform)	Myotonia	(Charlet-B. et al., 2002; Kim et al., 2014; Kino et al., 2009)
Sarcoplasmic/endoplasmic reticulum Ca(2+)-ATPase 1 (SERCA1 or ATP2A1)	Exon 22 inclusion	N/A	Skeletal muscle weakness and degeneration	(Hino et al., 2007; Kimura et al., 2005)
Bridging integrator-1 (BIN1 or amphiphysin 2)	Exon 11 skipping	N/A	Skeletal muscle weakness	(Fugier et al., 2011)
Ryanodine receptor 1 (RYR1)	Exon 70 or 82 exclusion	Exon 70 exclusion	Skeletal muscle weakness	(Kimura et al., 2005; Tang et al., 2015)
Dystrophin (DMD)	Exon 71 or 78 exclusion	N/A	Disrupted muscle structure maintenance and muscle development	(Nakamori et al., 2007; Rau et al., 2015)
Insulin receptor (IR)	Exon 11 skipping promoting insulin insensitive fetal isoform (IR-A)	Exon 11 skipping promoting insulin insensitive fetal isoform (IR-A)	Insulin intolerance in the skeletal muscles	(Dansithong et al., 2005; Paul et al., 2006; Savkur et al., 2001)
Cardiac troponin T (cTNT or TNNT2)	Exon 5 inclusion (fetal isoform)	Exon 5 inclusion (fetal isoform)	Cardiac conduction issues	(Kanadia et al., 2003;

				Ladd et al., 2001)
Cardiac sodium channel, SCN5A	Shift from exon 6B towards exon 6A	N/A	Reduced excitability of the heart	(Freyermuth et al., 2016)

Modifiers of DM pathogenesis

The mis-regulation of MBNL1 and CELF1, which is the primary mechanism underlying DM1, does not fully correlate with the differences in severity of symptoms. Indeed, other factors have been identified to modify the disease, which are discussed below.

Variant repeats in mutant DMPK allele may also be a modifier of the disease. Most of the DM1 patients have uninterrupted CTG repeats which, are unstable and likely to expand during mitosis and meiosis (Abbruzzese et al., 2002; Ashley and Warren, 1995; Harper et al., 1992). However, a small number of patients (2~5%) identified have variant repeats, including CCG/CTC/GGC/CAG, interrupting the expanded allele (Botta et al., 2017; Pešović et al., 2017; Santoro et al., 2013). A decrease in age of onset and severity of symptoms were observed in these patients due to poorly understood mechanisms.

Such modifiers include the DEAD-box helicases, DDX5 and DDX6, which can be recruited to CUG-repeats and modify their structure and/or association with RNA binding proteins (RBPs; de la Cruz et al., 1999). The helicase DDX6 unwinds the pathogenic repeats and dissociates MBNL1 protein which alleviates some DM1 phenotypes (Pettersson et al., 2014). It remains controversial whether DEAD-box helicase p68/DDX5, which co-localizes with the mutant DMPK RNA foci stabilizes or dissociates the mutant DMPK mRNA foci (Jones et al., 2015; Laurent et al., 2012).

Some other genetic modifiers were also identified in *Drosophila*, for example Csk, a Src family kinase, promotes proliferation of cells to suppress CUG repeat-containing RNA toxicity (Garcia-Lopez et al., 2008). Also in *C. elegans*, depletion of *smg-2*/UPF1 and other members of nonsense-mediated decay machinery were identified to negatively modulate CUG repeat-containing RNA foci and worm motor function (Garcia et al., 2014).

Summary

MBNL1 loss-of-function due to sequestration by CUG repeats and the subsequent altered RNA splicing events contribute to most phenotypes seen in DM1. Hence, sequestration of MBNL1 has been considered the primary cause of disease and remains the focus of the field. Altered function of CELF1, and other proteins that are either directly or indirectly affected by mutant DMPK expression can also help explain the pleiotropic effects on cells and tissues in DM1. As the molecular pathogenesis of DM1 continues to grow, it is evident that RNA toxicity due to the extensive CUG repeats in the mutant DMPK transcripts plays a key role. Many successful preclinical therapies aimed at inducing degradation of this toxic RNA rescue key DM1 phenotypes (see below in 1.1.3).

1.1.3 Preclinical therapeutic approaches

There is currently no cure or therapeutic avenue to slow down the progression of DM1, but research on preclinical treatments has focused on four strategies: 1) reducing transcription of mutant DMPK mRNA, 2) enhancing degradation of mutant DMPK mRNA, 3) displacing MBNL1 from toxic RNA, and 4) modulating individual genes and pathways downstream of RNA toxicity (Thornton et al., 2017).

1) Reducing transcription of mutant DMPK mRNA:

To eliminate the toxic effect of mutant DMPK mRNA, one promising approach is to inhibit the synthesis of such transcripts. Small molecules that interact directly with CTG/CAG repeats, such as Pentamidine (an antimicrobial; Coonrod et al., 2013) and Actinomycin D (ActD; a chemotherapeutic drug; Siboni et al., 2015), can inhibit transcription of mutant DMPK mRNA. Both these drugs are FDA approved, and can alleviate splicing defects and symptoms in HSA^{LR} transgenic mouse models although the dosage required may be too high to be used in patients.

Recently, researchers have adopted the new CRISPR/Cas9 system to delete or reduce the number of the toxic repeat expansion while leaving the DMPK 3' UTR mostly intact (van Agtmaal et al., 2017; Cinesi et al., 2016). This approach corrects the defect and restores normal DMPK function but is not yet completely controllable. Safety and efficacy issues associated with using CRISPR/Cas9 for genome editing are yet to be resolved (Li et al., 2017). Nevertheless, this approach renders great hope defeating DM1 and numerous other inherited diseases (Li et al., 2017).

2) Degradation of mutant DMPK mRNA

Many approaches to reduce the stability of mutant DMPK mRNA have been explored. RNA interference (siRNA, shRNA), antisense RNA, and antisense oligonucleotides (ASO) (Table 2) targeting CUG repeats or their flanking regions can reduce DMPK mRNA abundance by initiating decay through endonucleolytic cleavage (see deadenylation-independent decay in 1.2.6.1), which in turn alleviates mis-splicing events. It is impossible to specifically target the mutant DMPK transcripts using this method since the only difference between the wild type and mutant DMPK transcripts is

the number of CUG repeats. However, DMPK knockout mice only exhibit mild myopathy (Hamshere and Brook, 1996; Jansen et al., 1996; Reddy et al., 1996), which is not at all as harmful as the pleiotropic effects caused by mutant DMPK mRNA on cells and tissues. Therefore, this approach is worth developing and may bring drastic improvements in quality of life.

These approaches must have bypassed a rate-limiting step in decay of the DMPK mRNA to facilitate more rapid turnover. In addition, the fact that they work at all suggests that the repeat structure is not an insurmountable barrier to the decay machinery. It is important to note that the main reason targeting the DMPK mRNA for decay relieves the DM1 phenotype is that it releases MBNL1 and/or perhaps other proteins from the mutant DMPK mRNA (Wheeler et al., 2009; Wojtkowiak-Szlachcic et al., 2015).

3) Displacing MBNL1 from toxic RNA:

A primary reason for mutant DMPK mRNA toxicity is thought to be MBNL1 protein sequestration (Lee and Cooper, 2009). Therefore, dissociating MBNL1 protein from the mutant transcripts could allow the protein to resume its normal function and alleviate DM1 phenotypes tremendously. Small molecules that bind the CUG repeats in mutant DMPK mRNA and competitively dissociate MBNL1 protein, for example morpholino CAG25 (Wheeler et al., 2009), erythromycin (an antibiotic; Nakamori et al., 2016), and lomofungin (an antibacterial; Hoskins et al., 2014), remove nuclear foci, reduce the

Table 2: Agents used to reduce mutant DMPK RNA

Agents	Target sequence		Outcome	DM1 Model used	Reference
shRNA	5' of repeats	Nucleotide 10-30 (at start codon)	Mutant DMPK mRNA is reduced 51.5 ± 6.6% Wild type DMPK mRNA is reduced 64.2 ± 3.5%.	Primary DM1 myoblasts with ~3,200/18 CTG repeats	(Langlois et al., 2005)
		130-150 (5' of CDS)	Mutant DMPK mRNA is reduced 51.5 ± 6.6%. Wild type DMPK MRNA is redued 74.5 ± 2.3%.		
		1892-1912 (5' of the repeats in the 3' UTR)	Mutant DMPK mRNA is reduced 15.1 ± 3.3%. Wild type DMPK mRNA is reduced 26.5 ± 2.4%.		
siRNA	CUG repeat		~75% reduction of the mutant DMPK transcript in skeletal muscle was observed. Decrease in the number and intensity of nuclear foci were observed with MBNL1 regulated mis-splicing events rescued.	HSA^{LR} mice (250 CTG repeats inserted within 3' UTR of hACTA1)	(Sobczak et al., 2013)
			~52% knockdown of CUG repeat containing transcripts was observed.	HT1080 cells (fibrosarcoma cell line) stably transfected with DMPK 3' UTR with 800 CUG repeats (HT1080-800R)	
asRNA (antisense RNA)	5' UTR (Antisense RNA expressed from an 857-bp cDNA fragment from the 5' UTR)		No effect of knockdown was observed.	DM1 myoblasts containing mutant allele with ~750 CTG repeats	(Furling et al., 2003)
	Repeats and 3' UTR (Antisense RNA expressed from a 149-bp cDNA fragment containing 13 CTG repeats and 110 bp in the following region)		80% reduction of the mutant DMPK mRNA, 50% reduction of the wild type DMPK mRNA was observed. Muscle fusion was restored to normal level.		
	3' of repeats (ISIS 486178)		~90% reduction in mutant DMPK mRNA and ~70% reduction in normal wild type DMPK mRNA were observed with MBNL1 redistribution and corrected mis-splicing events.	Human DM1 muscle satellite cells with 3,200 CTG repeats	(Jauvin et al., 2017)
			~66% reduction in mutant DMPK mRNA and foci in skeletal muscle were observed. ~30% reduction of both in the heart were detected. Improved body weight, muscle strength, and muscle histology were observed.	DMSXL mice containing DMPK gene with 1,000-1,6000 CTG repeats	

ASO (RNase H1 active)	5' of repeats (ISIS 445569)	~90% reduction in mutant DMPK mRNA and ~70% reduction in wild type DMPK mRNA were detected with MBNL1 redistribution and corrected mis-splicing events.	Human DM1 muscle satellite cells	
		~41% reduction in mutant DMPK mRNA and foci in skeletal muscle were observed. No effect in the heart was detected. No significant effect on body weight, and a partial improvement of muscle strength was detected.	DMSXL mice	
	5' UTR (ASO 190403)	No effect on the level of repeat-containing mRNA was observed.	HSA^{LR} mice (Repeats contracted to 220 in this model)	(Wheeler et al., 2012)
	Coding region near 3' UTR (ASO 190401)	Strong knockdown of repeat-containing mRNA		
	3' of repeats (ASO 445236)	Strong knockdown (comparison between ASO 190401 and ASO 445236 cannot be analyzed from data).		
	Further 3' of repeats (ASO 445238)	Stronger knockdown compared to ASO 445236		
	CUG repeat	50% decrease in repeat-containing transcript, 40% decrease in average number of foci per nuclei and splicing events switching from fetal isoforms towards adult isoforms were detected.	EpA960/HSA-Cre mice (Mice contain DMPK 3' UTR with 960 interrupted CTG repeats and selectively expressed in skeletal muscle)	(Lee et al., 2012b)
		~70% splicing correction and ~75% reduction in nuclei containing CUG^{exp} RNA foci were detected.	DM1 fibroblasts	(Wojtkowiak-Szlachcic et al., 2015)
	CUG repeat	~90% reduction in repeat-containing mRNA. ASO preferentially targets RNA with expanded repeats. Mis-splicing events corrected.	DM500 cells (mixture of myoblasts and myotubes) generated from hDMPK (CTG)300 transgene mice	(Mulders et al., 2009)
Hammerhead ribozyme	5' of repeats in the 3' UTR	63% reduction of mutant DMPK mRNA, 50% reduction of the normal DMPK mRNA, and reduction in the number and intensity of nuclear foci in the nuclei were detected.	DM750 myoblasts	(Langlois et al., 2003a)

abundance of repeat-containing mRNA and rescue mis-splicing events caused by MBNL1 loss-of-function in DM1 cells and DM1 mouse models (Angelbello et al., 2016; Coonrod et al., 2013; Haghighat Jahromi et al., 2013; Luu et al., 2016; Rzuczek et al., 2015). These therapeutic effects suggest that dispersal of mutant DMPK mRNA foci and decrease in the abundance of mutant DMPK transcript after displacing MBNL1 may be caused by mutant DMPK mRNA destabilization. Interestingly, simply increasing the amount of MBNL1, for example enhancing MBNL1 transcription can rescue mis-splicing events seen in DM1 (Cerro-Herreros et al., 2016; Chen et al., 2016).

Though these MBNL1-centric approaches do not influence all pathological events caused by mutant DMPK mRNA, for example decreased expression of neighboring genes, they appear to represent a therapeutic avenue worthy of further development.

4) Targeting pathways downstream of RNA toxicity:

Another therapeutic strategy is to target pathways downstream of mutant DMPK mRNA expression. Several studies have aimed to normalize function of CELF1 to ameliorate CELF1-related mis-splicing events in DM1 (Jones et al., 2012b; Wang et al., 2009). In addition, drugs specifically aimed at fixing certain phenotypes can also obviously improve the quality of life of DM1 patient. For example, rapamycin induces muscle relaxation and increased muscle force without rescuing splicing (Brockhoff et al., 2017),

Summary

As the culprit of DM1 is the mutant DMPK transcripts, preclinical therapies have focused primarily on eliminating the toxic RNA and displacing MBNL1 with some emphasis on correcting the downstream effects. However, little was known about the natural decay

pathway of mutant DMPK mRNA, which could give valuable information to identify and optimize therapeutics to enhance turnover of mutant DMPK transcripts.

1.1.4 Models to study DM1

Since DM1 was first identified, scientists have adopted many models to study this debilitating disease. Different models have contributed to our understanding of the disease in different ways. *C. elegans* and *Drosophila* have given insights into factors that influence severity of DM1. For example, *smg-2*/UPF1 depletion enhances RNA foci formation in *C. elegans* expressing a reporter with 123 CUG repeats (Garcia et al., 2014). A screen to identify genes that impact the eye phenotype of a CUG toxicity model in *Drosophila* led to identification of export factor Aly, putative calcium binding protein CG4589, and transcription factor *cnc* (Garcia-Lopez et al., 2008). Mice are another often-used model in DM1 research and preclinical drug efficacy studies, because they can display the full spectrum of DM1 symptoms. Through the use of mouse models expressing transgenes with various lengths of CTG repeats, the most important disease contributors in DM1 were discovered. Mouse models revealed that CUG repeat-containing mRNA is the root cause of disease (Orengo et al., 2008; Seznec et al., 2001; Wang et al., 2007) and that MBNL1 loss-of-function is a primary contributor to DM1 phenotypes (Kanadia et al., 2003). These models have also been invaluable in testing a variety of pre-clinical approaches, for example ASO targeting the 3' region of the CUG repeats successfully reduced the level of mutant DMPK transcripts and rescued mis-splicing events (Jauvin et al., 2017).

However, studying the basic molecular mechanisms of disease is difficult and expensive in complex animal models. Many human cell lines were derived from DM1 patients,

including DM1 myoblasts and DM1 fibroblasts, have been used to examine the metabolism and effects of mutant DMPK mRNA at the cellular level (Davis et al., 1997; Ketley et al., 2014; Nakamori et al., 2007). In addition, transgenic cell lines expressing repeat containing mRNAs, including Hela, COS, and iPS cells have provided useful insights (Du et al., 2013; Jones et al., 2015; Timchenko et al., 2001). However, until the recent development of CRISPR/Cas9 mediated editing which allows removal of one or both copies of a gene, it was not possible to differentiate the wild type mRNAs from CUG repeat-containing transcripts to study their metabolism individually. Aside from the inability to distinguish the two transcripts, patient-specific differences may limit the reproducibility of the results when using patient-derived cell lines.

C2C12 cells have been employed by several groups to study DMPK mRNA metabolism. Expression of CUG repeats within the human DMPK 3' UTR in C2C12 cells recapitulates many characteristic phenotypes seen in DM1; for example, RNA foci (Amack and Mahadevan, 2001; Querido et al., 2011) sequestration of MBNL1 proteins (Ho et al., 2005b; Hoskins et al., 2014; Querido et al., 2011), disrupted splicing events (Tiscornia and Mahadevan, 2000), and defects in myogenesis (Amack and Mahadevan, 2001; Amack et al., 1999, 2002). This model has been used to understand numerous important aspects of DM1 pathogenesis, including the direct connection between toxic CTG repeats and phenotypes (Amack and Mahadevan, 2001), nuclear retention of CUG repeat-containing mRNA (Mastroyiannopoulos et al., 2005), separation of foci accumulation from mis-regulation of splicing (Ho et al., 2005b).

In this study, we developed our own cell culture model in C2C12 cells to begin uncovering the natural decay pathways of wild type and mutant DMPK transcripts (see details in 3.1.1).

1.1.5 Connections between DM1 and other repeat expansion diseases

DM1 belongs to a group of debilitating diseases called repeat expansion disorders. Some of these repeat expansion disorders, for example, DM2, Huntington's disease-like 2 (HDL2; Rudnicki et al., 2007; Wilburn et al., 2011), Spinocerebellar ataxia 8 (SCA8; Daughters et al., 2009), Fragile X-associated tremor/ataxia syndrome (FXTAS)/fragile X syndrome (FXS; Kong et al., 2017; Mila et al., 2017; Verkerk et al., 1991) exhibit RNA foci in the nucleus. In most cases, these RNA foci co-localize with MBNL1 as seen in DM1. The conditions most similar to DM1 are DM2, HDL2 and SCA8.

DM2, a quadruplet repeat expansion disorder, is closely related to DM1 with regard to RNA toxicity and MBNL1 sequestration. DM2 is caused by CCTG repeats expansion in an intron of the CNBP/ZNF9 gene. The repeat-containing pre-mRNA is normally spliced and exported for translation, however, the spliced intron accumulates in nuclear foci sequestering MBNL1 which causes mis-splicing events as seen in DM1 (Liquori et al., 2001; Lucchiari et al., 2008). The repeat length in DM2 is dramatically longer than DM1, but the phenotype is much less severe. This is could reflect that the CCUG repeats in the intron lariat are quickly targeted for decay after splicing. In HDL2, the sense strand of mutated JPH3 mRNA has CUG repeats in the coding region, which sequester MBNL1 proteins leading to some mis-splicing changes like those seen in DM1 (Rudnicki et al., 2007). Additionally, the sequestration of MBNL1 proteins by CUG repeats

ATXN8OS RNA derived from the SCA8 locus triggers MBNL1-related mis-splicing events that contribute to changes in neuro-transmission (Daughters et al., 2009).

It is interesting that repeats in different genes can give such a wide range of phenotypes if they share a mechanism. DM1 and HDL2 both have CUG repeat-containing RNAs forming foci in the nucleus with MBNL1 sequestration, however, due to their differences in the expression profile of the mutated gene, the tissues affected are different. DM1 is a multi-systemic disease, while as JPH3 gene is predominantly expressed in the brain, therefore HDL2 exhibits almost exclusively neurodegenerative symptoms (Margolis et al., 2001).

Some trinucleotide diseases do not have significant RNA toxicity. For example, Huntington's disease (HD; Finkbeiner, 2011; Raymond et al., 2011), Dentatorubral-pallidoluysian atrophy (DRPLA; Ikeuchi et al., 1995; Yamada et al., 2006) and SCA2 (Sanpei et al., 1996) have trinucleotide repeats in the coding region and protein toxicity is the major contributor to pathogenesis. The number of repeats in the coding region is generally much shorter than in noncoding regions (see Table 3), presumably because the coding region expansions are likely to be more toxic due to added effects from both protein and RNA toxicity.

Due to the shared features of these repeat expansion diseases, especially the ones with MBNL1 protein related mis-splicing events, what we learn from mutant DMPK transcripts decay may extrapolate to others and benefit therapeutics across the board.

Table 3: Repeat expansion disorders.

Disease	Symptoms	Affected gene	Repeat type, length and insertion site	Toxicity	Reference
DM2	Similar to DM1, but not as severe; no congenital form; proximal muscles affected first.	Zinc finger protein 9 (ZNF9) gene/CNBP	CCTG in intron 1. Normal: 7-24 interrupted CCTG repeats (rpts) Affected: 75-11,000 rpts	RNA toxicity: nuclear retained RNA associated with MBNL1 causing mis-splicing events.	(Liquori et al., 2001; Lucchiari et al., 2008)
HDL2	Chorea, dystonia, rigidity, bradykinesia, psychiatric symptoms, dementia leading to premature death.	Junctophilin-3 (JPH3)	CTG in coding region or 3' UTR of JPH3 CAG in antisense JPH3 strand Normal: 6-27 rpts Affected: 40-57 rpts	RNA toxicity: RNA foci containing MBNL1 in neurons in the brain. Protein toxicity: CAG in the antisense JPH3 strand translates to expanded polyglutamine (polyQ) protein.	(Rudnicki et al., 2007; Wilburn et al., 2011)
SCA8	Progressive cerebellar ataxia that affects gait, limb and eye coordination.	Ataxin-8 (ATXN8) Ataxin-8 opposite strand (ATXN8OS)	CAG in ATXN8 CTG in ATXN8OS non-coding region Normal: 16-91 rpts Affected: 110-130 rpts	RNA toxicity: CTG repeats induces toxic RNA containing MBNL1 in the nucleus of neurons. Protein toxicity: CAG repeat tracts are translated to expanded polyglutamine protein (RAN translation).	(Koob et al., 1999; Moseley et al., 2006; Zu et al., 2011)
FXTAS FXS	FXTAS: intention/cerebellar tremor, cerebellar ataxia, progressive neurodegeneration. FXS: post-pubertal macroorchidism, a long face, hyperextensible joints, prominent ears and moderate intellectual disability.	Fragile X mental retardation 1 (FMR1) on the X chromosome	CGG in 5'UTR Normal: 5-45 FXTAS 55-200 rpts Fragile X >200 rpts	RNA toxicity: RNA retained in the in the neuronal and astrocytic intranuclear inclusions with MBNL1. Protein toxicity: CGG repeat translates to expanded polyglycine protein (RAN translation).	(Kong et al., 2017; Mila et al., 2017; Verkerk et al., 1991)
HD	Chorea, cognitive and emotional deficits.	Huntingtin (HTT)	Coding CAG Normal 9-37 rpts Affected 37-121 rpts	Nuclear RNA foci in neuronal cells, fibroblasts sequestering MBNL1. Protein toxicity: polyQ expansion ubiquitously in the body	(Finkbeiner, 2011; Raymond et al., 2011)
DRPLA	Ataxia, choreoathetosis, myoclonus, epilepsy, and dementia.	Atrophin-1 (ATN1)	Coding CAG Normal: 6-34 rpts Affected: 35-90 rpts	Protein toxicity: polyQ expansion in the brain	(Ikeuchi et al., 1995; Yamada et al., 2006)
SCA2	Progressive ataxia, rigidity, tremors and muscle weakness, chorea.	Ataxin-2 (ATXN2)	Coding CAG Normal 15-35 rpts Affected 37-100 rpts	Protein toxicity: polyQ expansion	(Sanpei et al., 1996)

1.2 The DMPK mRNA life cycle

In eukaryotic cells, mRNAs are transcribed and processed (capped, polyadenylated, spliced etc.) in the nucleus, and then exported to the cytoplasm where they act as templates for protein translation. Eventually, mRNAs are degraded after serving their function. Under normal circumstances, if an mRNA fails to undergo processing and export efficiently, or if an error is made, the RNA decay machinery is recruited to degrade the aberrant message. This prevents accumulation of transcripts that lack the appropriate signals for export or translation. However, some normal mRNAs as well as many non-coding RNAs are retained in the nucleus permanently or transiently without being targeted for decay. The following section will discuss the current understanding of processing and export for wild type and mutant DMPK mRNAs.

1.2.1 Structure and transcription of DMPK mRNA.

The DMPK gene locus maps to chromosome 19q13.3 (Aslanidis et al., 1992; Jansen et al., 1992; Shutler et al., 1992). There are 15 exons which forms 7 different isoforms by alternative splicing (see 1.2.2) in human (Figure 3). Isoforms II and VII cause a frameshift in the open reading frame which occurs randomly in all tissues, and isoform VI also causes a frameshift which yields C-terminally truncated protein products (Groenen et al., 2000). In addition, these isoforms exhibit cell-type dependent expression (Groenen et al., 2000). The wild type DMPK gene contains 5-37 CUG repeats within the exon 15 in the 3’ UTR, while mutant DMPK gene carries from 50 to up to several thousand of these triplet repeats. Within the 3’ UTR, there is a single AAUAAA containing poly(A) signal (NCBI Accession NM_001081563.2). In addition, DMPK antisense transcription also occurs and the level of the antisense DMPK RNA is

proportional to disease severity. Antisense transcripts can be initiated at multiple start sites and terminated following multiple poly(A) sites (Gudde et al., 2017b).

It remains controversial whether the mutated CTG repeats positively or negatively affects the abundance of the mutant DMPK transcripts (Carango et al., 1993; Davis et al., 1997; Fu et al., 1993; Hamshere et al., 1997; Sabouri et al., 1993). The decrease in abundance of DMPK mRNA and its neighboring genes could be explained by a locally repressed, condensed chromatin conformation induced by the CTG repeats (Barbé et al., 2017; Boucher et al., 1995; Brouwer et al., 2013; Frisch et al., 2001; Hamshere and Brook, 1996; Lee and Cooper, 2009; Wang et al., 1994). In addition, the discrepancy in the abundance of DMPK mRNA could be due to tissue-specific effects on synthesis and/or decay and the use of difference methodologies used to measure abundance.

1.2.2 Capping and RNA splicing in DM1

Capping of DMPK pre-mRNA

A 7-methylguanosine (m7G) residue cap is added co-transcriptionally at the 5' end of pre-mRNA (Chiu et al., 2002; Moteki and Price, 2002; Wang et al., 1982). The RNA cap promotes RNA splicing as well as the subsequent cleavage and polyadenylation process (Flaherty et al., 1997; Ohno et al., 1987; Pabis et al., 2013) and translation (Wells et al., 1998). It also protects the mRNA from 5' → 3' degradation by XRN exonucleases (Hsu and Stevens, 1993), and serves as a quality control system (Andersen et al., 2013; Jiao et al., 2013). Both wild type and mutant DMPK mRNAs are capped (Davis et al., 1997).

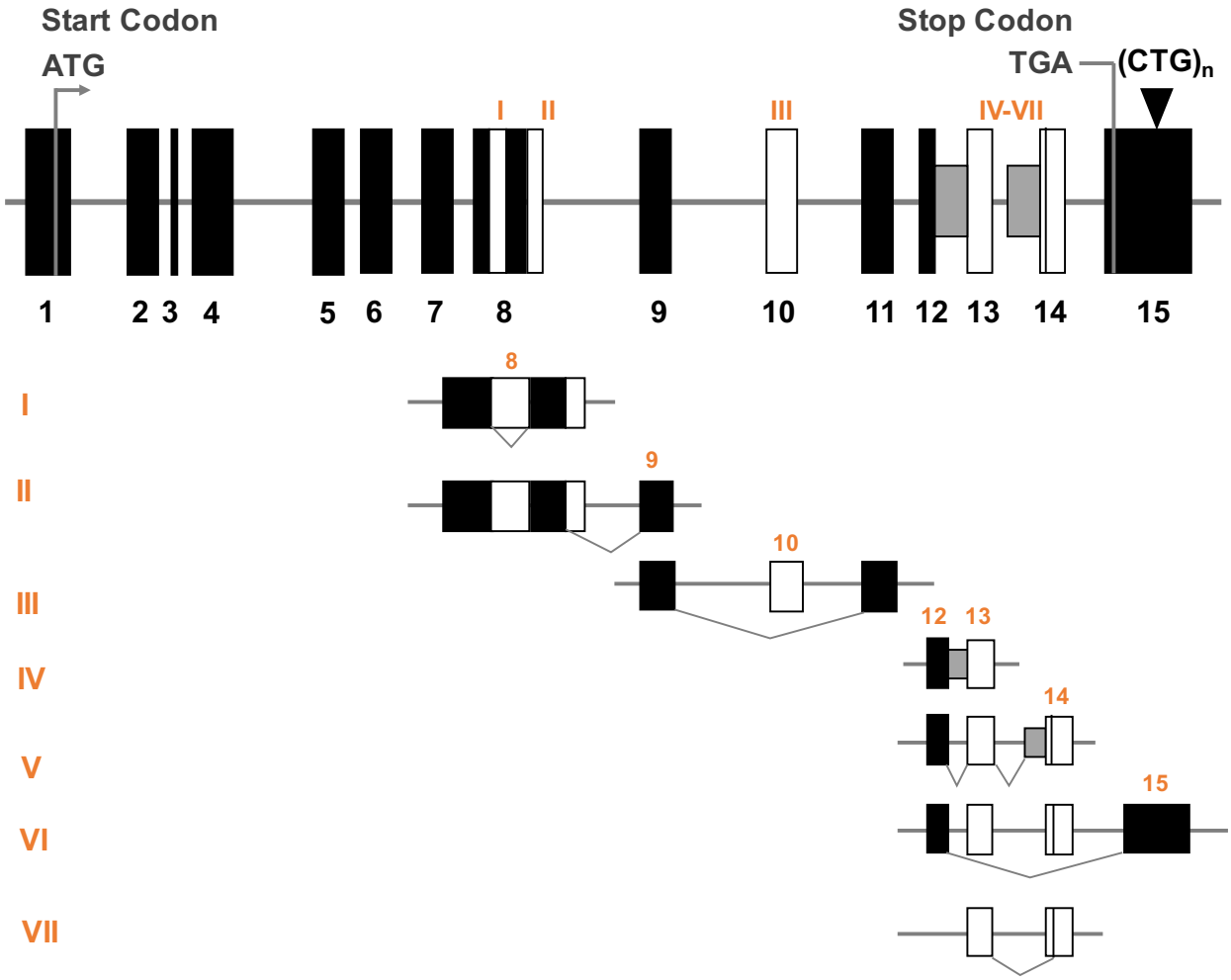

Figure 2: The DMPK gene consists of 15 exons. The CTG expansion is located within exon 15. Exons are depicted as black boxes. White boxes represent alternatively spliced exons and small grey boxes represent cryptic intron segments. Splicing of regions I (deletion of nucleotides 983-1069 of exon 8, mouse only), II (deletion of last 15 nucleotides of exon 8), III (deletion of exon 10, mouse only), IV (inclusion of complete intron 12), V (insertion of partial intron 13), VI (complete deletion of exon 13 and 14), VII (deletion of nucleotides 1654-1657 of exon 14) occurs. Figure is adapted from Groenen et al., 2000.

DMPK pre-mRNA splicing and alternative splicing

RNA splicing is the process that removes noncoding intragenic region sequences (introns) that are interspersed within coding regions (exons) in the pre-mRNAs which can influence mRNA metabolism. 80% of RNA splicing happens co-transcriptionally, but some introns located close to the 3' end are excised post-transcriptionally in the nucleoplasm including within nuclear speckles (Girard et al., 2012). In this respect, it is interesting to note that wild type DMPK mRNAs are readily detected within the nuclear speckles, but the mutant transcripts fail to enter this domain and accumulate in foci adjacent to the speckles (Smith et al., 2007).

During splicing, the spliceosome stably deposits several proteins on the mRNA upstream of the exon-exon junction, called the exon junction complex (EJC) (Le Hir et al., 2000a, 2000b). The EJC plays an essential role in mRNA localization (Fritzsche et al., 2013), serves as a platform for factors that promote mRNA export (Gromadzka et al., 2016; Le Hir et al., 2001), and stimulates translation (Chazal et al., 2013; Nott et al., 2004). In addition, the position of EJC relative to the transcription termination codon serves as quality control mechanism allowing EJC-dependent nonsense-mediated decay machinery (see 1.2.6.4).

The DMPK gene has 15 exons which can yield multiple splice isoforms (Figure 2; Groenen et al., 2000). The preponderance of evidence suggests that the mature mutant mRNA within the foci lacks introns supporting the conclusion that splicing is not dramatically affected (Davis et al., 1997; Gudde et al., 2017a). In comparison, the DM2 affected intron 1 of the ZNF9 mRNA is not spliced out and retained in the nucleus due

to MBNL1 sequestration onto the CCUG-repeat expansion mutation within intron 1 (Fardaei et al., 2002; Liquori et al., 2001; Lukáš et al., 2012).

1.2.3 Cleavage and polyadenylation of DMPK mRNA

The final step in co-transcriptional processing is 3' end cleavage and polyadenylation which is closely coupled with transcription termination. The mRNA is first cleaved downstream of the conserved AAUAAA sequence (poly(A) signal; Connelly and Manley, 1988; Mandel et al., 2006; Zarkower et al., 1986) and then a non-templated poly(A) tail of around 250 residues is added by poly(A) polymerase (Birnboim et al., 1973; Sheets and Wickens, 1989). The tail associates with various proteins to influence downstream metabolism including export (Das et al., 2003; Hector et al., 2002; Hilleren and Parker, 2001), translation (Grange et al., 1987; Sachs and Deardorff, 1992; Tarun and Sachs, 1996; Winstall et al., 2000) and decay (Bresson and Conrad, 2013; Bresson et al., 2015).

In the nucleus, the poly(A) tail interacts with nuclear poly(A) binding protein (PABPN1) (Bresson and Conrad, 2013; Kühn et al., 2017; Wahle, 1991), which helps to specify the length of poly(A) tail. However, when an mRNA is not processed correctly or too slow to be exported, PABPN1 acts as quality control mechanism to promote hyperadenylation which subjects the transcript to decay by the nuclear exosome (Bresson and Conrad, 2013). Another poly(A) binding protein, ZC3H14 (or Nab2 in yeast) also controls the length of nascent poly(A) tail (Kelly et al., 2014), but how the interactions between PABPN1 and ZC3H14 are coordinated is unknown. Additionally, nucleophosmin (NPM) is deposited on mRNA just upstream of the poly(A) tail after polyadenylation. This

protein also contributes to the control of poly(A) tail length (Palaniswamy et al., 2006; Sagawa et al., 2011).

Surprisingly, in human skeletal muscle cells, both wild type and mutant DMPK transcripts have ~500nt poly(A) tails (Gudde et al., 2017a). It is unclear, however, whether hyperadenylation influences DMPK mRNA export and/or decay.

1.2.4 The export of DMPK mRNA

Mature wild type DMPK mRNA must be exported to the cytoplasm to be translated. This process is coupled with splicing which deposits adaptor proteins such as ALY/REF of the TREX complex (a complex consisting of factors involved in transcription and the nuclear export of mRNAs) and serine/arginine-rich (SR) proteins on the mRNA before it reaches maturation (Huang and Steitz, 2001; Huang et al., 2003; Masuda et al., 2005; Meinel et al., 2013). These adaptor proteins recruit the export factor TAP(NXF1):p15 which interacts with the nucleoporins at the inside of nuclear pore complex—the key gateway between the nucleus and cytoplasm (Bachi et al., 2000; Cronshaw et al., 2002; Rout et al., 2000).

In fact, a large proportion of wild type DMPK mRNAs are found in the nucleus (Gudde et al., 2017a). This perhaps is an approach to restrict the expression of DMPK protein, as its overproduction is detrimental to mitochondrial clustering and cell viability (Oude Ophuis et al., 2009). Overall, mRNA nuclear localization is not uncommon (Bahar Halpern et al., 2015), and occurs when decay in the cytoplasm is more rapid than export, or when mRNAs fail to be exported efficiently.

The mutant DMPK mRNAs are also retained in the nucleus but they can be detected in bright foci in contrast to the diffuse pattern shown by the wild type mRNA. The retained mutant DMPK transcripts are flagged to be improper for export long before transcription termination (Holt et al., 2007; Kim et al., 2005a; Koch and Leffert, 1998; Smith et al., 2007). Mutant DMPK transcripts do not co-localize with nuclear speckles which is reported to be a check-point for export-ready mRNAs as described in 1.2.2 (Smith et al., 2007). Interestingly, the export defect can be overridden by inserting the woodchuck post-transcriptional regulatory element (WPRE) downstream of the repeats of the 3' UTR of mutant DMPK mRNA which allows it to use the CRM1-dependent viral RNA export pathway (Mastroyiannopoulos et al., 2005). This implies that the mutant DMPK transcripts may fail to efficiently recruit export factors, perhaps explaining their nuclear localization.

1.2.5 Translation of DMPK mRNA

Wild type DMPK transcripts are translated presumably like other mRNAs. Proteins binding the RNA cap (eukaryotic initiation factor 4F complex) interact with poly(A) binding protein (PABP) to stimulate effective translation (Imataka et al., 1998; López-Perrote et al., 2016; Searfoss et al., 2001; Uchida et al., 2002). Ribosomes assemble on the mRNA to synthesize peptides until reaching a stop codon (Alkalaeva et al., 2006; Chakrabarti and Maitra, 1991; des Georges et al., 2014; Pestova et al., 2000; Salas-Marco and Bedwell, 2004; Trachsel et al., 1977). The sense strand of mutant DMPK transcript, however, is not efficiently translated mostly due to nuclear retention (Mastroyiannopoulos et al., 2005; Smith et al., 2007). Interestingly, the very low level antisense strand of repeat-containing DMPK mRNA goes through repeat-associated

non-ATG (RAN) translation which generates toxic protein that may be toxic to the cell (Zu et al., 2011).

1.2.6 DMPK mRNA decay

RNA decay is an important posttranscriptional process that regulates up to 40-50% of changes in gene expression. Globally, it contributes to cellular processes of development, inflammation, aging and apoptosis, just to name a few (Cheadle et al., 2005; Jones et al., 2012a).

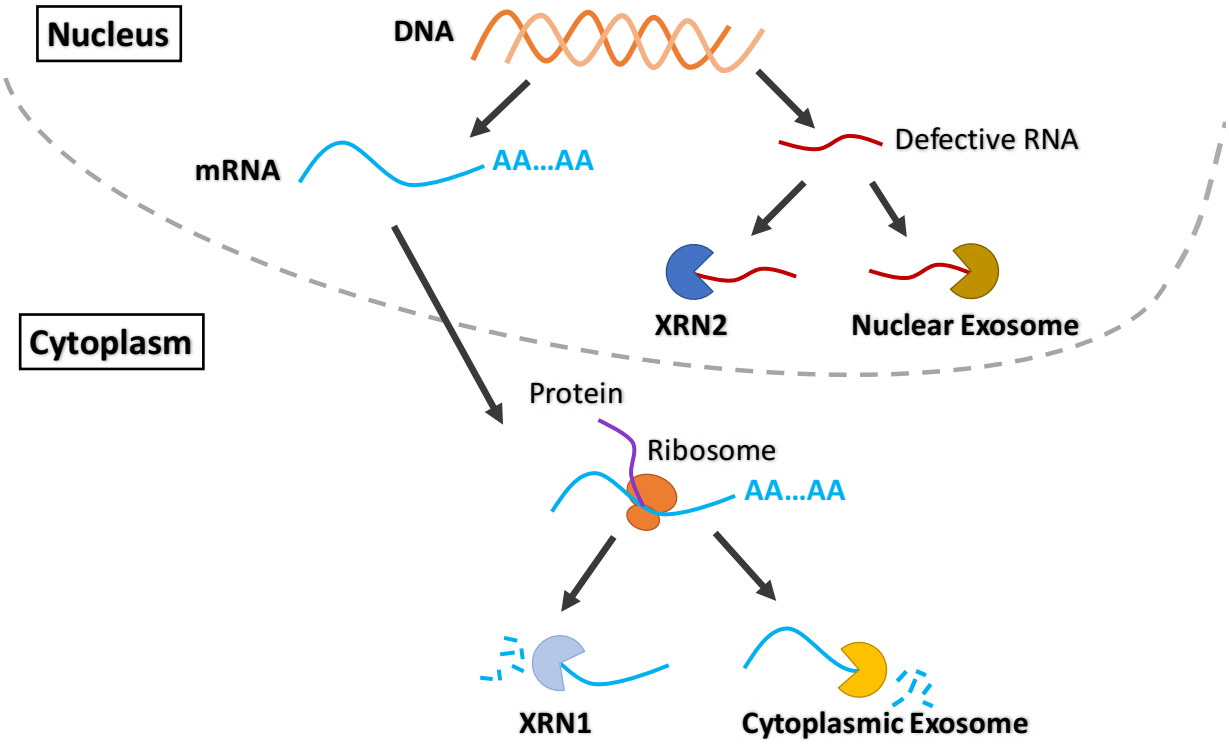

Figure 3: Cytoplasmic and nuclear decay of mRNA. Following deadenylation, mRNA is degraded either through decapping followed by 5' → 3' decay or 3' → 5' decay in the cytoplasm. Aberrant mRNAs can be degraded in the nucleus by 5' → 3' exonuclease XRN2 or 3' → 5' exonuclease the nuclear exosome.

Cytoplasmic pathway of mRNA decay

It is well-established that most mRNAs, presumably including the wild type DMPK mRNA, go through deadenylation-dependent decay in the cytoplasm (Muhlrad et al.,

1994; Wormington et al., 1996). In this case, mRNA decay is initiated by removal of the poly(A) tail, followed by 3' → 5' decay by the exosome and/or decapping and 5' → 3' decay by the exonuclease XRN1 (Figure 3).

Nuclear pathway of mRNA decay

Nuclear RNA decay pathways also exist, but are less characterized than cytoplasmic mRNA decay. The nuclear decay pathway is mainly used to process nuclear noncoding RNAs (ncRNAs), such as nucleolar RNAs (snoRNAs) and some nuclear restricted long ncRNA (>200 nt; Birney et al., 2007). Nuclear RNA decay is conducted by either XRN2 in the 5' to 3' direction (Amberg et al., 1992; Chang et al., 2011), or by the nuclear exosome (with catalytic subunit EXOSC10/RRP6) in the 3' to 5' direction (Figure 3; Bonneau et al., 2009; Januszyk and Lima, 2014; Wasmuth and Lima, 2012; Wolin et al., 2012).

Decay of the aberrant mRNAs

Both the cytoplasmic and nuclear decay pathways also play a major role in the quality control of mRNAs, which is essential to the homeostasis of the cell. In the nucleus, the nuclear decay machinery degrades unspliced and incorrectly polyadenylated Pol II transcripts (Houseley et al., 2006; LaCava et al., 2005; Milligan et al., 2005; Nagarajan et al., 2013). In the cytoplasm, aberrant transcripts that exhibit inappropriate ribosome translocation can be quickly degraded by nonsense-mediated decay (NMD; see 1.2.6.4), no-go decay (NGD), or non-stop decay (NSD) depending on the defect in the transcript.

1.2.6.1 Deadenylation

PARN (poly(A)-specific ribonuclease)

PARN is a processive poly(A) specific 3' exonuclease, whose activity is dependent on the existence of divalent metal ion (Martinez et al., 2000; Martînez et al., 2001). It interacts with both the 5' cap structure and the 3' poly(A) tail of mRNA during deadenylation. It is involved in regulation of maternal mRNA expression during development in *Xenopus* oocytes (Copeland and Wormington, 2001). In the nucleus, PARN inhibits 3' end processing and shortens nascent poly(A) tails in response to UV-induced DNA damage (Cevher 2010, Zhang 2010, Yan 2014).

CCR4-NOT (Carbon catabolite repression 4/negative on TATA-less)/CAF1 (CCR4 associated factor) and PAN2-PAN3 (poly(A) binding protein-stimulated poly(A) ribonuclease) complex

Deadenylation by PAN2-PAN3 and CCR4-NOT is a biphasic process. With the stimulation of PABP on the poly(A) tail, PAN2-PAN3 slowly trims the poly(A) tail to ~110nt. Subsequently, CCR4-NOT-CAF1 hydrolyzes the remaining adenosine nucleotides which creates a heterogeneous repertoire of mRNA with tail length ranging from ~110nt to ~20nt (Yamashita et al., 2005). The second phase is crucial in leading mRNA to 5' → 3' or 3' → 5' decay pathway.

Deadenylation-independent decay

Deadenylation-independent mRNA decay also exists which bypasses the removal of poly(A) tails and directly recruits decay enzymes (Badis et al., 2004; Muhlrad and Parker, 2005). Some preclinical therapeutics avenues involving RNAi and ASO for DM1 (see Table 2) utilize deadenylation-independent decay pathway. In the nucleus, with the

guidance of siRNA or processed shRNA (by DICER), AGO2 of the nuclear RISC complex (RNA-induced silencing complexes) cleaves the targeted mRNAs. This cleavage event invites the 3' → 5' nuclear exosome to degrade the upstream fragments and the 5' → 3' exonuclease XRN2 to decay the downstream fragments (Robb et al., 2005) to achieve the knockdown of certain gene of interest.

1.2.6.2 5'-3' decay

When deadenylation is completed, the 5' cap structure is removed by decapping enzymes (Wang et al., 2002). This results in a 5'-monophosphate on the mRNA that can be recognized by the XRN family of exonucleases to conduct 5' → 3' decay. 5' monophosphates generated by endonucleolytic cleavage can also be targeted by XRN enzymes.

Decapping

Classically, following deadenylation, the 3' end of the mRNA is associated with the heptameric Lsm1-7 complex. This complex activates the DCP2 decapping enzyme, a member of the Nudix superfamily of hydrolases (Ingelfinger et al., 2002; Tharun et al., 2000; Wang et al., 2002; Wu et al., 2014). However, DCP2 enzyme is not expressed ubiquitously (Song et al., 2010). DCP2 also exists in the nucleus (van Dijk et al., 2002; Liu et al., 2004) where it interacts with XRN2 to control premature transcription termination (Brannan et al., 2012). There are at least 3 other decapping enzymes—NUDT16, NUDT3 and DXO1 (decapping exonuclease; Song et al., 2010; Williams et al., 2015; Yue et al., 2014) – that target specific pool of RNA substrates. Interestingly, NUDT16 protein was found in the nucleus (Li et al., 2011; Taylor and Peculis, 2008), and DXO1 protein is able to hydrolyze unmethylated, incompletely capped RNA and

which contributes to mRNA quality control in the nucleus (Jiao et al., 2013). The decapping function of NUDT3 protein, however, has only been described in the cytoplasm (Grudzien-Nogalska et al., 2016; McLennan, 2006).

The 5' → 3' exonuclease

After decapping, the 5'-monophosphate on the mRNA is recognized and degraded processively by the highly conserved XRN family of 5' → 3' exoribonucleases. In the mammalian cells, there are two types of XRN proteins: XRN1/PACMAN in the cytoplasm, and XRN2/RAT1 in the nucleus. XRNs are indispensable for rRNA maturation and quality control (Wang and Pestov, 2011), mRNA transcription termination (Morales et al., 2016; Sansó et al., 2016), mRNA quality control (Davidson et al., 2012a; Hilleren and Parker, 2003), degradation of noncoding RNA (van Dijk et al., 2011; Geisler et al., 2012; Watanabe et al., 2013), mRNA decay (Hsu and Stevens, 1993), gene silencing (Orban and Izaurralde, 2005), and nonsense-mediated decay (Lejeune et al., 2003).

Presumably, wild type DMPK mRNA is degraded solely in the cytoplasm by XRN1 like other normal mRNAs. However, the enzyme responsible for degrading the CUG repeat-containing transcripts was unknown until completion of this dissertation.

1.2.6.3 3' → 5' decay

The 3' → 5' decay pathway is largely carried out by the exosome, an essential ribonuclease complex, in both the nucleus and cytoplasm. The exosome is involved in degradation and/or processing of nearly all classes of RNA. The nuclear exosome is responsible for maturation and quality control of rRNA (Milligan et al., 2008; Schilders et al., 2005), noncoding RNA processing (Peng et al., 2003), and degradation of mis-

folded tRNA and aberrant mRNA degradation (Schneider et al., 2012). The cytoplasmic exosome play a vital role in regulated mRNA-decay pathways (Mukherjee et al., 2002), gene silencing as well as quality control pathways (Doma and Parker, 2006; van Hoof et al., 2002; Mitchell and Tollervey, 2003).

The exosome comprises a non-catalytic nine-subunit core (Exo9), which forms a central pore (Wasmuth and Lima, 2012). Additional subunits are required for enzymatic activity: DIS3/RRP44 and EXOSC10/RRP6. DIS3 has processive exoribonuclease activity, and its human homologs are present in both the nucleus (DIS3, with an additional endoribonucleolytic activity) and the cytoplasm (DIS3L and DIS3L2) (Malecki et al., 2013; Tomecki et al., 2010). Interestingly, DIS3L2 does not interact with the exosome components, prefers 3' uridylated substrates and can efficiently degrade structured substrates (Lubas et al., 2013; Malecki et al., 2013). EXOSC10/RRP6 has distributive exonuclease activity and resides primarily in the nucleus (Bonneau et al., 2009; Januszyk and Lima, 2014; Wasmuth and Lima, 2012). In the nuclear exosome complex, EXOSC10/RRP6 appears to enhance the activity of DIS3 (Wasmuth and Lima, 2012), however, it is unknown how RNAs are differentially targeted to DIS3 or EXOSC10/RRP6 in the nucleus. In addition, as the central pore of the exosome is only large enough for a single stranded RNA to possibly pass through, RNA secondary structures must be unwound by either TRAMP (Trf4/5-Air1/2-Mtr4 polyadenylation) complex in the nucleus or SKI (superkiller) complex in the cytoplasm before entering (Araki et al., 2001; LaCava et al., 2005; Mitchell and Tollervey, 2003).

Following deadenylation, the remnants of poly(A) tail provide a 3' OH and region of unstructured RNA required for exosome recruitment (Lee et al., 2012a). The

cytoplasmic exosome can then degrade the wild type transcripts processively to free nucleotides. The Scavenger Decapping enzyme DcpS cleaves and recycles the 5' cap before the last few nucleotides are degraded (Chen et al., 2005; Liu et al., 2002; Wang and Kiledjian, 2001).

As mutant DMPK transcript aggregates in nuclear foci, it is tempting to speculate that it may also be degraded in the nucleus where the nuclear exosome is the primary degradation machinery (Hilleren et al., 2001; Szczepinska et al., 2015). Interestingly, the nuclear exosome does not visibly co-localize with nuclear DMPK foci in either *Drosophila* or DM1 patient neurons (Houseley et al., 2005; Jiang et al., 2004). This does not rule out a role for the exosome in decaying the mutant transcript, however, it is important to keep in mind that there is no evidence that the foci are the sites of decay of the RNA. If the mutant DMPK mRNA is eventually exported, then it is possible that the exosome-independent DIS3L2 exoribonuclease participates in its degradation as knocking down DIS3L2 worsens the phenotype of DM1 in *C. elegans* (Garcia et al., 2014).

1.2.6.4 Nonsense-mediated decay

Nonsense-mediated decay (NMD) is a translation-dependent mRNA quality control mechanism which triggers degradation of aberrant mRNA harboring a premature termination codon (PTC) (Amrani et al., 2004). Interestingly, it also functions as a regulator for maintaining appropriate gene expression (Ni et al., 2007; Sureau et al., 2001; Weischenfeldt et al., 2008).

The up-frameshift protein 1 (UPF1/RENT1) is an essential NMD factor which binds transiently to newly synthesized and exported mRNAs promiscuously to survey for a

PTC (Chakrabarti et al., 2011; Gregersen et al., 2014; Zünd et al., 2013). Once a PTC is recognized, serine/threonine-protein kinase SMG1 is recruited to phosphorylate UPF1 under tight regulation from other NMD factors (Deniaud et al., 2015). The hyperphosphorylated UPF1 not only represses further translation initiation on this mRNA (Isken et al., 2008), but also interacts with SMG5, SMG6, SMG7 and PNRC2 that trigger the subsequent decay (Chakrabarti et al., 2014; Okada-Katsuhata et al., 2012). The endonuclease SMG6 cleaves the NMD target near the PTC (Eberle et al., 2009; Lykke-Andersen et al., 2014). In addition, SMG7 recruits the CCR4-NOT deadenylases complex (Loh et al., 2013), and SMG5 with PNRC2 recruits the mRNA-decapping complex DCP2/DCP1a (Cho et al., 2009, 2013). Thereafter, the cleaved mRNA lacking the 5' cap or the 3' poly(A) tail can be readily degraded by 5' → 3' and 3' → 5 decay machineries as described previously.

The distance between the termination codon and the PABPC1 bound poly(A) tail in the mutant DMPK RNA is extended due to the extended CUG repeats, which could subject the transcript to NMD. In support of this idea, inactivating UPF1 protein by RNAi in human DM1 patient fibroblasts causes an increase in the number of toxic RNA foci, while no nuclear foci is observed in normal fibroblasts with or without UPF1 protein depletion (Garcia et al., 2014).

UPF1 protein is not only an NMD factor, but it also participates in Staufen1-mediated decay (Kim et al., 2005b). Additionally, it is predicted bioinformatically that UPF1 protein interacts with many nuclear proteins including the 5' → 3' exonuclease XRN2, EXOSC10 of the nuclear exosome, PABPN1 (that binds the poly(A) tail in the nucleus),

decapping enzyme DCP2, 3' end associated enzyme factor LSM1, and DM1-disease modifier helicase DDX6 (Varsally and Brogna, 2012).

Collectively, NMD, or at least UPF1 protein, may have an effect on the degradation of DMPK mutant transcripts.

1.3 Rationale

As discussed in this chapter, the pathogenesis of DM1 is greatly associated with the nuclear retained mutant DMPK mRNA. One promising avenue of preclinical research has sought to get rid of this mutant transcript using siRNA or ASO (see Table 2), which is likely to be very beneficial to the DM1 phenotypes. However, such approaches can likely be significantly augmented by increasing natural processes of mutant DMPK mRNA decay. However, little is known about how and where DMPK mRNAs are naturally degraded, and what enzymes are responsible. Our goal is to address this knowledge gap. By studying DMPK mRNA decay, we will also determine the role mutant DMPK mRNA stability plays in DM1 pathogenesis. We hypothesize that wild type DMPK mRNA and mutant DMPK transcripts are degraded via different pathways. Previous reports of complex structures stalling the 5' → 3' exonuclease XRN1 by poly(G) tract structures or a three helix junction in the flavivirus 3' UTRs (Chapman et al., 2014a; Muhlrad et al., 1994) provide precedence that RNA structure can influence key aspects of mRNA decay. Thus we propose to determine whether the CUG repeat/MBNL1 protein complex present in mutant DMPK transcripts can affect their decay. Specifically we propose that the structure of CUG repeat – with or without MBNL1 protein – can stall the 5' → 3' exonuclease XRN causing partially degraded mutant DMPK mRNA to accumulate in the nucleus and contribute to DM1 toxicity. In

addition, the stalling of XRN enzymes at expanded CUG repeat structures may also cause XRN malfunction/repression due to slow off-rates of a normally highly processive exoribonuclease. Finally, the presence of expanded CUG repeats in a DMPK mRNA may make that mutant transcript a target for nonsense-mediated decay due to the extended distance between the stop codon and the poly(A) signal. Thus we propose to explore a role for nonsense-mediated decay in targeting transcripts containing expanded CUG repeats in their 3' UTR. Collectively, we anticipate that our results further our understanding of DM1 pathogenesis and perhaps provide new insights into therapeutic avenues to treat the disease.

CHAPTER 2: MATERIALS AND METHODS

2.1 Cell culture and transfection

2.1.1 Cell line maintenance

2.1.1.1 C2C12 mouse myoblasts

C2C12 mouse myoblasts (ATCC #CRL1722) were transfected and selected by Dr. Mary Schneider (see details in 2.1.2) to make stable cell lines capable of inducibly expressing DMPK 3' UTR with or without 700 CTG repeats (Figure 5A).

Maintenance of CUG0 and CUG700 cell lines

Both CUG0 and CUG700 cells were maintained at or below 70% confluency in Dulbecco's Modified Eagle's Medium (DMEM; Cellgro #50-003-PC) containing 10% tet-system approved fetal bovine serum (Clontech #631106), penicillin (50 units/ml) and streptomycin (50 µg/ml; Hyclone #SV300100) as well as puromycin (1 µg/ml; Sigma #P8833) in 5% CO_2 at 37ºC. Cells were passaged when 70% confluent at a split ratio of 1:10 using 0.25% trypsin- EDTA (Hyclone #SH30042.01) in Phosphate Buffered Saline (PBS; Hyclone#21-040-CV).

2.1.1.2 Immortalized human myoblasts

Both control human myoblasts (MB-C) and DM1 patient myoblasts (MB-DM480; with 480 CTG repeats) from MTCC were immortalized by Dr. Hend Ibrahim. HIV7/CNPO viral vectors carrying the human telomerase (hTERT; Kowolik et al., 2004) and cyclin-dependent kinase 4 with a FLAG-tag (FLAG-hCDK4; 75ng) were transduced into MTCC MB-C and MB-DM480 cell lines using 2µl Polybrene (Millipore #TR-1003-G). Pools of

neomycin/G418 resistant cells were selected in 1 mg/ml G418 (Goldbio #G-418-1) for 7-10 days. We transduced multiplicity of infection (MOI) of 5. Following immortalization, hCDK4 expression was verified by western blot and cells were passaged successfully for >20 generations.

Immortalized human myoblasts were maintained at or below 70% confluency in Dulbecco's Modified Eagle's Medium/high glucose (DMEM/HIGH GLUCOSE; Hyclone #SH30022.01) containing 20% newborn calf serum (heat inactivated at 55ºC for 30 min; PEAK #PS-NB1), insulin (10 µg/ml; ThermoFisher #12585014), basic human fibroblast growth factor (bFGF, 25 ng/ml; Goldbio #1140-02-1000), epidermal growth factor (EGF; Sigma #SRP3027), G418 sulfate/geneticin (1mg/ml; Goldbio #G-418-1) in 5% CO_2 at 37ºC. Cells were passaged when 70% confluent at a split ratio of 1:10 using 0.25% trypsin-EDTA (Hyclone #SH30042.01) in Phosphate Buffered Saline (PBS; Hyclone #21-040-CV).

2.1.2 Plasmid preparation and transfection

All plasmids (Table 5) were transformed and amplified in *E coli* DH5α and purified using Purelink Hipure plasmid maxiprep kit (Invitrogen #K210007) followed by MiraClean endotoxin removal kit (Mirus #MIR5910) or ZymoPURE Plasmid Maxiprep Kit (Zymo Research #D4203). C2C12 mouse myoblasts were transfected in suspension after counted under a microscope using Lipofectamine 2000 (Invitrogen #11668-019) with Opti-MEM1 Reduced Serum Medium (ThermoFisher #31985-070) according to the manufacturer's instructions. Transfection reactions were performed inside the biosafety

Table 4: Transfection reactions

Culture vessel	Purpose	Tube 1	Tube 2	Cells
100 mm dish	Tet-off promoter activation	12 µg pTET-OFF + 600 µl OptiMEM	24 µl Lipofectamine 2000 + 600 µl OptiMEM	1,400,000 cells per dish
60 mm dish	Tet-off promoter activation	4 µg pTET-OFF + 200 µl OptiMEM	8 µl Lipofectamine 2000 + 200 µl OptiMEM	500,000 cells per dish
	Transfection with any plasmid containing shRNA	4 µg pTET-OFF + 4 µg plasmids encoding shRNA + 400 µl OptiMEM	16 µl Lipofectamine 2000 + 400 µl OptiMEM	
	siGFP transfection	4 µg pTET-OFF + 12 µl siGFP (10 µM) + 800 µl OptiMEM	32 µl Lipofectamine 2000 + 800 µl OptiMEM	
	siXRN2 + siMBNL1 transfection	4 µg pTET-OFF + 6 µl siXRN2 (10 µM) + 6 µl siMBNL1 (10 µM) + 800 µl OptiMEM	32 µl Lipofectamine 2000 + 800 µl OptiMEM	
	siSCRAMBLED or siRRP6 transfection	4 µg pTET-OFF + 6 µl siRNA (10 µM) + 500 µl OptiMEM	10 µl Lipofectamine 2000 + 500 µl OptiMEM	
One well in a 12-well plate	Tet-off promoter activation	0.6 µg pTET-OFF + 30 µl OptiMEM	1.2 µl Lipofectamine 2000 + 30 µl OptiMEM	80,000 cells per well
One well in a 96-well plate	Tet-off promoter activation	0.06 µg pTET-OFF + 3 µl OptiMEM	0.12 µl Lipofectamine 2000 + 3 µl OptiMEM	8,000 cells per well

Tube 1 and tube 2 were incubated separately at room temperature for 5 min, then mixed together and incubated at room temperature for 20 min before adding to cells in suspension. Media without any antibiotics was used during transfection to minimize cell death. (Reactions were scaled up to avoid pipetting small volumes.)

cabinets with autoclaved Eppendorf tubes or sterile DNase free, RNase free conical tubes. The amount of plasmid and reagents used were calculated according to the surface area of the dish/well used (Table 4). Reactions can be scaled up depending on the number of transfections needed.

Table 5: Plasmids and siRNAs used in this study

Plasmid Name	Origin & key sequence
pTRE3G-BI-ZsGreen1	Clontech #631334
pTRE3G-Luc-CUG0	Figure 5A left
pTRE3G-Luc-CUG700	Figure 5A right
Linear Puromycin Marker	Clontech #631626
pTET-OFF	Clontech, 1st generation #631017
pLKO.1	Sigma-Aldrich #SHC002
Mouse XRN2 shRNA	Sigma-Aldrich; TRCN0000119960 CCGGCAACGATACTACAAGAACAAACTCGAGTTTGTTCTTGTAGTA TCGTTGTTTTTG
Mouse MBNL1 shRNA	Sigma-Aldrich; TRCN0000219085 GTACCGGTGACAGCACAATGATTGATACCTCGAGGTATCAATCATT GTGCTGTCATTTTTTG
Mouse UPF1 shRNA	Sigma-Aldrich; TRCN0000274486 CCGGAGCTATGTGGCTTAGTCTATCCTCGAGGATAGACTAAGCCA CATAGCTTTTTTG
Mouse siXRN2	Sigma-Aldrich; SASI_Mm01_00193520 5'-GAAAUUCCGACGUAAGGUU-3'
Mouse siMBNL1	Sigma-Aldrich; SASI_Mm01_00086352 5'-CGUCAUUAGCCAUAUUGUA-3'
Mouse siRRP6	Sigma-Aldrich; SASI_Mm01_00138650 5'-CUCUCAAGCAGCAAAGUUU-3'
Human siXRN2	Sigma-Aldrich 5′ -CACUGGAAGUAUGUAGAGA
Human siMBNL1	Sigma-Aldrich 5'-UCGCUAUUACAUAGCUGAUCGUUUA-3'
sieGFP	Sigma-Aldrich5'-GCAAGCUGACCCUGAAGUUCAU-3'
siSCRAMBLED Universal Negative Control	Sigma-Aldrich #SIC001-10NMOL; proprietary sequence

Generation of CUG0 plasmid (pTRE-3G-Luc-CUG0)

The pTRE3G-BI-ZsGreen1 vector (Clontech #631334) was prepared by digesting with *EcoRV* restriction enzyme (NEB). The insert was produced by overlap extension PCR using Pfu DNA Polymerase (Agilent #600390) according to the manufacturer's instructions (Figure 4). First, firefly luciferase fragment was amplified from pGL3-Basic

vector (Promega #U47295) with forward primer (TRE3G-*EcoRV*-Luc-F): 5'-GCGGCCGCCGGCGATatggaagacgccaaaaacataaagaaaggc-3' and reverse primer (Luc-DT0-R): 5'-TATGATCCTCTGGAGATttacaatttggactttccgcccttcttg-3'. Second, DT0 fragment was amplified from DT0 plasmid (plasmid containing human DMPK 3' UTR with 0 CTG repeats kindly provided by Dr. Thomas Cooper; Ho et al., 2004) with forward primer (Luc-DT0-F): 5' AAGTCCAAATTGTAAaccctagaactgtcttcgactccg-3' and reverse primer (DT0-TRE3G-R): 5'-TATGATCCTCTGGAGATccagagctttgggcagatgga-3'. Third, products from the first two PCR reactions were gel purified and amplified with forward primer (TRE3G-*EcoRV*-Luc-F: 5'-GCGGCCGCCGGCGATatggaagacgc caaaaacataaagaaaggc-3' and reverse primer (DT0-*EcoRV*-TRE3G-R): 5'-TATGATCCTCTGGAGATttacaatttggactttccgcccttcttg-3'. The insert was gel purified and ligated with the pTRE3G-BI-ZsGreen1 vector. After ligation, the reactions were transformed into *E coli* DH5α cells, and plated onto a LB plate containing ampicillin

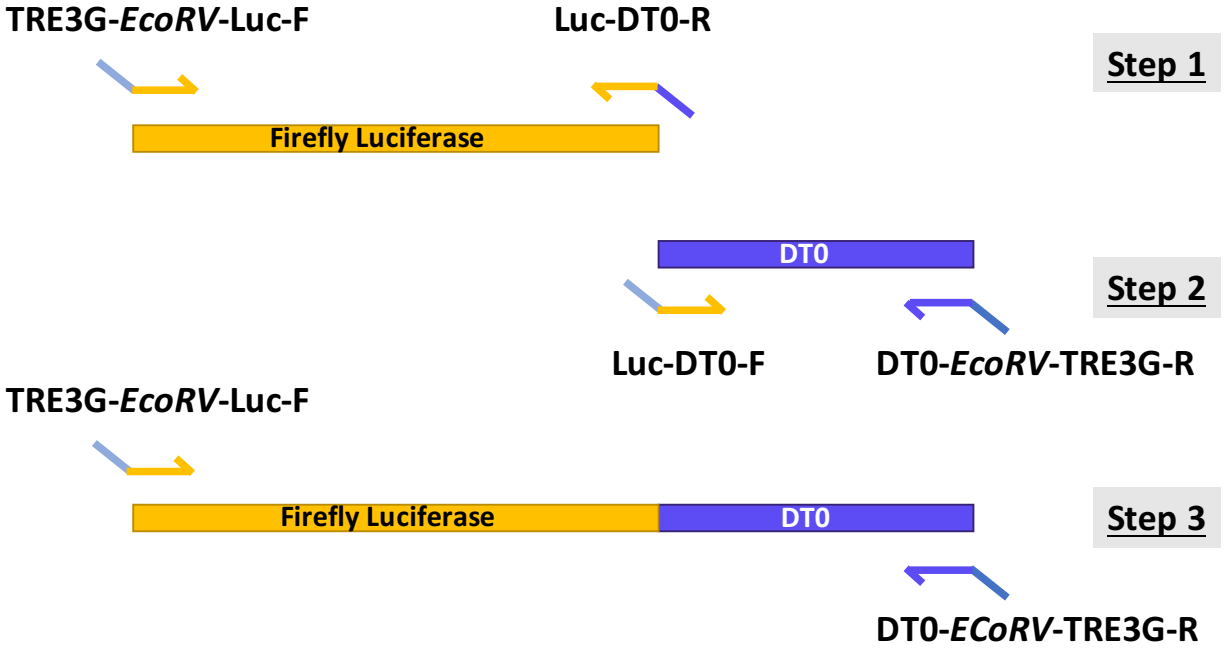

Figure 4: 3-step PCR primer map for creating insert for pTRE3G-Luc-CUG0.

overnight. Colonies were selected from the LB plate for miniprep and screened by PCR (forward primer (TRE3G-*EcoRV*-Luc-F): 5'-GCGGCCGCCGGCGATatggaagacgccaaaa acataaagaaaggc-3' and reverse primer (DT0-*EcoRV*-TRE3G-R): 5'- TATGATCCTCTG GAGATttacaatttggactttccgcccttcttg-3'). Positive colonies were maxiprepped and verified by sequencing before transfection.

Generation of CUG700 plasmid (pTRE3G-Luc-CUG700)

We subcloned the DMPK 3' UTR with CTG repeats into pTRE3G-BI-ZsGreen1 vector by digesting CUG0 plasmid with XmaI and AvrII and inserting a XmaI/ArII fragment containing the repeats from the CT960 plasmid (plasmid containing DMPK 3' UTR with 960 CTG repeats, kindly provided by Dr. Thomas Cooper; Ho et al., 2004). After ligation, the reactions were transformed into SURE (Stop Unwanted Rearrangement Events) Competent cells (Agilent #200238) which were engineered to avoid DNA rearrangement and deletion of nonstandard secondary and tertiary structures. Further analysis showed that some repeats were lost during the cloning and culture; ~700 CTG repeats remained. As 700 CTG repeats is sufficient to cause significant pathogenesis in patients, we proceeded to use this plasmid for the remaining experiments.

Generation of CUG0 and CUG700 cell lines

We transfected pTRE3G-Luc-CUG0 and pTRE3G-Luc-CUG700 (Figure 5A) separately into C2C12 cells, together with a Linear Puromycin Marker (Clontech #631626) plasmid. A pool of puromycin resistant cells were selected in 2 µg/ml puromycin (Sigma #P8833) and clonal cell lines were selected from this pool. Several independent clonal cell lines were screened microscopically for expression of ZsGreen and response to

DOX/transactivator and two lines with inducible expression were selected for subsequent experiments.

2.2 RNA preparation and quantification

2.2.1 RNA isolation and quality control

Total RNA was extracted from cultured cells using TRIzol® reagent (Life Technologies #15596018) according to the manufacturer's recommendations. Column-based RNA purification was used in some experiments (Zymo Research #R1054/R1055). DNase I treatment (ThermoFisher #DN0525) was performed for 20-30 min at 37 °C to remove genomic DNA and the RNA was recovered by phenol/chloroform/IAA extraction and ethanol precipitation. Total RNA yield was measured by Nanodrop (ThermoFisher #2000c).

2.2.2 Reverse transcription (RT)

We utilized 1 µg of total RNA in a standard reaction with 0.5 µg random hexamers (Integrated DNA Technologies #51-01-18-01) in a final volume of 5 µl. Improm II reverse transcriptase (Promega #A3800) was used according to manufacturer's instructions.

2.2.3 Quantitative PCR (qRT-PCR)

To perform quantitative PCR (qPCR), a master mix was prepared for each reaction using 17.5 µl iQ SYBR Green 2X Supermix (Bio-Rad # 170-8887; IDT), 1.4 µl forward primer (2.5 µM), 1.4 µl reverse primer (2.5µM), 11.9 µl ddH2O, and 2.8 µl cDNA. 10 µl of the master mix was transferred to 3 wells of a 96-well plate and loaded into a CFX96 Real-Time PCR Detection System (Bio-Rad) after a quick spin. A two-step amplification protocol was used with an annealing temperature of 60ºC for 30s and a melting

temperature of 95ºC for 30 sec for 40 cycles. The melt curve was generated by starting at 60ºC with an increase of 0.5ºC every 5 sec until 95ºC was reached. Data was analyzed with CFX Manager software (Bio-Rad). Target gene expression was normalized to murine GAPDH (mGAPDH) mRNA to determine abundance. The CFX Manager software applied the Pfaffl Method (Pfaffl, 2001) to determine expression relative to the reference gene.

All primer pairs were standardized using six 5-fold cDNA serial dilutions to allow determination of PCR efficiency. All primers used had a PCR efficiency between 90-110% and a R^2 value (correlation coefficient) >0.98. Primers were designed and chosen using Primers3 Plus (http://bioinfo.ut.ee/primer3-0.4.0/) and Primer-BLAST (https://www.ncbi.nlm.nih.gov/tools/primer-blast/). Primer sets were designed to have a GC content between 50-60%, annealing temperature between 60-63ºC, and length of 18-24 nucleotides. Primers used and their efficiencies are listed in Table 6.

2.2.4 Digital droplet PCR (ddPCR)

Each PCR reaction was assembled as follows: 10 µl QX200™ ddPCR™ EvaGreen Supermix (Bio-Rad # 1864034), 1 µl each primer (2.5 mM), 1 µl cDNA (diluted as necessary), and nuclease-free water for a final volume of 20 µl. A no template control and no reverse transcriptase control was included for each experiment. Droplets were generated using the Bio-Rad Droplet Generator (Bio-Rad #1864002) and transferred to a 96-well plate (Eppendorf # 951020346), sealed with a foil seal (Bio-Rad cat# 1814040) and subjected to thermocycling: 95°C for 5 min, 40 cycles of (95°C for 30 sec followed by 60°C for 1 min), 90°C for 5 min, hold at 4°C in a BioRad C1000 Touch thermal cycler (Bio-Rad #1851197). The droplets were read and parsed into positive

Table 6: List of primers used for PCR, (q)RT-PCR and ddPCR

Primer Name	Gene ID	Sequence	Product size	Efficiency	Note
TRE3G-*EcoRV*-Luc-F	N/A	5'-GCGGCCGCCGGCGATatggaagacgccaaaaacataaagaaaggc-3'	N/A	N/A	
Luc-DT0-R	N/A	5'-TATGATCCTCTGGAGATttacaatttggactttccgcccttcttg-3'	N/A	N/A	
Luc-DT0-F	N/A	5' AAGTCCAAATTGTAAaccctagaactgtcttcgactccg-3'	N/A	N/A	
DT0-*EcoRV*-TRE3G	N/A	5'-TATGATCCTCTGGAGATccagagctttgggcagatgga-3'	N/A	N/A	
Tet-Luc-5' (Firefly Luciferase)	N/A	F: 5'-GCT ATG AAG AGA TAC GCC CTG GTT-3' R: 5'-CAA CAC CGG CAT AAA GAA TTG AAG-3'	252 nt	90.6%	
Tet-3' (Human origin)	1760	F: 5'-GCG ATC TCT GCC TGC TTA C-3' R: 5'-CGG AGG ACG AGG TCA ATA AA-3'	151 nt	94.4%	
ZsGreen	N/A	F: 5'-GTC AGC TTG TGC TGG ATG AA-3' R: 5'-CCC CGT GAT GAA GAA GAT GA-3'	210 nt	99.0%	
Mouse 45S rRNA	100861531	F: 5'-GCG TGT TGG TCT TCT GGT TTC -3' R: 5'-AAC TTT CTC ACT GAG GGC GG -3'	105 nt	95.2%	
Mouse MT-RNR1	17724 Mitochondria	F: 5'-ATT TCA TTG GCC GAC AGC TA-3' R: 5'-AGG TAG AGC GGG GTT TAT CG-3'	Sequence N/A	89.7%	(Zhang et al., 2014)
Mouse XRN1	24127	F: 5'-GCC AAG TAA GAA GCT GAC ATG C-3' R: 5'-TGT CCA CCG ATG CCA CAT TT-3'	77 nt	106.9%	
Mouse RRP6	50912	F: 5'-CCG ATG CAG ACA GCT TCG TA-3' R: 5'-CCT GGA AGG CAG GGA AAC TT-3'	123 nt	97.1%	
Mouse H19	14955	F: 5'-AGG TAT CGG ACT CCA GAG GG-3' R: 5'-CAG TGC CTC ATG GGA ATG GT-3'	86 nt	94%	
Mouse MyoD	17927	F: 5'-TGG GAT ATG GAG CTT CTA TCG C-3' R: 5'-GGT GAG TCG AAA CAC GGA TCA T-3'	119 nt	107.1%	
Human/mouse GAPDH	14433	F: 5'-TCA CCA CCA TGG AGA AGG-3' R: 5'-GCT AAG CAG TTG GTG GTG CA-3'	169 nt	90.3%	
Human DMPK 5'	1760	F: 5'-GGA CCT TGA CTT CTG AGA GGC-3' R: 5'-AGC CCA TCT CTC AGT CCT CC-3'	87 nt		ddPCR primers
Human DMPK 3'	1760	F: 5'-GCG ATC TCT GCC TGC TTA CT-3' R: 5'-CGG AGG ACG AGG TCA ATA AA-3'	151 nt		ddPCR primers
Human 45S rRNA	100861532	F: 5'-GAA CGG TGG TGT GTC GTT-3' R: 5'-GCG TCT CGT CTC GTC TCA CT-3'	130 nt	91.0%	
Human $tRNA^{Tyr}$	100009601	F: 5'-CCT TCG ATA GCT CAG CTG GTA GAG CGG AGG-3' R: 5'-CGG AAT CGG AAC CAG CGA CCT AAG GAT GTC C-3'	84 nt	102.7%	

nt: nucleotide

and negative populations using the QX200™ Droplet Reader (Bio-Rad #1864003). The copy number of the mRNA of interest was derived via QuantaSoft™ software (provided with QX200™ droplet reader) which applies a Poisson distribution to infer the number of copies of template cDNA per µl of sample.

2.2.5 Measuring mRNA half-life

2.2.5.1 Doxycycline shut-off

CUG0 and CUG700 cells were transfected with pTET-OFF and grown in 60 mm dishes for 24 hours to 70% confluency. Transcription of both ZsGreen and Luciferase was shut off by treating cells with 1 µg/ml doxycycline (DOX; Clontech #631311). Cells were collected 0, 1, 2, and 4hr after DOX addition and RNA was extracted and assessed by qRT-PCR or northern blot. The abundance of the luciferase reporter at each timepoint was normalized to mGAPDH mRNA abundance (qRT-PCR) or the abundance of a non-specific band detected by the CAG-linker probe (northern). The mRNA abundances were plotted to provide a slope (k) of the exponential curve, which was used to derive a half-life based on the equation below.

$$t_{1/2} = \frac{\ln(0.5)}{k}$$

Experiments with Actinomycin D (ActD; Sigma #A9415-2MG) were performed as described above, but global transcription was first shut off by treating cells with 8 µg/ml ActD (diluted in DMSO) for 30min prior to adding doxycycline and cells were collected 0, 2, 4, and 8 hours after DOX addition.

2.2.5.2 4sU labeling

Control and patient myoblasts were cultured to 70% confluency in 100 mm dishes. 4sU (Sigma #T4509) was added to the cells at a final concentration of 400 μM (diluted from a 100 mM stock) for 4 hours. At the end of the labeling period, the media was removed and total RNA was extracted as previously described. Biotinylation was accomplished with biotinylation buffer (100mM HEPES [pH 7.5], 10mM EDTA) and 10 ml MTSEA-biotin-XX (1 mg/mL dissolved in dimethylformamide; Biotium #90066) and nascent and pre-existing fractions were separated with a streptavidin magnetic bead kit (μMacs streptavidin kit; Miltenyi #130-074-101) on a magnetic stand (Miltenyi #130-042-602) as described in Russo et al., 2017.

Each fraction was resuspended in 50 μl of nuclease-free water. Then, 1 μl of RNA in each fraction was reverse transcribed in a standard reaction with a 3:1 mixture of random hexamers (Integrated DNA Technologies #51-01-18-01) and oligo$(dT)_{18}$ (Integrated DNA Technologies #51-01-15-07) as primers. After Improm II reverse transcriptase (Promega #A3800) was used to perform the reverse transcription, the abundance of specific RNAs from each fraction was determined using gene specific primers in digital PCR (dPCR) as described in 2.2.4.

The half-life of DMPK mRNA was calculated using the following equation (Rädle et al., 2013) assuming first order kinetics.

$$t_{1/2} = -t_L * \ln(2) / \ln(1 - R)$$

t_L = labeling time (minus 5 min for 4sU incorporation to begin).

R = abundance in nascent RNA fraction/abundance in total RNA fraction, normalized to R calculated for the positive control RNA.

2.2.6 Fluorescent *in situ* hybridization (FISH)

This protocol is based on Taneja et al., 1995, and modified based on Urbanek et al., 2015 and Urbanek et al., 2015.

CUG0 and CUG700 cells were transfected with pTET-OFF (Table 5) to turn on the promoter as described in 2.1.2 and plated onto coverslips in a 12-well plate.

Coverslips were washed with 1 ml PBS 24 hours after transfection. To fix the cells, the coverslips were incubated for 15 min with 4% paraformaldehyde (in PBS) at room temperature, which was followed by 10 min incubation in 1 ml methanol to permeabilize the cells. Cells were then washed with 1 ml 70% ethanol, and rehydrated with 1 ml PBS for 10 min. After incubation in prehybridization buffer (40% formamide, 2x SSC) for 10 min, cells were hybridized with 1 µl/ml 5'-/5Cy3/$(CAG)_6$-3' probe in hybridization buffer (40% formamide, 2x SSC, 0.2% BSA) for two hours at 37ºC in the dark. Two hours later, cells were washed with 40% formamide, 1x SSC for 30 min at 37ºC, and 1x SSC at room temperature for 15 min twice. After removing the excess SSC, the coverslips were mounted onto glass microscope slides using ProLong Gold Antifade Mountant with DAPI (Life Technologies #P36930) or ProLong Diamond Antifade Mountant with DAPI (Life Technologies #P36962) and allowed to cure at room temperature for 24hrs.

After sealing with clear nail polish, the cells were visualized using an Olympus IX71 inverted fluorescent microscope at 100X magnification using the 31000 DAPI/Hoechst filter (EX360, EM460) for DAPI and the 41002 TRITC (Rhodamine)/Cy3 filter (EX535,

EM610) for Cy3. Images were captured using a digital camera (Q Imaging Retiga 2000R) and analyzed using SlideBook 4.0 (Intelligent Imaging Innovations).

2.2.7 Northern blotting

2.2.7.1 Electrophoresis, blotting and hybridization

30 µg of total RNA was resolved on a 1% formaldehyde agarose gel (15 ml 1x MOPS buffer and 25.5 ml 37% formaldehyde in a total volume of 250 ml) at 80V for 5 hours at room temperature. The gel was treated with 0.05N NaOH for 20 min to break down the phosphate backbone of RNA for easier transfer and washed with 20x SSC for 40 min before capillary transfer to a Hybond-XL nylon membrane in 10x SSC overnight at room temperature. Nucleic acids were immobilized by UV-crosslinking.

Membranes were pre-washed in 1x SSC, 1% SDS at 60ºC for 1 hour and pre-hybridized in 0.45 µm filtered hybridization buffer (250 mM Na_2HPO_4 pH 7.5, 7% SDS, 1 mM EDTA and 1% BSA) at 55°C for 1 hour. Membranes were then hybridized to probe with CAG-linker overnight at 55ºC in the hybridization buffer. Blots were washed twice with 2x SSC, 0.1% SDS for 5 min at room temperature, and once with 0.5x SSC, 0.5% SDS for 20 min at room temperature. Membranes were exposed to storage phosphor screens and imaged on the Typhoon Trio Imager (GE Healthcare) which was analyzed using Image Quant software (GE Healthcare).

2.2.7.2 Generation of γ^{32}P-labeled probe

To 5’ end label a probe, a 50 µl reaction with 100 ng or 1 µl of 100 nM oligonucleotides (we used CAG-linker probe: 5'-$(CAG)_2$TCGAG$(CAG)_4$-3'), 5 µl T4 PNK buffer, 1 µl γ^{32}P-ATP (PerkinElmer), and 2 µl T4 PNK (New England Biolabs #M0201S) was incubated

at 37°C for 30-60 min. Unincorporated ATPs were removed with a Microspin™ G-25 column (GE healthcare #27-5325-01). 1 µl was evaluated using a liquid scintillation counter. The entire reaction was added to 5 ml hybridization buffer and filtered (0.45 µm) to remove debris before adding to the blot.

2.2.8 Cytoplasmic and nuclear cell fractionation

Detergent-based subcellular fractionation was used to separate nuclear and cytoplasmic cellular fractions based on a previously published protocol (Weil et al., 2000). Cells were cultured to 70% confluency and scraped into cold PBS in 15 ml. The tubes were centrifuged at 500 x g for 5 min and the supernatant was discarded before addition of 1ml of NP-40 lysis buffer (0.5% V/V NP-40, 10 mM Tris-HCl pH 8.5, 1.5 mM MgCl2, 10 mM EDTA, 140 mM NaCl). The cells were incubated on ice for 20 min and a small amount was stained with trypan blue to verify adequate cell lysis under a microscope. The nuclei were pelleted by centrifugation for 5 min at 500 x g at 4°C. The cytoplasmic supernatant was removed carefully from the pellet and placed in a new tube. The nuclear pellet was washed twice with 500 µl of NP-40 lysis buffer to remove any remaining cytoplasmic fractions with the first wash saved and added to the cytoplasmic fraction. Equivalent amount of TRIzol® was added to the cytoplasmic fraction, and 500 µl of TRIzol® was added to the nuclear pellet. The nuclear and cytoplasmic RNA pellets were each resuspended in an equal volume of nuclease-free water. 1 µg of RNA of the cytoplasmic fraction and equal volume of the nuclear fraction were subjected to qRT-PCR as described in 2.2.2 and 2.2.3. The relative abundance of each transcript in each fraction was determined and the percentage of each transcript in the nuclear fraction was then determined and graphed.

2.3 Protein preparation and assays

2.3.1 Protein knockdown

Expression of RNA decay factors and RNA binding proteins was reduced through transfection of shRNA-encoding plasmids or siRNAs at the time of pTET-OFF transfection, see 2.1.2 for transfection and Table 5 for list of shRNA and siRNA. Following transfection, knockdown was evaluated by qRT-PCR (XRN1, RRP6) or by western blot (all other factors).

2.3.2 The TRIzol® protein extraction method

After 24-48 hours of incubation following transfection with siRNAs or shRNA plasmids, cells in 60 mm dishes were collected into 500 µl TRIzol®, mixed with 100 µl of chloroform and centrifuged for 10 min at 4°C after mixing with 100 µl of chloroform. The organic phase containing proteins was combined with 150 µl 100% ethanol, incubated for 2-3 min and centrifuged at 2,000 x g for 5 min. The supernatant was transferred to a fresh tube and 750 µl isopropanol was added and incubated for 10 min before centrifugation at 12,000 x g for 10min. The pellet was washed three times by breaking down the pellet in wash buffer (0.3M guanidine hydrochloride in 95% ethanol) and incubating for 20 min before centrifugation at 7,500 x g for 5 min. Finally, the pellet was washed with 1.5 ml 100% ethanol and resuspended in equal volume of 8 M Urea and 1% SDS. This protocol is adapted according to the manufacturer's user guide.

2.3.3 Western blot analysis

To determine the total protein concentration, the Pierce™ BCA Protein Assay Kit (ThermoFisher #23225) was used according to the manufacturer's instruction. Equal amount (25-40 µg) of proteins were prepared for SDS-PAGE by adding 2x SDS protein

dye (0.5 M Tris-HCl pH 6.8, 20% glycerol, 2% SDS, 20% β-mercaptoethanol, and trace amount of bromophenol blue) and boiling at 95°C for 2-3 min. All samples in this dissertation were separated on 6% or 8% SDS-PAGE gels and transferred to 0.45 μm PVDF Immobilon®-P transfer membrane (Millipore #IPVH00010) either in 1x transfer buffer (25mM Tris base and 192 mM glycine, pH 8.3) containing 20% methanol with Trans-blot SD Semi-dry transfer cell (Bio-rad) or in 1x SDS running buffer (25 mM Tris base, 192 mM Glycine, and 3.5 mM SDS) containing 20% methanol in the wet transfer apparatus according to the protein size. Membranes were then blocked and incubated in 5% non-fat dry milk in 1x TBS and 0.05% Tween-20 (TBST) at room temperature for 1 hr or overnight at 4°C. Primary antibody was added directly to the blocking buffer and was incubated for 1 hour at room temperature or overnight at 4°C followed by three 10-min washes with 1x TBST at room temperature. Secondary antibody incubation took place for 1 hour at room temperature followed by three 10-min washes with 1x TBST at room temperature. SuperSignal West Pico Chemiluminescent Substrate (ThermoFisher #34080) was used for detection of protein abundances with a ChemiDox XRS+ System (Bio-Rad). Quantification analysis was performed using ImageLab3.0 software (Bio-Rad). Antibodies used are listed below in Table 7.

2.3.4 Immunofluorescence microscopy

This protocol was created with help from Dr. David G. Maranon.

CUG0 and CUG700 cells were transfected with pTET-OFF and grown on coverslips in a 12-well plate for 24 hours. After media were discarded, the coverslips were washed with cold 1x PBS. The cells were fixed and permeabilized with 1 ml cold 100% methanol (stored at -20°C) for 10 min at room temperature, followed by three 1x PBS washes.

The coverslips were incubated in 1x PBS at 4°C overnight. The coverslips were incubated in blocking buffer (5% BSA in 1x PBS) for 30min at room temperature. Primary antibodies were added to the blocking buffer and incubated for 1 hour at room temperature, followed by two 3-min warm 1x PBS (37°C). Secondary labeling took place for 1 hour at room temperature followed by two 3-min warm 1x PBS (37°C). After removing the excess PBS, the coverslips were mounted onto glass microscope slides using ProLong Gold Antifade Moutant with DAPI (Life Technologies #P36930) or ProLong Diamond Antifade Mountant with DAPI (Life Technologies #P36962) and allowed to cure at room temperature for 24hrs. After sealing with clear nail polish, the cells were visualized.

The MBNL1 immunofluorescence microscopy slides were visualized at 63x magnification with Axio Zeiss Axio Imager.72 microscope (# 35340005343) using DAPI filter (EX4359/EM461) for DAPI and Texas red filter (EX590/EM461) for Alexa 594. Images were captured using a digital camera (CoolSNAP ES2), and analyzed using ZEN2 Blue Edition. The MBNL1 and XRN2 immunofluorescence microscopy slides were visualized with Zeiss LSM510 META laser scanning confocal microscope at 63x magnification using 405nm filter for DAPI, 532nm filter for Alexa 594 and 644nm filter for Alexa 647. The images were analyzed using ZEN 2009.

Table 7: Antibodies used in this study

Antibody Name & Target	Size	Type	Dilution	Vendor
Anti-GAPDH	~38 kDa	mouse monoclonal	1: 20,000	Millipore #MAB374
Anti-XRN2	~117 kDa	rabbit polyclonal	1: 4,000	Novus #NB100-57541
Anti-MBNL1	42 kDa	mouse monoclonal	1: 200	Santa Cruz #sc-136165
Anti-UPF1	~124 kDa	rabbit polyclonal	1: 10,000	Bethyl #A301-902A
Goat anti-mouse IgG-HRP		secondary	1: 1,000	Santa Cruz #sc-2005
Goat anti-rabbit IgG (H/L)-HRP		secondary	1: 1,000	Bio-Rad #5196-2504

Goat anti-mouse Alexa 594		fluorescent secondary	1: 1,000	Life Tech #A11032
Goat anti-mouse Alexa 647		fluorescent secondary	1: 1,000	Invitrogen #A31633
Goat anti-rabbit Alexa 647		fluorescent secondary	1: 1,000	Life Tech #A21235

2.3.5 Luciferase assay

Luciferase assay were performed with either combined ViviRen™ *in vivo* Renilla Luciferase Substrate (Promega #P1231)/ViviRen™ Live Cell Substrate (Promega #E6491) and Luciferase Assay System (Promega #E4550), or dual-luciferase reporter assay systems (Promega #E1980) using Victor™ X5 2030 Multilabel Reader (PerkinElmer). Data were analyzed with PerkinElmer 2030 workstation software. The emission filter used was D615 Europium chelate emission filter (centre wavelength 615 nm, bandwidth (full width half maximum ca 8.5 nm, maximum transmittance at peak wavelength ca 80%).

Combined ViviRen™ Substrate and Luciferase Assay System

Cells were transfected with pTET-OFF and grown in 96-well plates for 24-48 hours. To read renilla luciferase activity, after removing the media, 25 µl of diluted ViviRen™ (1: 3,000 for ViviRen™ *in vivo* Renilla Luciferase Substrate or 1: 1,000 ViviRen™ Live Cell Substrate in fresh media) was added to each well and read for 0.5 sec. With ViviRen™ Live Cell Substrate, a 2-min incubation occurred before reading. To evaluate firefly luciferase, after ViviRen™ was discarded, cells were washed with 1x PBS, and lysed with 20 µl diluted lysis buffer (1: 5 in nuclease-free water) for 10 min at room temperature. Meanwhile, injection apparatus was washed twice with nuclease-free water and filled with 5 ml of luciferase assay substrate (resuspended in luciferase assay

buffer). Wells were automatically injected with 100 µl luciferase assay substrate and shaken for 3 sec before reading each well for 0.5 sec.

CHAPTER 3: RESULTS

3.1 Mouse myoblasts expressing the DMPK 3' UTR with CUG repeats exhibit phenotypes seen in DM1 patient cells

3.1.1 Overview of luciferase reporters bearing the human 3' UTR

The goal of this project was to bridge the gap in our understanding of the decay of DMPK mRNA by determining where and how the wild type and mutant DMPK mRNAs are degraded, what enzymes are responsible, and assessing how the CUG repeat/MBNL1 ribonucleoprotein structure affects decay. However, it remains a challenge to study the decay patterns of wild type and mutant DMPK transcripts in heterozygous DM1 patient cells where both types of transcripts exist and the only distinguishing feature is the length of the CUG repeats. We therefore first needed to develop a system where we could express and detect wild type and mutant transcripts independently and repress their transcription without affecting global gene expression.

In light of this, we generated two reporter constructs: one containing firefly luciferase fused to the human DMPK 3' UTR with the CTG repeats deleted (pTRE3G-Luc-CUG0; Figure 5A left), and another containing the same sequences but with 700 CTG repeats within the human DMPK 3' UTR (pTRE3G-Luc-CUG700; Figure 5A right). We did not include any CTG repeats in the pTRE3G-Luc-CUG0, because introduction of even 5 CTG repeats in a mouse model induces cardinal features of myotonic dystrophy (Mahadevan et al., 2006). The DMPK 3' UTR sequences were derived from plasmids pDT0 and pDT960 kindly provided by Tom Cooper (Ho et al., 2004). We included the entire DMPK 3' UTR because the 3' UTR is a primary determinant of mRNA stability for

many transcripts and also because the context of the CUG repeats within the full DMPK 3' UTR contributes to DM1 pathogenesis (Mahadevan et al., 2006; Mankodi et al., 2000; Orengo et al., 2008; Storbeck et al., 2004).

We used a bidirectional Tet-responsive promoter to allow us to turn expression both on and off at will without interfering with other cellular mechanisms while also providing a control transcript (ZsGreen, a brighter alternative to GFP) that is co-expressed and should behave similarly in both reporters.

We expressed our reporter constructs in C2C12 mouse myoblasts cells which are relatively easy to culture, can be differentiated into myotubes which more closely resemble adult muscle, and can be readily transfected (Blau et al., 1985; Yaffe and Saxel, 1997). Most importantly, this cell line has been used extensively for DM1 research and is known to recapitulate many features of DM1 upon expression of CUG repeat-containing mRNAs – for example, characteristic nuclear foci, mis-splicing events and defect in myogenesis, besides its short doubling time and satisfying transfection efficiency (Hoskins et al., 2014; Mastroyiannopoulos et al., 2005; Querido et al., 2011; Tiscornia and Mahadevan, 2000; Usuki et al., 1997). Additionally, the mouse and human DMPK gene are sufficiently divergent that the endogenous mouse DMPK transcripts can easily be distinguished from our reporter transcripts.

Generation of CUG0 and CUG700 cell lines

The cell lines were generated by transfecting pTRE3G-Luc-CUG0 and pTRE3G-Luc-CUG700 (Figure 5A) into C2C12 cells respectively, together with a Linear Puromycin Marker (Clontech #631626) plasmid. Single colonies were selected using cloning cylinders to create monoclonal cell lines. Several independent clonal cell

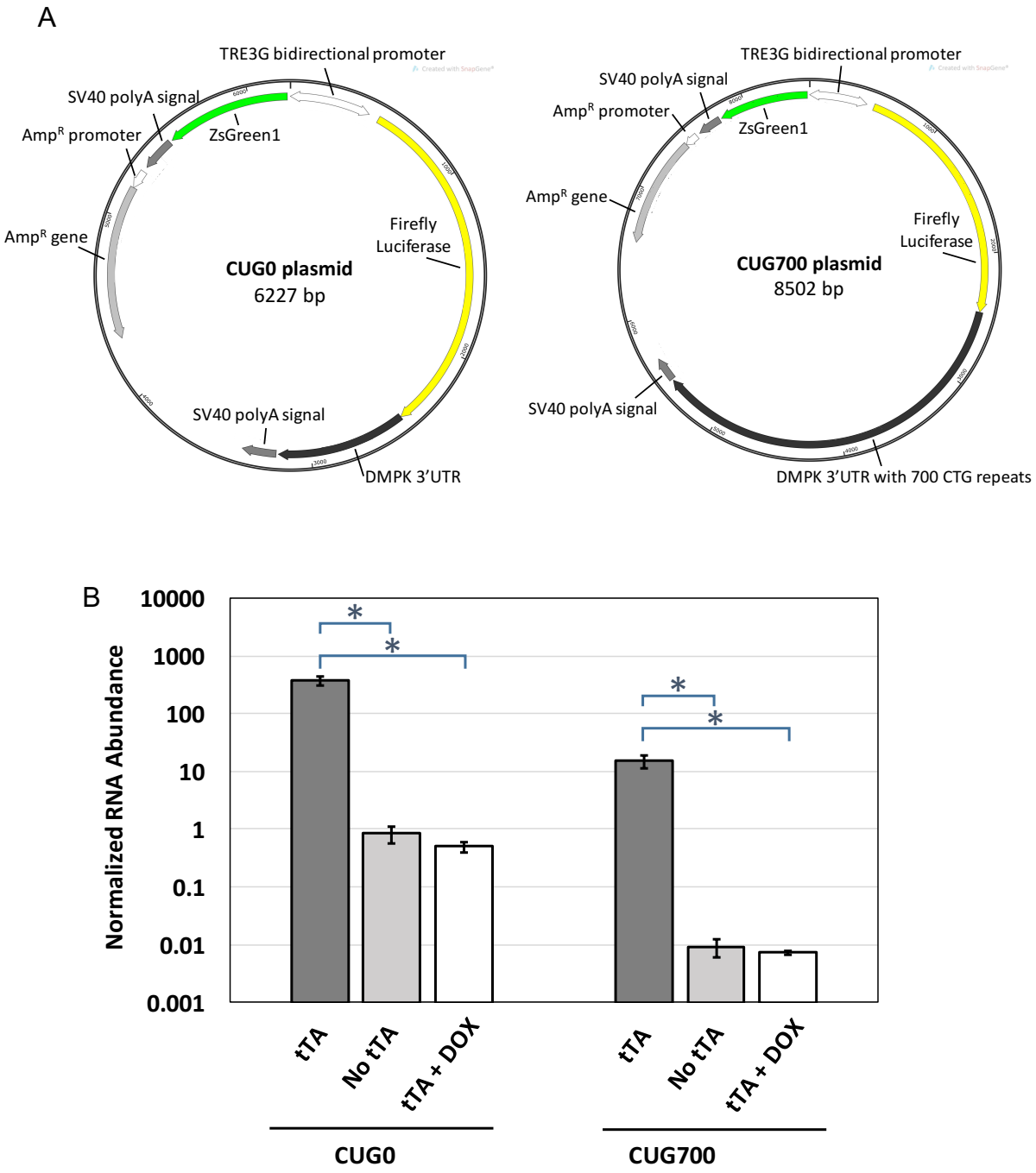

Figure 5: CUG0 and CUG700 cell lines exhibit tight regulation of expression of reporter mRNA in response to DOX. A. Maps of reporter constructs. B. Both CUG0 and CUG700 cells were transfected with pTET-OFF, or transfection reagents alone, or pTET-OFF in the presence of 1 µg/ml DOX. RNA was isolated 24 hours later and expression of luciferase was evaluated by qRT-PCR. Abundance of luciferase mRNA was normalized to mGAPDH mRNA. Error bars represent the standard deviation of 3 biological replicates. *p<0.05 by two-tailed Student's t-test.

lines were screened visually for the expression of ZsGreen, and then selected based on their resistance to puromycin. Importantly, these stable cell lines show minimal expression of the transgene in the absence of the tetracycline transactivator (Figure 5B) allowing them to be cultured without experiencing toxicity due to the repeat containing mRNAs. As transcription can also influence repeat stability (Harley et al., 1992; Harper et al., 1992; Hunter et al., 1992), keeping the transgene in a repressed state also minimizes the opportunities for repeat contraction and expansion over time.

The TRE3G promoter can be specifically turned on by transfection of a plasmid (pTET-OFF) encoding the tetracycline transactivator (tTA) and transfection efficiency can be readily monitored by evaluating ZsGreen expression microscopically. Conversely, addition of doxycycline (DOX) inactivates tTA to rapidly turn off transgene expression with negligible effect on other aspects of cell metabolism (Wishart et al., 2005).

CUG cell lines demonstrate regulated expression in response to DOX

In order to evaluate regulation of reporter mRNA expression, we measured the abundance of the reporter mRNA in response to transfection of tTA and concomitant addition of doxycycline. Cells were collected 24 hours after transfection to isolate total RNA. Total RNA was subjected to qRT-PCR using primers targeting firefly luciferase and endogenous murine GAPDH (mGAPDH) mRNA. As shown in Figure 5B, negligible amount of reporter mRNA expression was detected without tTA transfection (light gray bars). Cells transfected with tTA (darker grey bars) expressed ~450-fold more in CUG0 cells compared to without tTA transfection, and ~1600-fold more in CUG700 cells indicating that tTA transfection is efficient at turning on the promoter. Additionally, cells transfected with tTA in the presence of DOX (white bars) also expressed negligible

amount of reporter mRNA, indicating that our tet-responsive promoter can be readily shut off upon DOX addition. Above all, this demonstrates regulated expression of the reporter in response to DOX.

We noted that the abundance of the reporter mRNA was ~20-fold higher in the CUG0 cell line than in the CUG700 cell line (Figure 5B). This could be due to the site of integration of the CUG0 and CUG700 plasmids, or could reflect chromatin repression in the CUG700 cell lines as it has been reported that repeat expansion in the DMPK gene represses transcription of DMPK and its neighboring genes (Brouwer et al., 2013).

The rate of decay is not likely to be heavily dependent on the abundance, so the difference in expression level is not a major concern. Assessment of mRNA decay requires collecting cells at different time points after transcription inhibition and comparing the mRNA abundance at each time point to that at time 0 within the same cell line. Therefore, it is possible to draw a direct comparison of half-lives between cell lines without requiring that the transcripts are expressed at the same level.

The CUG700 reporter mRNA accumulates in foci and sequesters MBNL1 protein

Before initiating experiments to evaluate decay of the DMPK mRNA, we first needed to establish that the luciferase reporter mRNAs behaved the same way as the DMPK mRNA in patient cells. The primary unique property of repeat-containing DMPK mRNA is accumulation in nuclear foci (Davis et al., 1997; Taneja et al., 1995). We therefore used fluorescence *in situ* hybridization (FISH) with Cy-3 labeled $(CAG)_6$ probe to assess the subcellular localization of the CUG700 mRNA in our cell lines. Characteristic nuclear RNA foci were detected in the CUG700 cells (Figure 6 top). As expected, there is no

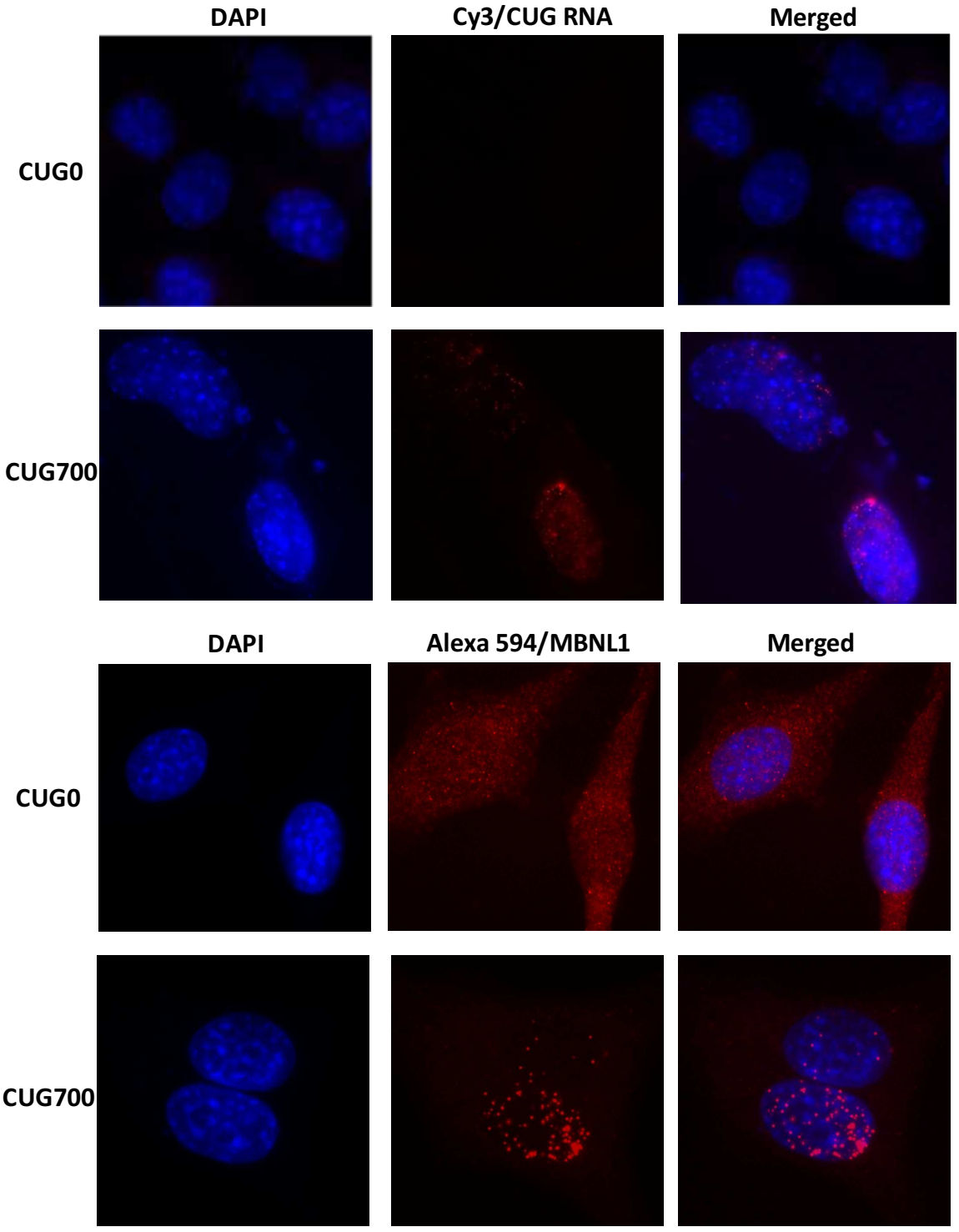

Figure 6: CUG700 mRNA accumulates in nuclear foci and induces sequestration of MBNL1 proteins. Fluorescent *in situ* hybridization (FISH) and immunofluorescence was carried out on activated CUG0 and CUG700 cells to examine DMPK mRNA (probe: 5'-Cy3/$(CAG)_6$-3') and MBNL1 protein expression pattern. DAPI was used to visualize the nucleus.

foci signal in CUG0 cells (Figure 6 top) as neither the endogenous mouse DMPK gene or the human DMPK 3' UTR has any CTG repeat. Another characteristic of DM1 cells is the accumulation of MBNL1 proteins in nuclear foci (Mankodi et al., 2001). MBNL1 was detected in fixed cells via immunofluorescence microscopy. In the CUG0 cell line, MBNL1 protein is distributed throughout the nucleus and cytoplasm (Figure 6 bottom), as reported previously (Kino et al., 2014). However, in the CUG700 cell line, MBNL1 accumulates in nucleus foci, similar to those seen in DM1 (Figure 6 bottom).

3.1.2 Both CUG0 and CUG700 transcripts are predominantly nuclear

In order to assess more quantitatively what proportion of the CUG700 mRNA is retained in the nucleus, we adopted a detergent-based subcellular fractionation method to separate the nuclear and cytoplasmic fractions in CUG0 and CUG700 cells following transfection with pTET-OFF (see MATERIALS & METHODS 2.1.4). We extracted total RNA from each fraction and resuspended the RNA from each fraction in an equal volume. Effective separation of nucleus and cytoplasm was verified by assessing the partition of 45S pre-rRNA (primarily nuclear), and MT-RNR1 (mitochondria-encoded rRNA, cytoplasmic). The relative amount of reporter mRNA in the nucleus and cytoplasm was determined by qRT-PCR.

As expected, the CUG700 reporter mRNA is 93.4 ± 5.9% nuclear (white bar in Figure 7A), which recapitulates the phenotype reported previously (Davis et al., 1997; Taneja et al., 1995) It is not clear whether all the nuclear reporter mRNA is in foci or not(Ho et al., 2005b). To our surprise, the reporter mRNA in the CUG0 cells also appeared to be predominantly nuclear (88.7% ± 6.0%). ZsGreen mRNA from both

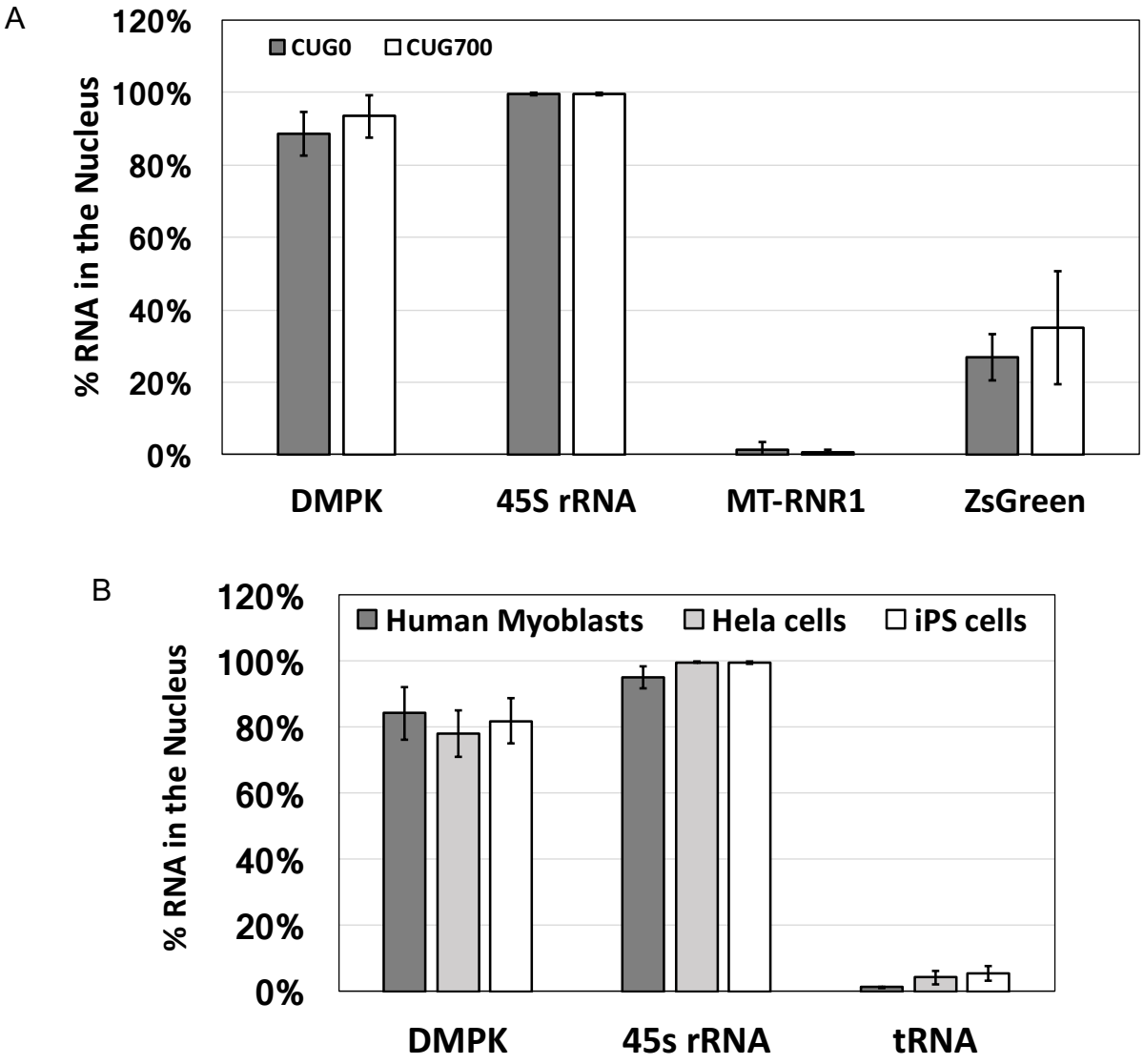

Figure 7: Both CUG0 and CUG700 reporter mRNAs are mostly nuclear. A. Detergent-based subcellular fractionation was used to separate nuclear and cytoplasmic cellular fractions in CUG0 and CUG700 cells. 45S rRNA=nuclear control, tRNA=cytoplasmic control. Error bars represent standard deviation of three biological replicates. B. Cell fractionation in normal human myoblasts (MB-C), HeLa cells, and iPS cells to show natural DMPK mRNA localization. Error bars represent standard deviation of two (human myoblasts) or three (the rest) biological replicates.

CUG0 and CUG700 cells are mostly cytoplasmic which showed that the nuclear localization is not due to over expression of transcripts from the tet-responsive promoter. In order to rule out that this was due to aberrant export or processing of our reporter transcript, perhaps due to the fact that it lacks introns, we assessed localization of endogenous DMPK mRNAs in human cell lines. We performed nuclear/cytoplasmic fractionation experiments in the same manner with three human cell lines: normal human myoblasts (MB-C), HeLa cells, and induced pluripotent stem (iPS) cells. The localization of DMPK mRNA in all three cell lines agreed with our observations in the reporter cell line, which confirms that wild type DMPK mRNA resides mostly in the nucleus (Figure 7B). This finding is also supported by a recent report from the Wansink lab (Gudde et al., 2017a). Nuclear retention may be achieved by slow export and/or rapid decay in the cytoplasm. This could facilitate controlled expression of DMPK protein, as overexpression of DMPK protein is destructive to mitochondria clustering and cell viability (Oude Ophuis et al., 2009).

3.1.3 Only the CUG0 reporter mRNA gets translated efficiently

The fact that both CUG0 and CUG700 reporters are primarily nuclear would suggest that neither one can be translated, although previous studies clearly show that normal DMPK mRNA is translated to produce protein (Davis et al., 1997; Smith et al., 2007) and that the mutant transcript can be detected in the cytoplasm (Dansithong et al., 2008; Jones et al., 2015). Therefore, we performed luciferase assays to determine whether they are translated. For this experiment, we transfected pTET-OFF as before, along with a Renilla luciferase (RLuc) plasmid to control for variation in transfection efficiency. The activity of both firefly luciferase (FLuc) and the co-transfected RLuc was

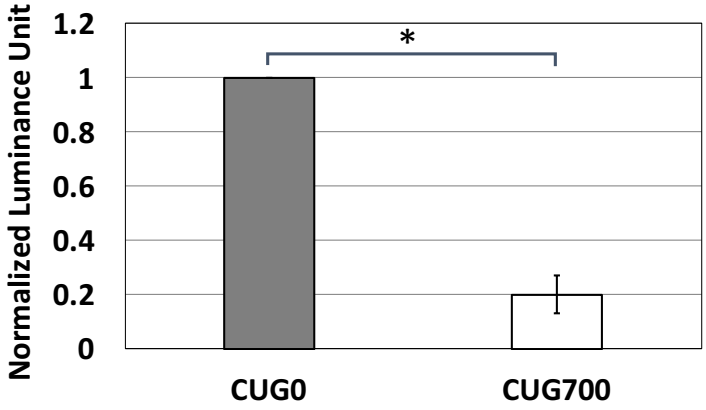

Figure 8: Only CUG0 reporter mRNA gets translated efficiently.
Luciferase assays were performed to measure the translation of reporter mRNAs in CUG0 and CUG700 cells. Error bars represent standard deviation of three biological replicates. *$p<0.05$ compared to CUG0 samples by two-tailed Student's t-test.

measured. In addition, the abundance of FLuc reporter transcript was assessed by qRT-PCR. FLuc activity was normalized to both the activity of RLuc (to control for transfection efficiency) and the level of total FLuc mRNA (to control for differences in mRNA abundance between the two reporters). Of note, the proportion of each population of reporter mRNA that is in the cytoplasm is similar between CUG0 and CUG700 cells, as there are 11.3 ± 6.0% of reporter mRNA in the CUG0 cells and 6.6 ± 5.9% of reporter transcripts in the CUG700 cells (Figure 7A). Despite being predominantly nuclear, the CUG0 mRNA is efficiently translated (Figure 8). This may indicate that the CUG0 mRNA is degraded soon after translation.

The CUG700 transcript, however, produced ~5-fold less protein per mRNA than the CUG0 construct (Figure 8). While this could be due to failure to export (Holt et al., 2007; Koch and Leffert, 1998; Smith et al., 2007), it could be explained by inefficient translation and/or mRNA could be targeted for nonsense-mediated decay (NMD). The extended distance between the stop codon and the poly(A) signal in mutant transcript caused by the CUG repeat expansion may render it to be targeted by NMD (Amrani et al., 2004; Bühler et al., 2006).

Taken together our results demonstrate that our cell lines recapitulate the basic phenotypes shown in normal and DM1 patient and validate their use as a model to study DMPK mRNA decay: CUG700 cells exhibit characteristic nuclear RNA foci and MBNL1 foci, both CUG0 and CUG700 transcripts exhibit nuclear localization, and the repeat-containing mRNA is inefficiently translated.

3.2 Both CUG0 and CUG700 reporter mRNAs are surprisingly unstable

It was previously reported that both wild type and mutant DMPK mRNAs are very stable (half-life of 9-17 hours) and the mutant DMPK mRNA foci dissolve ~15hrs following inhibition of transcription via Actinomycin D (ActD; Davis et al., 1997; Holt et al., 2007; Krahe et al., 1995; Langlois et al., 2003b).

In order to evaluate the half-life of our reporter mRNAs, both CUG0 and CUG700 cells were transfected with pTET-OFF to induce expression. After 24 hours, DOX was added to shut-off transcription. Cells were collected 0, 1, 2, and 4 hours after DOX addition. RNA was isolated and then qRT-PCR was performed to measure RNA abundance. The reporter mRNA abundances were normalized to the abundance of endogenous mGAPDH mRNA and plotted over time to generate a half-life. Both the CUG0 and CUG700 mRNAs degraded rapidly with first order exponential decay kinetics (Figure 9). The short half-lives of just over one hour indicate these transcripts are surprisingly unstable; for comparison the median half-life of mRNAs in C2C12 cells is 2.9 hours (Lee et al., 2010).

Considering that ActD is notorious for interfering with cell metabolism as a global transcription inhibitor (Bansal et al., 1991; Ljungman et al., 1999), and that it inserts preferentially at CTG repeats to affect transcription of the mutant DMPK mRNA (Siboni et al., 2015), we suspected that ActD treatment in previous studies may have interfered with the natural decay of the transcript. In order to evaluate this possibility, we measured reporter mRNA half-lives in the presence of both DOX and ActD.

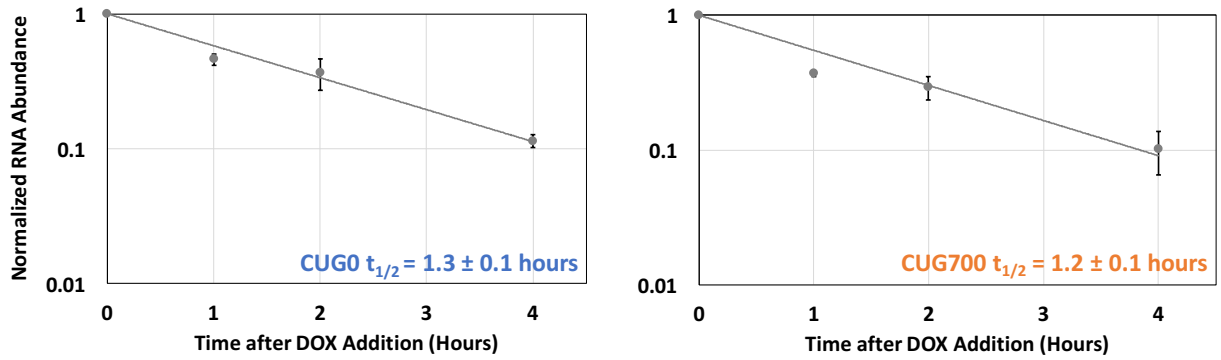

Figure 9: Both CUG0 and CUG700 mRNAs are unstable. Both CUG0 and CUG700 cells were collected 0, 1, 2, and 4hrs after DOX treatment, RNA was isolated and then qRT-PCR was performed to measure RNA abundance. The reporter mRNA abundances were normalized to mGAPDH and plotted over time. Error bars on both the graph and the half-life represent standard deviation of three biological replicates. There is no statistical difference in half-life between CUG0 and CUG700 reporter mRNAs by two-tailed Student's t-test.

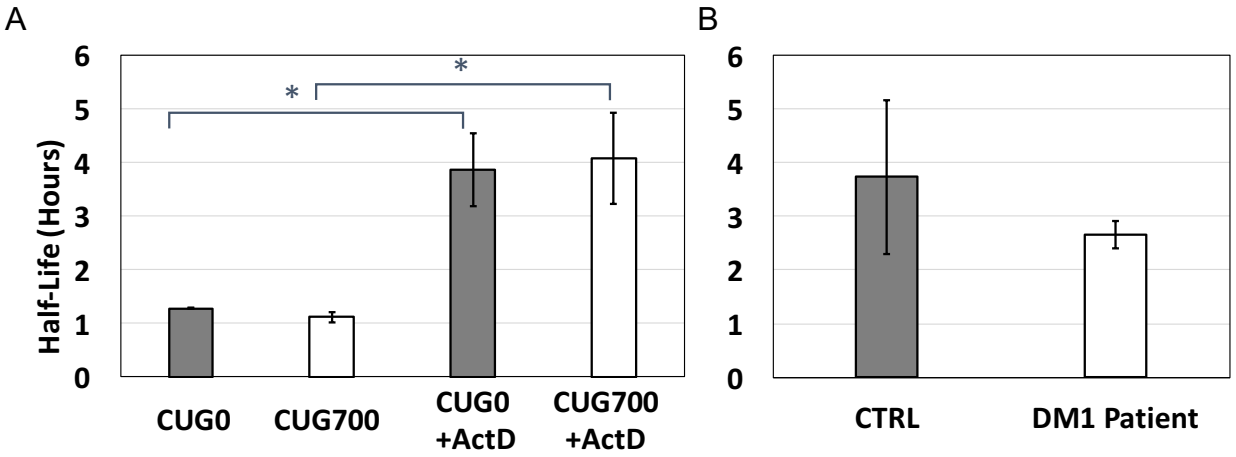

Figure 10: ActD treatment stabilizes CUG0 and CUG700 mRNAs. A. Graph showing DMPK mRNA half-lives using DOX or DOX + ActD to shut off transcription measured by qRT-PCR. B. Half-lives of DMPK mRNA measured by ddPCR in Normal human myoblasts (MB-C) and DM1 patient myoblasts (MB-DM480) using metabolic labeling method by Adam M. Heck. Error bars represent standard deviation of three biological replicates. *p<0.05 compared to DOX treatment alone by two-tailed Student's t-test.

After pTET-OFF was transfected, cells were treated with ActD 30 min prior to addition of DOX. Cells were collected 0, 2, 4, and 8 hours later. Reporter mRNA half-life was assessed in the same manner as previously described.

Interestingly, both reporter transcripts are ~3 fold more stable compared to with DOX treatment alone (Figure 10A), indicating ActD treatment does indeed result in longer half-lives. Thus, previous assessments of DMPK mRNA half-life likely over-estimated stability (Davis et al., 1997; Holt et al., 2007; Krahe et al., 1995; Langlois et al., 2003b).

In order to evaluate the decay of DMPK mRNAs in a more disease relevant system, we adopted a metabolic labeling method to measure the half-life of DMPK mRNA in normal human (MB-C) and DM1 patient myoblasts (MB-DM480). This approach relies upon the isolation of nascent transcripts labeled with 4-thiouridine (4sU) and allows estimation of mRNA decay rates without interfering with transcription rates (Dölken et al., 2008; Russo et al., 2017). As predicted, the half-lives of DMPK transcripts (3.7 ± 1.4 hours in control human myoblasts, 2.7 ± 0.3 hours in DM1 patient myoblasts) were significantly shorter than those reported in DM1 patient cells (Davis et al., 1997; Krahe et al., 1995) with no significant difference between wild type and mutant transcripts (Figure 10B). Of note, this experiment does not distinguish between wild type and mutant DMPK transcripts in the DM1 patient myoblasts. The half-lives in the human myoblasts were not as short as we observed for our reporter transcripts. This discrepancy could be due to variations in mRNA decay between cell types (Lee et al., 2010; Sharova et al., 2009; Yang et al., 2003) or due to the fact that our reporters do not contain the entire DMPK mRNA sequence.

3.3 CUG0 and CUG700 transcripts are degraded in different compartments

Both reporter mRNAs reside in the nucleus, and both degrade rapidly but only the CUG0 transcripts get translated efficiently. Based on our observations, we could not distinguish whether CUG700 transcripts are exported but degraded rapidly prior to or concomitant with translation, or if they degrade in the nucleus without experiencing export. In order to evaluate how the reporter mRNAs are degraded, we knocked down the primarily cytoplasmic 5'-3' exonuclease, XRN1, by transfecting plasmid encoding XRN1 shRNA into both CUG0 and CUG700 cell lines at the same time as transfection of the transactivator. XRN1 mRNA abundance was reduced to 59.3 ± 25.9% compared to control for CUG0 cells and 55.5 ± 12.6% for CUG700 cells (Figure 11A) as verified by qRT-PCR. We were unable to find any commercially available antibodies to reliably detect mouse XRN1 protein. Cells were treated with DOX to shut off transcription 48 hours after transfection. Total RNA was extracted 0, 1, 2, and 4 hours after doxycycline addition to generate a half-life for the reporter transcripts. As expected for a normal transcript, CUG0 reporter mRNAs were stabilized to 2.1 ± 0.2 hours after XRN1 knockdown, but the half-life of CUG700 reporter transcripts was unaffected (Figure 11D), indicating that the predominantly cytoplasmic exonuclease XRN1 degrades wild type CUG0 reporter mRNA but is not targeting mutant CUG700 reporter mRNA.

In the same manner, we knocked down the predominantly nuclear 5' → 3' exonuclease, XRN2. The XRN2 protein was depleted to 42% ± 3% for CUG0 cells and 36% ± 13% for CUG700 cells as measured via western blot (Figure 11B&C). In this case, the half-life of the CUG0 reporter mRNA was unchanged, while the CUG700 reporter transcripts were significantly stabilized to 2.2 ± 0.1 hours (Figure 11D). This indicates that the

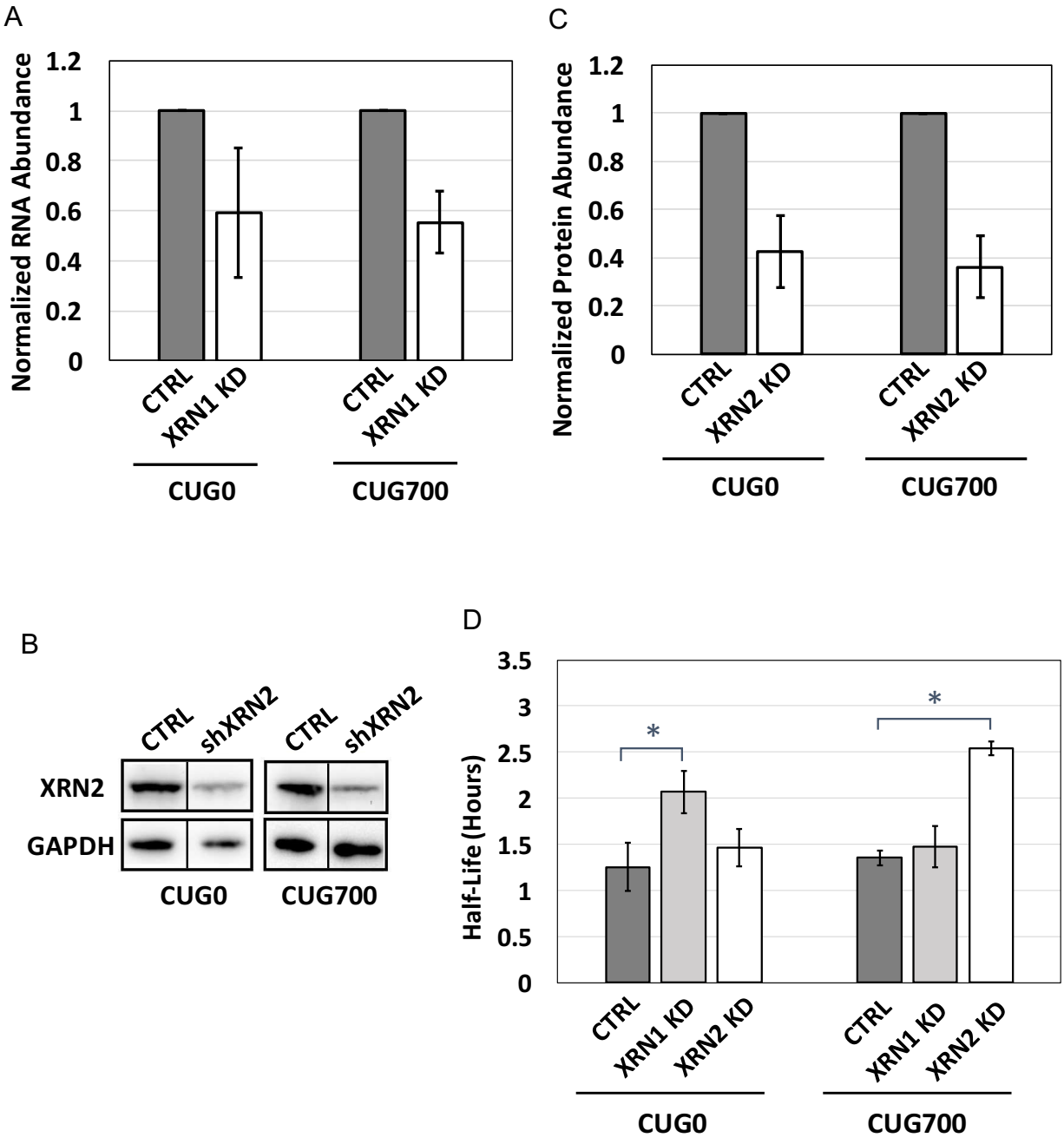

Figure 11: CUG0 mRNAs are degraded in the cytoplasm by XRN1 while repeat-containing transcripts are decayed in the nucleus by XRN2. A. XRN1 mRNA abundance was assessed by qRT-PCR and normalized to mGAPDH. B. XRN2 KD protein abundance was assessed by western blot. C. Quantification of western blot. D. CUG0 and CUG700 cells are transfected with XRN2 shRNA for 48hrs before DOX was added. Cells were collected 0, 1, 2, and 4hours after DOX addition to generate total RNA for half-life analysis by qRT-PCR. Error bars represent standard deviation of 3 biological replicates. *$p<0.05$ compared to CTRL (pLKO.1) by two-tailed Student's t-test.

predominantly nuclear exonuclease XRN2 decays the CUG700 reporter mRNA, but not the CUG0 reporter mRNAs. Therefore, we concluded that even though both reporter transcripts are predominantly nuclear, the CUG0 mRNAs are degraded in the cytoplasm by XRN1, while repeat-containing transcripts are decayed by XRN2 in the nucleus. This is consistent with our observation and previous findings that repeat-containing transcripts are mostly nuclear (Davis et al., 1997; Gudde et al., 2017a; Taneja et al., 1995).

3.4 The 3' end of CUG700 transcripts is more stable than the 5' end suggesting a limitation of XRN2 processivity

The complex structure of the CUG-repeat is reminiscent of G- or GC-rich RNA structures found in viral RNAs that impede processing by the 5' → 3' decay exonuclease XRN1 (Chapman et al., 2014b; Moon et al., 2013, 2015). Furthermore, recent studies have suggested that artificial association of RNA binding proteins with repeated regions can also block XRN1-mediated decay (Garcia and Parker, 2015; Heinrich et al., 2017). Therefore we hypothesized that the extensive CUG repeat structure either on it's own, or in association with MBNL1 proteins, may slow or block XRN2 and allow the toxic CUG repeats and sequences 3' of them to persist. The primers used to assess the reporter mRNA abundance so far bind to the luciferase transcript upstream of the expanded CUG repeats. Thus, we had no knowledge of the half-life of the repeat itself or the region downstream of the repeat.

We therefore measured the half-life of the RNA region downstream of the repeats using a different set of primers (3' primers; Figure 12A). As expected, there was no difference in half-life between the 5' and 3' of the reporter mRNA in CUG0 cells. This indicates that

the 5’ → 3’ exonuclease XRN1 is able to degrade the transcript without delay. Excitingly, the 3’ end of the repeat-containing transcripts is significantly more stable than the 5’ end (Figure 12B), indicating a limitation of XRN2 processivity. This suggests that XRN2 either is dramatically slowed by the CUG repeats or completely fails to digest them. In the latter case, another enzyme would need to be recruited to decay the repeat region and the 3’ end. Notably, although it decays more slowly than the 5’ end, the 3’ region is still degraded relatively rapidly, with a ~2 hr half-life (Figure 12B).

Next, we examined if this phenomenon also exists in DM1 patient myoblasts. We labeled the control and DM1 patient myoblasts with 4sU, and measured the 5’ and 3’ end half-life via dRT-PCR (see Materials and Methods 2.2.4). As expected, there is no difference in half-life between the 5’ and 3’ wild type DMPK mRNAs in the control human myoblasts (MB-C; Figure 13).

Interestingly, the 3’ end of the DMPK transcripts in the DM1 patient cells trends towards being more stable than the 5’ end, although the difference is not statistically significant ($p=0.07$). Here we meet the technical difficulty of being unable to differentiate wild type and mutant DMPK mRNAs in patient cells using PCR based approaches. Since both wild type and mutant DMPK transcripts exist in DM1 patient cells, increased stability of the 3’ end of the mutant DMPK mRNA may be obscured by the more rapid decay of the wild-type 3’ end.

Decay of the 3’ end of the CUG700 mRNA is not dependent on XRN2

Next, we wanted to evaluate the role of the 5’ → 3’ exonuclease XRN2 in decay of the

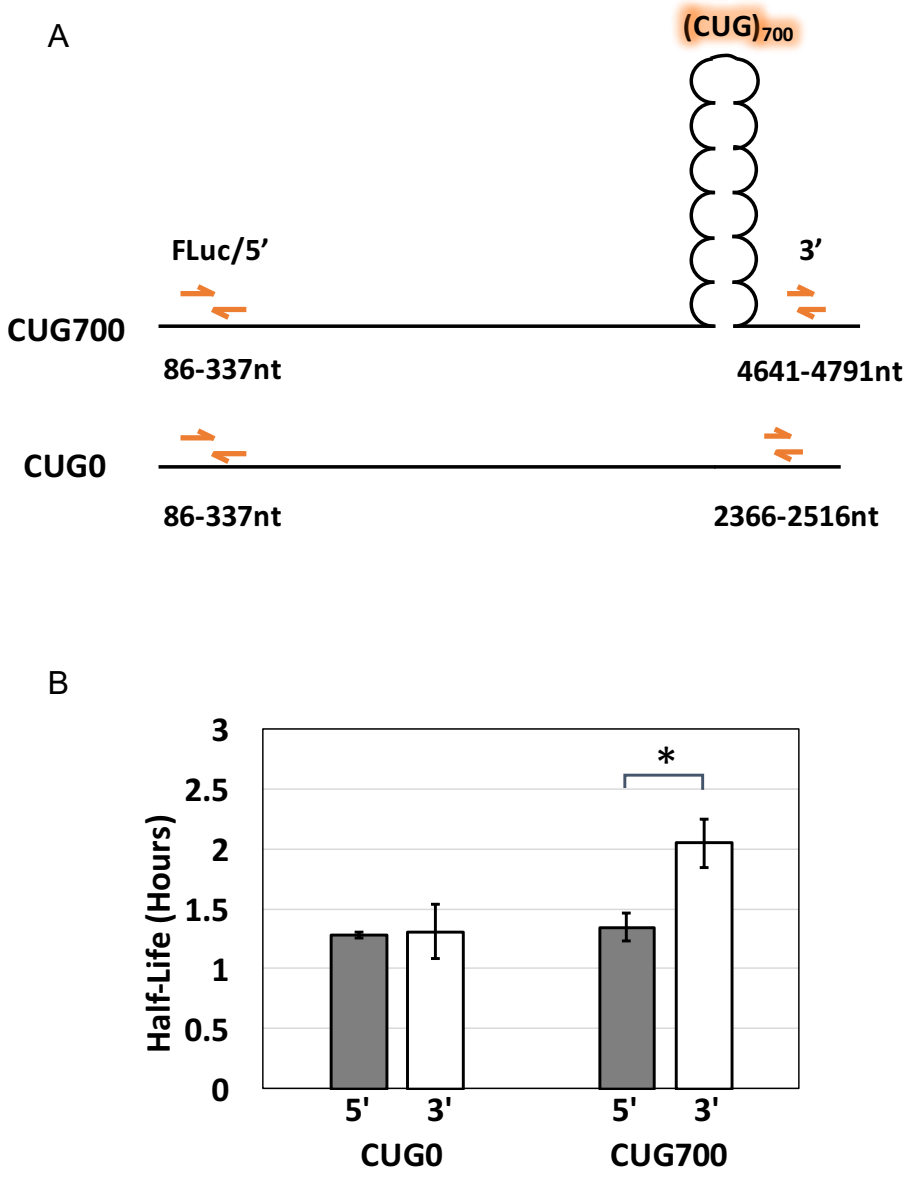

Figure 12: 3' end of the CUG700 reporter mRNA is more stable than the 5' end suggesting a limitation of XRN2 processivity. A. Two primers were designed, one to amplify a region upstream of the CUG repeats (FLuc/5') and one to detect the region 3' of the repeats (3'). B. RNA was extracted from cells 0, 1, 2, and 4hr post DOX addition for half-life analysis by qRT-PCR. Error bars represent the standard deviation of 3 biological replicates. Note that the 5' data are the same with Figure 9. *p<0.05 for the half-life of the 3' end compared to the 5' end in CUG700 transcripts by two-tailed Student's t-test.

3’ end of the CUG700 transcript. To achieve this, we retested samples from the earlier XRN1 KD and XRN2 KD experiments with the 3’ primers in CUG0 and CUG700 cells (Figure 12A).

Neither end of the CUG0 mRNA was affected by depletion of XRN2 protein (Figure 14A) consistent with our earlier observation that it is degraded by the cytoplasmic 5’ → 3’ exonuclease XRN1 (Figure 11A). Interestingly, when we knocked down XRN2 in the CUG700 cells, the 3’ end of the repeat-containing transcript was not stabilized (Figure 14B). This supports the idea that XRN2 is impeded by the CUG repeat in the mutant DMPK transcripts. However, as the 3’ region is degraded at the same rate regardless of XRN2 activity, this also implies that a different enzyme, likely a 3’-5’ exonuclease such as the exosome, degrades the 3’ region and possibly the repeats themselves.

We hypothesized that XRN2 protein may be retained in the nuclear foci with MBNL1 and the repeat-containing mRNA, therefore we performed co-immunofluorescence microscopy to detect both XRN2 and MBNL1 proteins. CUG700 cells were transfected with pTET-OFF 24 hours prior to performing immunofluorescence microscopy (see Materials and Methods 2.3.4). MBNL1 protein appeared as distinct foci similar to Figure 4C. Unfortunately, it is hard to determine whether XRN2 is in foci with MBNL1 due to the distribution of XRN2 staining throughout the nucleus (Appendix A1).

The 3’ end of the mutant DMPK transcript is degraded by the nuclear exosome

In order to determine whether a 3’ → 5’ exonuclease, for example the exosome, degrades the CUG700 transcripts from the 3’ side, we knocked down RRP6, the

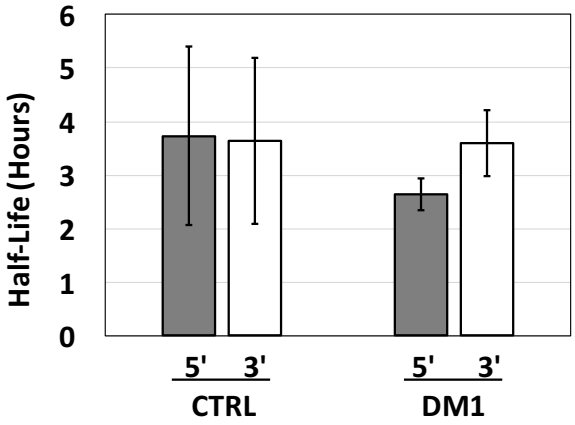

Figure 13: The 3' end of the DMPK mRNA may be more stable than the 5' end in patient cells. Normal human myoblasts (MB-C) and DM1 patient myoblasts (MB-DM480) were 4sU labeled for 4hrs prior the cell collection to extract total RNAs for generating half-life by ddPCR. Error bars represent standard deviation of three biological replicates performed by Adam Heck. Two-tailed Student's t-test showed no significant differences between the half-lives of the 5' and 3' ends in either CTRL or DM1 myoblasts.

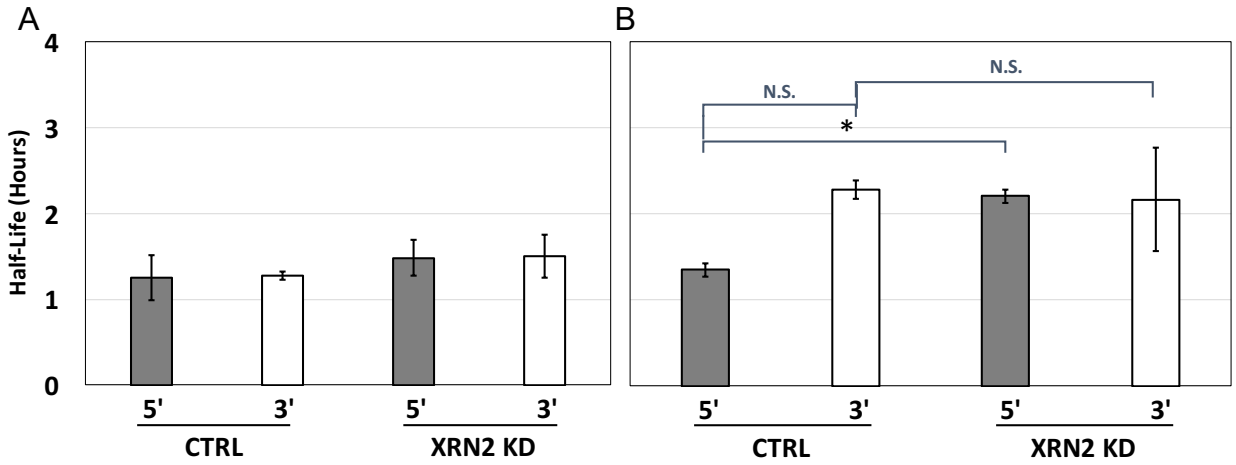

Figure 14: Depletion of XRN2 only affects the 5' end of the CUG700 RNA.
A.& B. CUG0 and CUG700 cells were transfected with XRN2 shRNA to knock down XRN2 protein. Cells were treated with DOX 48hrs after transfection and RNA was extracted 0, 1, 2, and 4hr after DOX addition. Half-lives were generated by qRT-PCR. Error bars represent standard deviation of 3 biological replicates. *$p<0.05$ compared to the 5' end in the CTRL sample by two-tailed Student's t-test.

catalytic component of nuclear exosome. We achieved this by transfecting plasmid containing RRP6 shRNA for CUG0 cells and RRP6 siRNA for CUG700 cells (see Materials and Methods 2.1.2). The RRP6 mRNA was knocked down 77.1% ± 18.7% compared to control in CUG0 cells and 85% ± 2.7% compared to control as verified by qRT-PCR (Figure 15A). Half-life of the reporter mRNA was assessed as previously described.

There was no change in half-life of either 5' or 3' end in CUG0 cells after RRP6 knockdown (Figure 15B). However, the half-life of the 3' end of the reporter mRNA is significantly elevated to 3.0 ± 0.3 hours after RRP6 knockdown compared to 2.3 ± 0.2 hours in the control group (Figure 15C), indicating that the nuclear exosome indeed degrades the CUG700 transcripts from the 3' side. Interestingly, the half-life of the 5' end of the mutant reporter mRNA is elevated to 2.0 ± 0.3 hours compared to 1.5 ± 0.4 hours in the control group (Figure 15A). However, this increase in half-life is not statistically significant (p=0.3). This indicates that the nuclear exosome may contribute to decay of the 5' end but it is not the primary factor.

3.5 The repeat region is not dramatically more stable than the flanking regions

Next, we wanted to determine the half-life of the CUG repeats. In order to measure it, we performed northern blotting with RNA from CUG0 cells at CUG700 cells (see detail in Materials and Methods 2.2.7). CUG700 cells were treated with DOX 24 hours after transfected with pTET-OFF. RNA was extracted 0, 1, 2, and 4 hours after DOX addition. RNA from CUG0 cells was extracted 24 hours after pTET-OFF transfection as control. Northern blot was performed with 5' end γ^{32}P-ATP labeled CAG with linker probe (5'-$(CAG)_2TCGAG(CAG)_4$-3'; Coonrod et al., 2013).

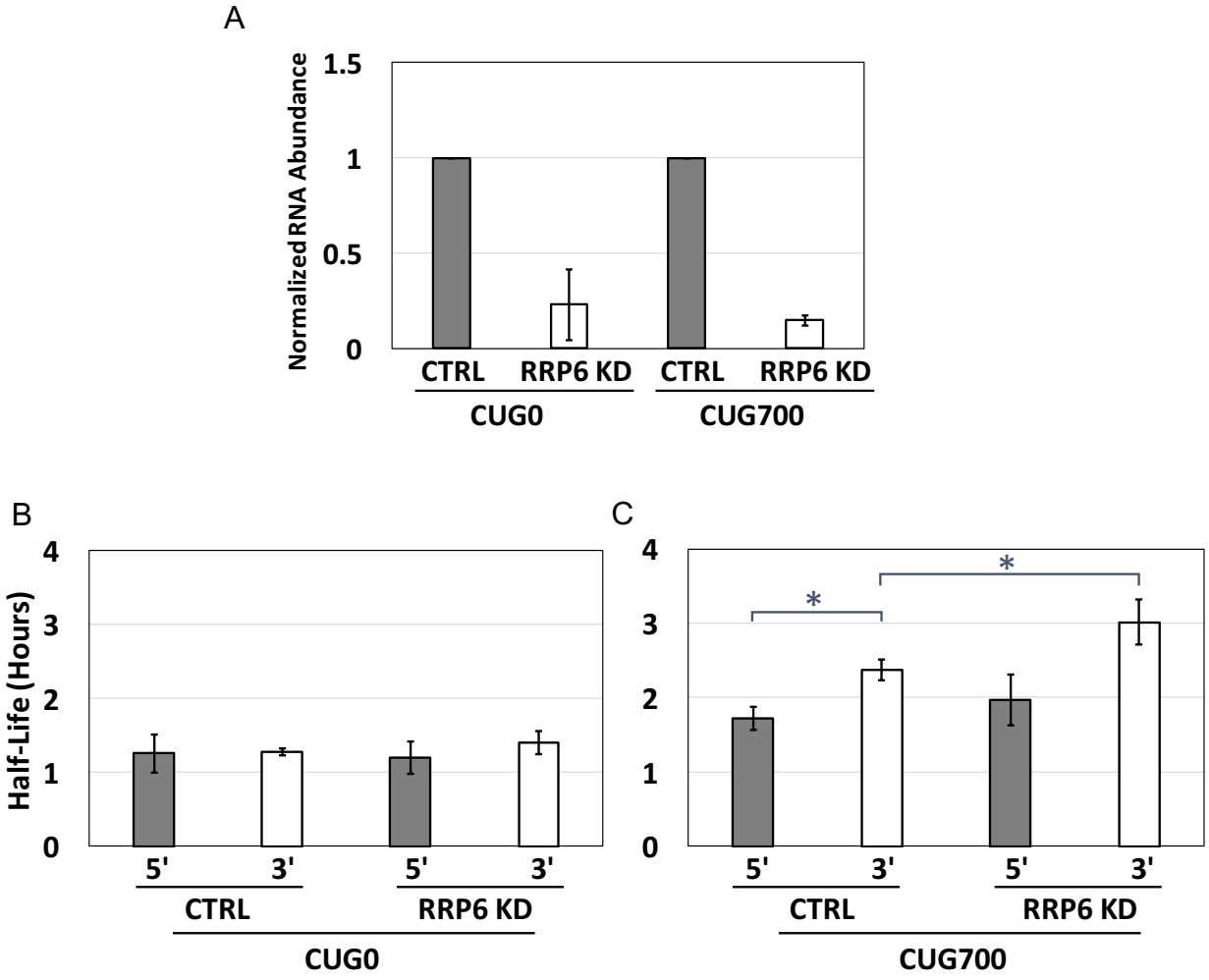

Figure 15: Only the half-life of the 3' end of the reporter mRNA is significantly elevated after RRP6 depletion. A. RRP6 mRNA abundances assessed by qRT-PCR. B. CUG0 cells were treated with DOX 48 hours after transfecting with plasmid expressing shRRP6. RNA was extracted 0, 1, 2, and 4 hours after DOX addition. RNA abundances were measured by qRT-PCR to generate a half-life. C. CUG700 cells were treated with DOX 48 hours after siRRP6 transfection. Cells were collected 0, 1, 2, and 4 hours after DOX addition to extract RNA. RNA abundances were measured by qRT-PCR to generate a half-life. Error bars represent standard deviation of 3 biological replicates. *$p<0.05$ comparing the half-lives of 5' and 3' end in CTRL samples and comparing the half-life of the 3' end of RRP6 KD samples to CTRL samples by two tailed Student's t-test.

From the northern blot, we cannot detect any CUG containing RNA in the CUG0 lane, which is expected as there is no CUG repeats in either the CUG0 reporter mRNA or the endogenous mouse DMPK mRNA (Figure 16A). We do however detect a band at ~2.7 kb in the CUG700 cells that is likely to be either intact or partially decayed CUG700 mRNA. The half-life of repeat containing mRNA in CUG700 cells is 3.0 ± 0.5 hours (Figure 16B). With the caveat that we are comparing half-life data generated using two different methods, the half-life of repeat-containing mRNA appears significantly longer than both the half-life of the 5' (1.3 ± 0.1 hours; p=0.006) and 3' (2.0 ± 0.2 hours; p=0.045). We conclude that the CUG repeats region persist in the nucleus longer than the flanking regions.

3.6 MBNL1 protein association prevents the 5' → 3' exonuclease XRN2 from accessing the 3' end of the transcript

Next, we wanted to know if the RNA structure adopted by the repeat region is sufficient to prevent XRN2 from reaching the 3' end of the transcripts or if MBNL1 protein association is required.

To study this, we depleted MBNL1 protein by transfecting plasmid expressing MBNL1 shRNA. MBNL1 protein was depleted to 27% ± 11% of normal levels in CUG0 cells and18% ± 14% in CUG700 cells (Figure 17A). The half-lives of the 5' and the 3' end of the reporter mRNA were measured as previously described.

As expected, the stability of CUG0 reporter mRNAs is not affected by MBNL1 protein knockdown since these transcripts lack a binding site for MBNL1 protein (Figure 17B). Furthermore, MBNL1 protein depletion had no effect on decay of the 5' end of the

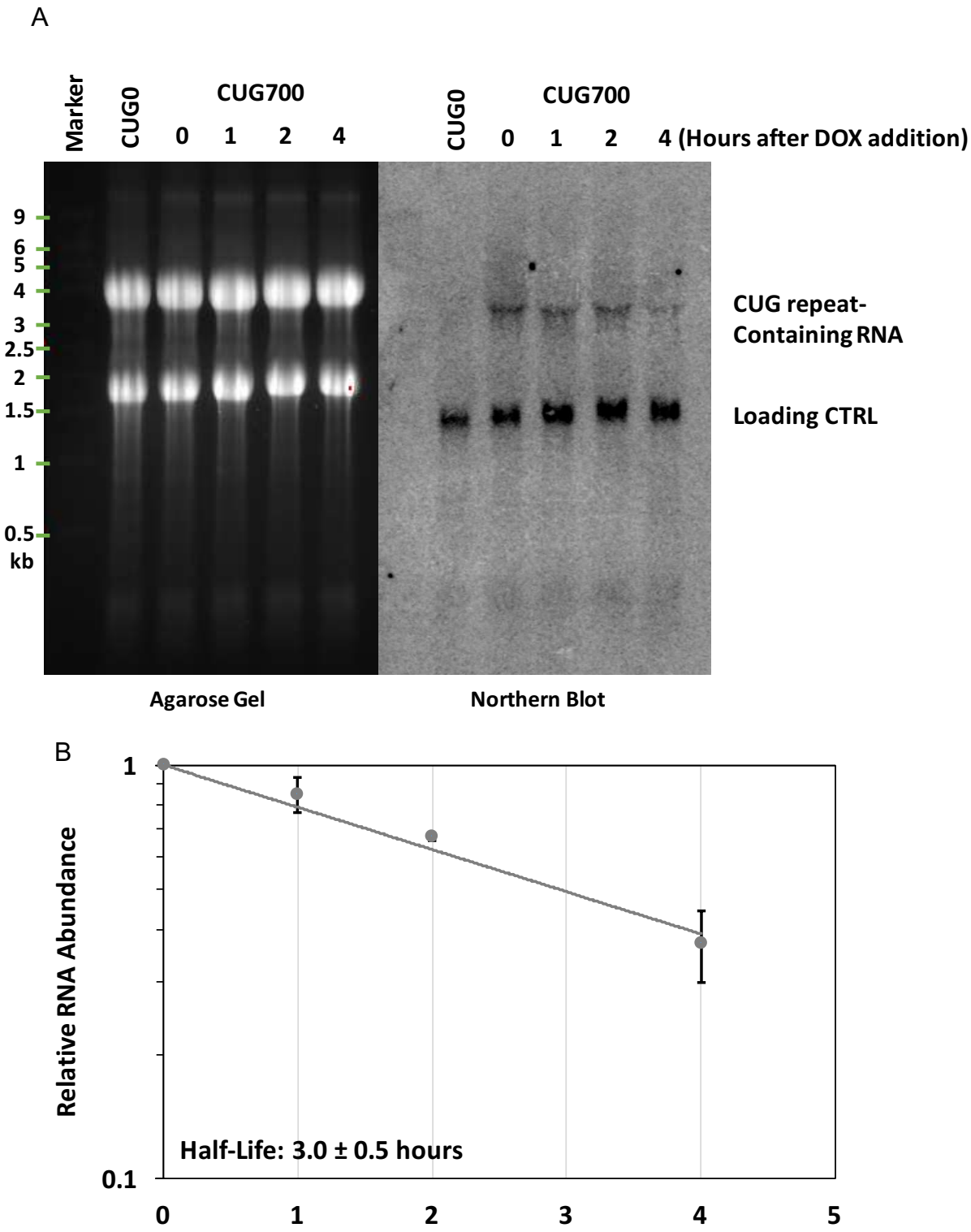

Figure 16: The half-life of repeat region is not dramatically more stable than the flanking regions. A. Agarose gel picture depicting RNA marker, 28S and 18S rRNA. Northern blot performed with RNA from CUG0 and CUG700 cells using 5' end γ^{32}P-ATP labeled 5'-$(CAG)_2TCGAG(CAG)_4$-3' probe. B: Quantification of northern blots. Error bars represent standard deviation of two biological replicates for the 1 hr time point and three biological replicates for the rest of the time points.

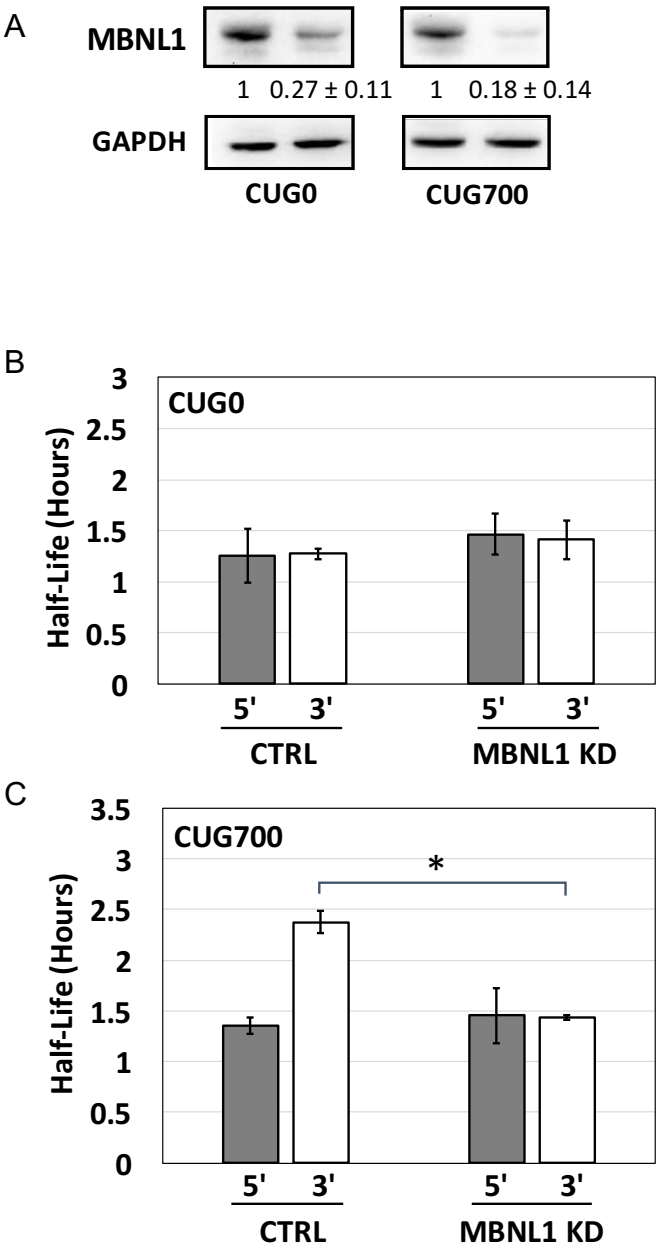

Figure 17: The 3' end of CUG700 mRNA is destabilized by MBNL1 protein knockdown. A. MBNL1 protein abundance was assessed by western blot. B&C. CUG0 and CUG700 cells were transfected with MBNL1-shRNA. DOX was added after 48hrs of transfection. Cells were treated with TRIzol™ 0, 1, 2, and 4hrs after DOX addition to extract total RNA. Half-lives were generated by qRT-PCR. Error bars represent standard deviation of 3 biological replicates, *$p<0.05$ for 3' end half-life in CTRL samples compared to both 5' end in CTRL sample and 3' end in MBNL1 KD sample by two-tailed Student's t-test.

repeat-containing reporter RNA suggesting that MBNL1 protein association does not dramatically influence the activation of the decay process for this transcript. Nevertheless, the 3' end of the mutant transcripts was destabilized, restoring decay of the 3' end to the same rate as the 5' end (Figure 17C), as seen for the CUG0 reporter mRNA. There are two possible explanations for this result. (i) MBNL1 protein binding to the repeats is required for impeding exonuclease XRN2 and following its depletion, XRN2 effectively processes the entire message. (ii) Depletion of MBNL1 protein, which results in dissolution of foci (Querido et al., 2011; Smith et al., 2007), also activates an alternative decay pathway that processes the 3' end more effectively.

3.7 Following depletion of MBNL1, XRN2 processes the entire transcript efficiently

Many studies have shown that dissociation of MBNL1 protein from mutant DMPK transcripts diffuses toxic foci, reduces the abundance of the mutant transcript and rescues DM1 phenotypes (Haghighat Jahromi et al., 2013; Nakamori et al., 2016; Wheeler et al., 2012). However, it is not clear whether the mutant DMPK mRNA is degraded in the nucleus or if MBNL1 protein depletion allows it to be exported to the cytoplasm for decay. We wondered whether MBNL1 protein depletion might alter the relative abundance of the transcript in the cytoplasm. Therefore, we knocked down both XRN2 and MBNL1 proteins by transfecting siRNAs targeting both into CUG700 cells. In the control group, an equal amount of GFP siRNA was transfected. Cells were treated with DOX 24 hours post transfection, and collected 0, 1, 2, and 4 hours afterwards. RNA was isolated to generate half-life as previously described.

XRN2 protein was knocked down 71 ± 3% and MBNL1 protein was depleted 76 ± 6% (Figure 18A). The 5' end of the reporter mRNA is stabilized after XRN2 + MBNL1

knockdown, which further confirmed that after MBNL1 protein depletion, CUG700 transcripts are still degraded by XRN2 (Figure 18B) and therefore likely remain in the nucleus. The 3' end of the reporter mRNA is stabilized (compared to MBNL1 KD alone in Figure 17C) suggesting that the mutant DMPK transcripts are targeted by the 3' → 5' decay machinery when both MBNL1 and XRN2 proteins are depleted. Thus, we believe that the pathway for decay of CUG700 involves decapping followed by rapid 5' → 3' decay of the region upstream of the repeats by XRN2. XRN2 either cannot process the repeats at all due to their association with MBNL1 proteins, or it slows dramatically and must wait for MBNL1 to dissociate to move forward. The decay of the 3' region of the transcript, which requires RRP6 protein, and likely the nuclear exosome, appears to be activated later resulting in a longer half-life for this region.

3.8 UPF1 protein is required for degradation of the CUG700 mRNA

In *C. elegans*, the nonsense-mediated decay (NMD) pathway influences the formation of nuclear foci by CUG repeat-containing mRNA, as depleting NMD essential factors *smg-2* (homologue for UPF1), *smg-1* (homologue for SMG1) and *smg-6* (homologue for SMG6) proteins increases the abundances of CUG repeat-containing mRNAs and the depletion of smg-2 enhances the toxic mRNA nuclear foci formation (Garcia et al., 2014). Therefore, we hypothesized that nonsense-mediated decay factors such as UPF1 may play a role in the degradation of our reporter transcripts.

In order to determine this, we first treated the cells with cycloheximide (CHX), which inhibits the translocation step during protein synthesis in eukaryotic cells (Schneider-Poetsch et al., 2010; Wilkinson and MacLeod, 1988). CHX inhibits cytoplasmic decay

A

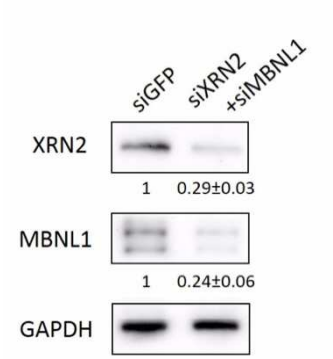

B

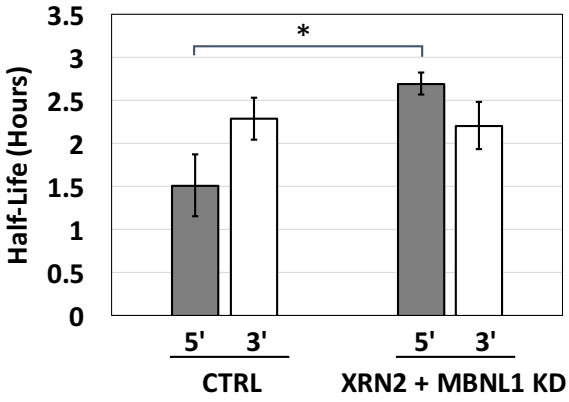

Figure 18: Co-depletion of MBNL1 and XRN2 proteins only stabilizes the 5' end of the CUG700 transcripts. A. XRN2 and MBNL1 protein abundances were assessed by western blot. B. CUG700 cells were transfected with siXRN2 and siMBNL1. DOX was added after 48hrs of transfection. RNA was extracted 0, 1, 2, and 4hrs after DOX addition to extract total RNA for half-life analysis generated by qPCR. *$p<0.05$ compared to 5' in the CTRL samples by two-tailed Student's t-test. Error bars represent standard deviation of 3 biological replicates.

including translation-dependent nonsense-mediated decay (Carter et al., 1995; Cougot et al., 2004; Zhang et al., 1997), but does not directly affect nuclear RNA metabolism (Yeilding et al., 1998).

CUG0 and CUG700 cells were transfected with pTET-OFF, and 10 μg/ml CHX was added to the media after 24 hours. Cells were collected 3 hours after CHX treatment to isolate RNA. The reporter mRNA abundance was measured by qRT-PCR as previously described.

As predicted, an increase of 1.9 ± 0.5 fold in abundance for CUG0 mRNA was detected (Figure 19A). The abundance of the cytoplasmic mRNA MyoD (positive control) is increased 3.0 ± 0.6 fold, while the abundance of nuclear long noncoding RNA (lncRNA) H19 (negative control) remains unchanged in both cell lines (Figure 19A&B).

Interestingly, CUG700 transcripts accumulated after CHX inhibition (Figure 19B). It seems unlikely such a dramatic effect is due to cytoplasmic stabilization (given that the majority of the mutant mRNA is degraded in the nucleus; Figure 7A). We therefore suggest that is due to an indirect effect of CHX on transcription of the reporter (Peresleni et al., 1988; Wong et al., 1987) or translation of RNA decay factors(Gokal et al., 1986).

We depleted UPF1 protein to 8% ± 8% in CUG0 cells and 6% ± 7% in CUG700 cells by transfecting plasmid expressing UPF1 shRNA (Figure 20A). Cells were treated with DOX 48 hours' post transfection, and collected 0, 1, 2, and 4 hours after DOX addition to isolate RNA. The half-life of the reporter mRNA was generated as previously described.

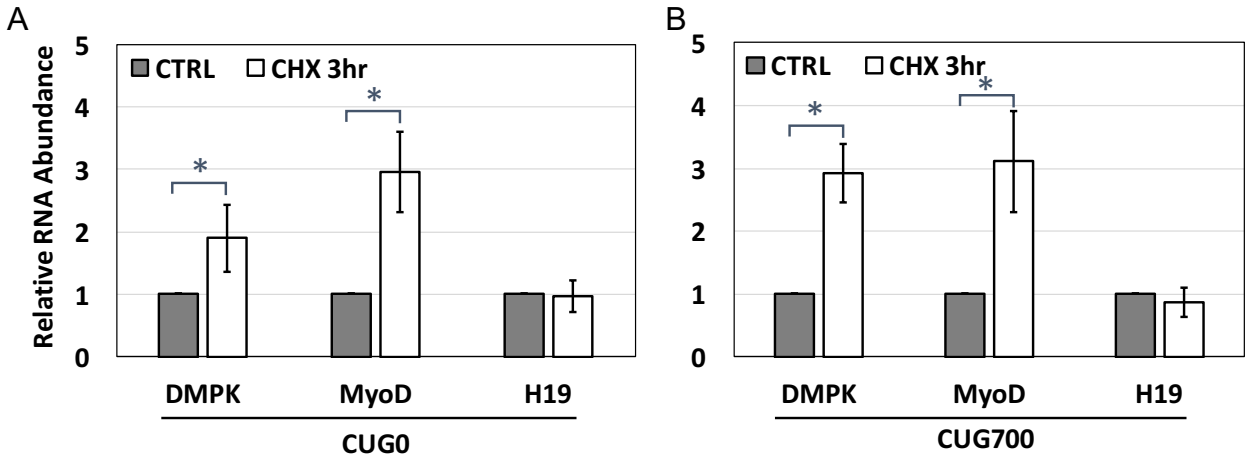

Figure 19: Cycloheximide treatment causes accumulation of mutant DMPK transcripts. Both CUG0 and CUG700 cells were treated with 10 µg/ml CHX for 3 hours before collected to generate RNA whose abundances were quantified via qRT-PCR. Cytoplasmic mRNA MyoD=positive control, nuclear lncRNA H19=negative control. Error bars represent standard deviation of 3 biological replicates. *p<0.05 compared to control samples by two tailed Student's t-test.

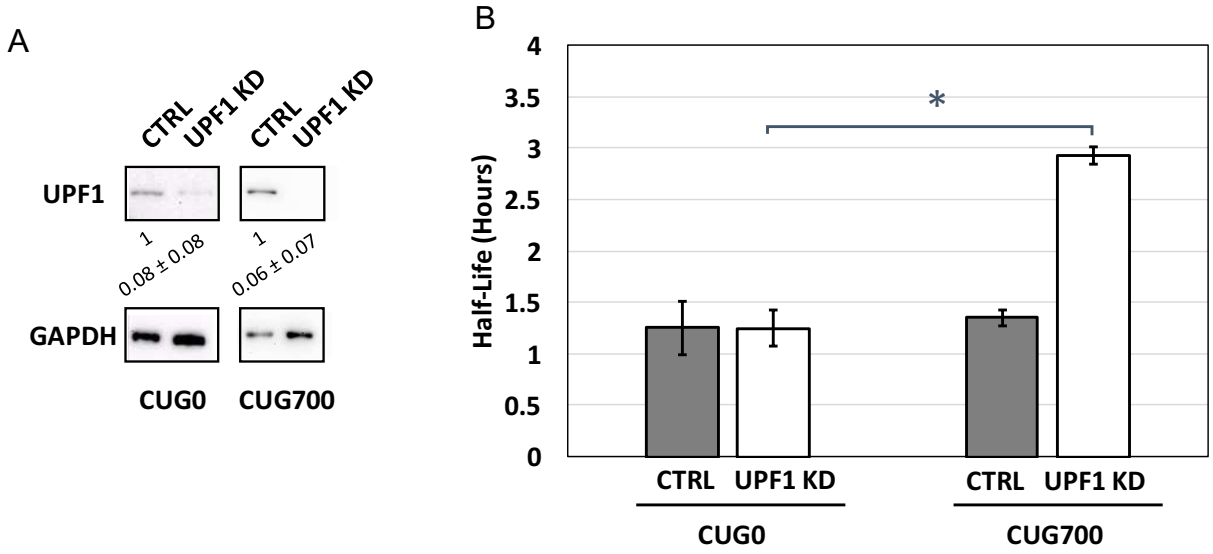

Figure 20: UPF1 is involved in the degradation of mutant DMPK transcripts. A. Cells were transfected with plasmids expressing UPF1 shRNA for 48 hours. Cells were collected 0, 1, 2, and 4 hours after DOX addition. Half-life was generated by qRT-PCR. Error bars represent standard deviation of 3 biological replicates. *p<0.05 of mutant DMPK mRNA half-life compared to control samples in CUG700 cells by two-tailed Student's t-test. B. Western blot analysis of UPF1 KD efficiency.

As predicted, the half-life of the 5’ end of the CUG0 mRNA was not affected by UPF1 knockdown. In contrast, the 5’ end of the CUG700 transcripts were significantly stabilized (Figure 20B), indicating that UPF1 protein is required for decay of the repeat-containing transcript. This is consistent with previous findings in patient fibroblasts that UPF1 protein depletion resulted in increased foci (Garcia et al., 2014). It is very interesting to note that unlike MBNL1 protein knockdown, UPF1 protein depletion delays entry of the CUG700 mRNA into the decay pathway (as the 5’ end is stabilized). However, this data alone does not prove the involvement of NMD in the degradation of mutant DMPK transcripts as UPF1 protein is also involved in staufen1-mediated decay (Kim et al., 2005b) and has some nuclear functions (Choe et al., 2014; Varsally and Brogna, 2012). Therefore, further endeavor is needed to determine what role UPF1 protein plays (directly or indirectly) in the degradation of CUG700 transcripts.

CHAPTER 4: DISCUSSION

4.1 A new and valuable model for studying DMPK mRNA metabolism

We have generated C2C12 mouse myoblast cell lines that inducibly express a luciferase reporter bearing either 0 or 700 CUG repeats within human DMPK 3' UTR. The CUG700 cell line exhibits characteristic nuclear foci containing the reporter mRNA and MBNL1, as well as predominantly nuclear localization and weak translation of the reporter mRNA – all key features exhibited by the repeat-containing DMPK transcript in DM1 patient cells. In parallel, we made a control cell line that only expresses the human 3' UTR without any CTG repeat. We used these two reporter cell lines to study and compare the decay of transcripts containing or lacking CUG repeats. These experiments would be very challenging to do in DM1 patient cells for two reasons. First, the only difference between the wild type and mutant DMPK mRNAs in most cell lines is the number of CUG repeats, thus the 5' and 3' regions of the wild type and mutant mRNAs cannot be distinguished in unmanipulated DM1 patient cells (Figure 13). Second, it is not simple to assess decay of a single gene without influencing cell metabolism, either by adding a toxic transcription inhibitor such as actinomycin D (ActD; Bansal et al., 1991; Ljungman et al., 1999; Siboni et al., 2015) or 5,6-dichloro-1-beta-D-ribofuranosylbenzimidazole (DRB; Stoimenov et al., 2011) or by using modified nucleotides, such as 4sU, to distinguish nascent and pre-existing mRNAs. Metabolic labeling also has some unwanted effects (Burger et al., 2013; Slomovic et al., 2006) and can be laborious with regards to sample processing and analysis.

With this cell culture model, we have determined that the reporter mRNAs in CUG0 and CUG700 cells are predominantly nuclear, but are degraded in different compartments. We have also discovered that the ribonucleoprotein structure formed by the CUG repeats expansion in the CUG700 cells inhibits XRN2-mediated decay, which could poteintially be contributing to DM1 pathogenesis.

Possible future applications of the model

With this cell culture model, we can study the roles of other proteins that associate with the CUG repeats and of factors that modify the phenotype associated with their expression. One such example is the RNA helicase, DDX6 (Pettersson et al., 2014). Overexpression of the DDX6 protein improves some of the phenotypes seen in DM1, for instance, a reduction in the mutant DMPK mRNA foci and rescued mis-splicing events (Pettersson et al., 2014). One hypothesis is that the DDX6 protein unwinds the double-stranded CUG repeats in the mutant mRNA and/or dissociates MBNL1 proteins in order to facilitate decay. If so, overexpression of DDX6 protein, may destabilize the 3' end, similar to MBNL1 depletion as XRN2 should be able to process the repeats more efficiently. Besides DDX6, there are also other proteins that associate with the CUG repeats or modify the disease phenotype which could affect decay of the repeat-containing RNA, for example dsRNA-binding protein Staufen1, RNA helicase DDX5 protein, RNA splicing factor hnRNP H.

As some RNA-binding proteins and factors associated with mRNA decay are differentially expressed in differentiated cells (Neff et al., 2012), one can speculate that the degradation rate and/or pattern of mutant DMPK transcripts may be different. For example, increased expression of the adult-isoform-favoring MBNL1 protein in

differentiated C2C12 cells was reported (Bland et al., 2010). The degradation of the CUG repeats may be more challenging as more available MBNL1 proteins are associated with the repeat structure. We can study the decay pathway for mutant DMPK transcripts in more differentiated myotubes, which more closely resemble adult muscle cell.

Additionally, antisense oligonucleotide (ASO) drugs and siRNAs in preclinical research that target the mutant DMPK transcripts for decay showed beneficial effects, relieving some DM1 phenotypes (Jauvin et al., 2017; Lee et al., 2012b; Pandey et al., 2015; Sobczak et al., 2013; Wheeler et al., 2012). We can use our system to test if targeting upstream or downstream of the repeats is more efficient at getting rid of the whole transcript by measuring the decay rate of the 5', 3' and the repeats region of the mutant mRNA after drug administration.

In conclusion, our cell lines are a valuable model specifically designed for studying the effect of CUG-repeat expansion on the degradation of mutant DMPK transcripts in the context of DMPK 3' UTR. Though there may be potential limitations, overwhelmingly, our cell line is bringing the field forward by providing the option to study the molecular mechanism of DM1 from a new angle.

4.2 Both CUG0 and CUG700 mRNAs are degraded surprisingly rapidly

Prior to this study, wild type and mutant DMPK transcripts as well as the mutant DMPK mRNA foci were believed to be very stable in either DM1 fibroblasts or DM1 myoblasts (Davis et al., 1997; Holt et al., 2007; Krahe et al., 1995; Langlois et al., 2003). Interestingly, our results have shown that both reporter mRNAs in our CUG cell lines are surprisingly unstable (~1 hour). However, when we treated the CUG cells with DOX

in the presence of ActD, the reporter mRNAs are 4-fold more stable compared to cells treated with DOX alone. Therefore, we infer that ActD treatment stabilizes DMPK mRNA. This could be due to ActD interfering with cell metabolism as a global transcription inhibitor (Bansal et al., 1991; Ljungman et al., 1999; Siboni et al., 2015). Additionally, after addition of ActD, some nuclear proteins are translocated to the cytoplasm (Wishart et al., 2005). This kind of translocation may also happen for nuclear decay factors, which might in turn inhibit the decay of mutant DMPK transcripts.

To support this idea, we tested the stability of DMPK mRNAs in both the control and DM1 patient myoblasts with 4sU labeling. Their half-lives were at least 4-fold less than previously reported. In a separate study, the wild type DMPK transcripts in the Huh7.5 cells (a hepatocyte carcinoma cell line) have a half-life of 1.23 hours with 4sU labeling (Moon et al., 2015). The differences of these half-lives could be due to cell type differences. Overall, we have demonstrated that neither the wild type nor the mutant DMPK transcripts are as stable as previously reported. Though our reporter mRNAs degrade faster than DMPK transcripts in the DM1 myoblasts, we can still detect the characteristic nuclear foci and sequestration of MBNL1 protein. Therefore, this new information points us to study how even rapidly decayed CUG-repeat containing transcripts contribute to the pathogenesis of DM1.

4.3 Both CUG0 and CUG700 mRNAs are mostly nuclear, but are degraded in different compartments.

We have discovered that both the reporter mRNAs in CUG0 and CUG700 cells as well as wild type DMPK mRNAs are predominantly nuclear. Our results also showed that CUG0 mRNAs are primarily degraded in the cytoplasm by the 5 → 3' exonuclease

XRN1, and the CUG700 transcripts are predominantly decayed in the nucleus by the 5' → 3' exonuclease XRN2.

4.3.1 The nuclear localization of CUG700 mRNA

We have demonstrated that the reporter mRNA in the CUG0 cell line is mostly nuclear, and the wild type DMPK mRNAs in DM1 myoblasts, HeLa cells and iPS cells are also mostly nuclear. This finding was somewhat unexpected as most mature mRNA localize in the cytoplasm (Solnestam et al., 2012). We suggest that this is an approach to limit expression of DMPK protein, whose overexpression is detrimental to cell metabolism (Oude Ophuis et al., 2009). This theory could be tested by using different concentrations of DOX to control how much reporter mRNA in CUG0 cell line is transcribed. If the cell is limiting how many CUG0 transcripts are exported, the amount of CUG0 mRNA in the cytoplasm would cease to increase after enough CUG0 mRNA is transcribed.

4.3.2 The nuclear localization of CUG700 mRNA

The nuclear localization of the reporter mRNAs in CUG700 cells is consistent with previous reports describing the human mutant DMPK transcript localization (Davis et al., 1997; Taneja et al., 1995). But it was unclear whether the nuclear localization of this mRNA is caused by inefficient export or if they are exported to the cytoplasm and quickly get degraded. We demonstrated that XRN1 protein knockdown does not significantly affect the stability of the CUG700 reporter mRNA, though it remains possible that a small fraction could still get exported and degraded in the cytoplasm since we detected some luciferase activity from the CUG700 reporter. Evidence implying mutant DMPK transcripts cannot recruit export factors is piling up. 1) Mutant

DMPK mRNA fails to enter the nuclear speckles which is reported to be a check-point for export-ready mRNAs (Smith et al., 2007). 2) The mutant reporter DMPK transcripts can be efficiently exported through CRM1-dependent export pathway when the woodchuck post-transcriptional regulatory element (WPRE) is inserted downstream of the repeats (Mastroyiannopoulos et al., 2005). 3) Mutation of the mRNA export factor Aly enhances the eye phenotype in a DM1 *Drosophila* model (Garcia-Lopez et al., 2008). We can further validate this hypothesis by analyzing the interaction between CUG0 and CUG700 mRNA with export factors TAP(NXF1):p15, ALY/REF or SR proteins. Failure to associate with these export factors indicates that the mutant DMPK transcripts are retained in the nucleus due to inability to recruit export factors.

4.3.3 CUG0 and CUG700 mRNAs are degraded in different compartments

The degradation site of the reporter mRNA in CUG0 cell line, in the cytoplasm, is consistent with the mechanism experienced by most protein encoding mRNAs (Muhlrad et al., 1994; Wormington et al., 1996). Our results also suggest that the CUG0 mRNAs degrade rapidly after export.

However, we do not fully understand why the CUG700 transcripts are degraded in the nucleus – does the cell recognize it as aberrant or label it as a non-coding RNA?

Aberrant transcripts are degraded in the nucleus by either 5’ → 3’ exonuclease XRN2 or 3’ → 5’ exonuclease exosome (Davidson et al., 2012a; Hilleren et al., 2001). This is consistent with the fact that the 5’ end of the repeat-containing mRNA in our CUG700 cells are degraded by XRN2, while the 3’ end is degraded by the nuclear exosome. The cell may recognize the repeat-containing transcripts as aberrant and target them for decay.

Unlike aberrant mRNAs that are often degraded co-transcriptionally (Davidson et al., 2012b), evidence of co-localization of DMPK DNA and DMPK mRNA is scarce (Mankodi et al., 2003; Taneja et al., 1995). This indicates that mutant DMPK transcripts are not degraded at the site of transcription. Interestingly, aside from site of degradation, there are other aspects that mutant DMPK transcript are similar to nuclear nonconding RNA. 1) Most annotated long noncoding RNAs (lncRNAs) are transcribed by RNA Pol II, and are capped, spliced and polyadenylated. Some have longer than usual poly(A) tails like mutant DMPK mRNA, for example NEAT1 and XIST (Bresson and Conrad, 2013). 2) LncRNA NEAT1 and MALAT1 are retained in the nucleus and can be detected as foci using FISH, though unlike mutant DMPK mRNA foci, NEAT1 and MATLA1 foci are localized to paraspeckles and nuclear speckles, respectively (Hutchinson et al., 2007). 3) LcRNAs act as sponge or decoy which sequester RNA-binding proteins normally to regulate gene expression (Morriss and Cooper, 2017). For example, NEAT1 acts as a sponge to sequester splicing factors SFPQ (splicing factor proline/glutamine-rich) and NONO (p54nrb) in the paraspeckles to regulate gene expression (Hirose et al., 2014), which is somewhat similar to MBNL1 sequestration by CUG repeats. However, little is known about the degradation pathway of lncRNAs, therefore, information is limited for us to compare them to mutant DMPK transcripts.

4.4 The ribonucleoprotein structure formed by CUG repeats expansion and the sequestered MBNL1 proteins prevents the 5'→3' exonuclease XRN2 from accessing the 3' end of the mutant DMPK transcript

As we have demonstrated, the CUG700 transcripts are turned over relatively rapidly yet they still accumulate in nuclear foci which sequester MBNL1 proteins. Our studies

sought to test the hypothesis that the ribonucleoprotein structure formed by extensive CUG repeats combined with MBNL1 proteins suppresses the activity of the predominantly nuclear 5' → 3' exonuclease XRN2. We demonstrated that the ribonucleoprotein structure blocks the access of XRN2 to the 3' end of the mutant DMPK mRNAs. Later, the nuclear exosome is then recruited to degrade the mRNA from the 3' side.

This brings up a brand-new perspective that there are 3 rate limiting steps of the degradation of the mutant DMPK transcripts (Figure 21). 1) Initiation of 5' → 3' decay, probably involving decapping. 2) The 5' → 3 exonuclease XRN2 is stalled upon reaching the CUG repeats/MBNL1 protein structure. 3) Initiation of the 3' → 5' decay by the nuclear exosome either after XRN2 is stalled, or at least some time later than 5'->3' decay. Due to second and third limiting steps, the function of XRN2 may be impaired, and uncapped degradation intermediates may accumulate. These could contribute to the pathogenesis of DM1 and are discussed below.

4.4.1 Possible effects generated by limiting XRN2 processivity

Though the 5' end of the mutant DMPK transcript is degraded rapidly, the delay in processing caused by failure of XRN2 may allow the repeat region to persist and sequester MBNL1 long enough to alter cell function and may also lead to persistence of the 3' end beyond it's normal life span. Additionally, one can ponder the cascading effects an inhibited XRN2-mediated decay can bring about.

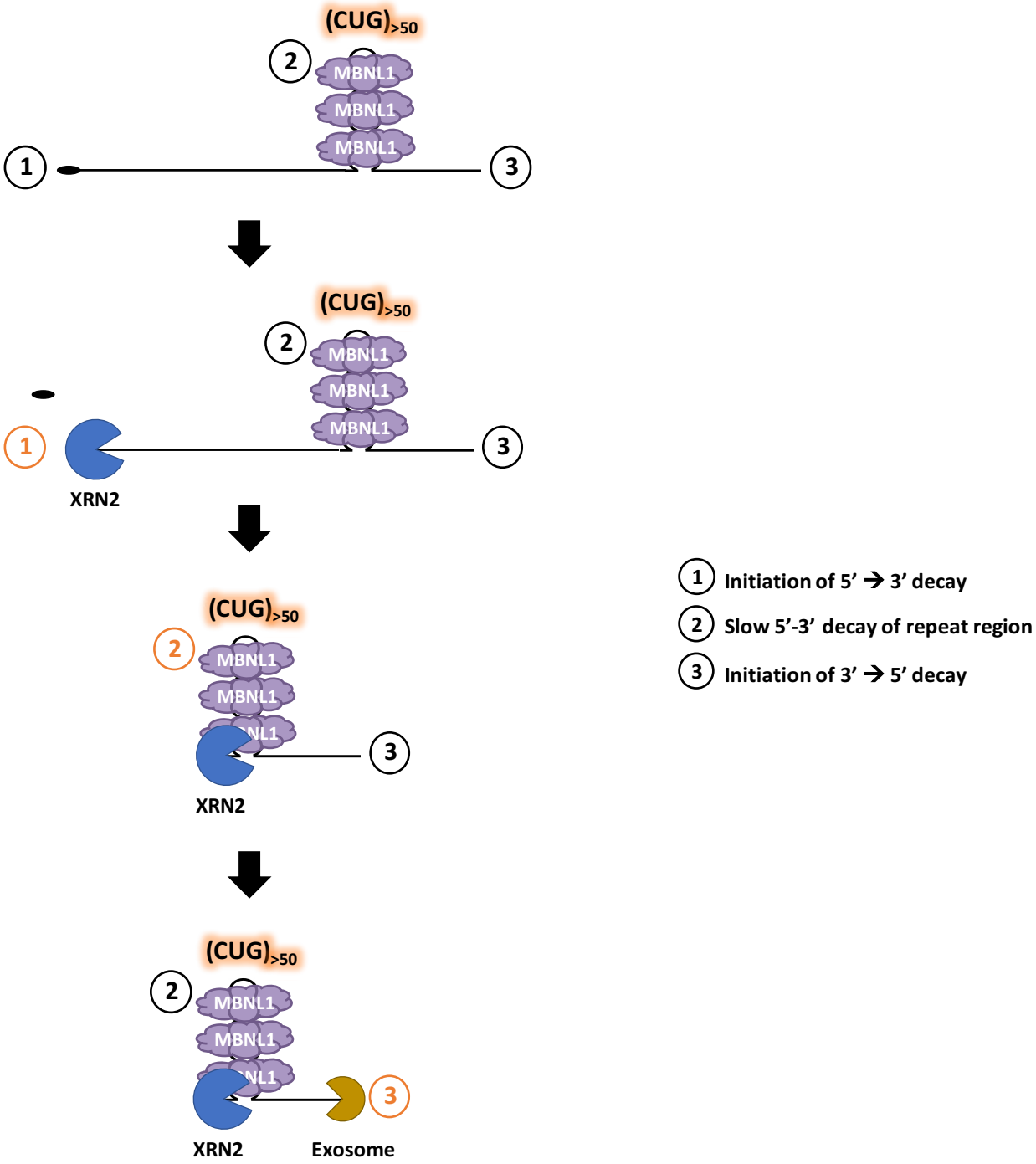

Figure 21: Diagram of 3 rate-limiting steps of mutant DMPK mRNA decay.

1) XRN2 function may be impaired

The stall of XRN2 exonuclease caused by the ribonucleoprotein structure formed by the CUG repeats expansion and the MBNL1 proteins in the mutant DMPK transcripts may limit the availability of the XRN2 proteins for other aspects of cell metabolism.

The primarily nuclear 5' → 3' exonuclease XRN2 is involved in transcription termination by RNA Pol II (mRNA, microRNA; Ballarino et al., 2009; Fong et al., 2015; Tollervey, 2004; West et al., 2004) according to the "torpedo" model. XRN2 is also responsible for the maturation and degradation of pre-ribosomal RNAs (pre-rRNAs; Wang and Pestov, 2011) and noncoding RNAs, for example snoRNA (small nucleolar RNA; Miki and Großhans, 2013). XRN2 also acts as the nuclear quality control that degrades aberrant RNAs and products of abortive transcription (Brannan et al., 2012; Davidson et al., 2012a).

Therefore, if the availability of the exonuclease XRN2 is limited due to prolonged association with the CUG repeats, it could have a global effect on cell metabolism: aberrant mRNA may arise, rRNA may not be processed properly to generate ribosomes, a delay in transcription termination of RNA Pol II products (West et al., 2004) may limit the availability of RNA Pol II for other transcription events.

We have tried to investigate if pre-rRNA is properly processed in our reporter cell line to determine the function of XRN2. However, we did not detect any differences between CUG0 and CUG700 cells. This could be because not every promoter in the pTRE3G-Luc-CUG700 construct in our cell line received tTA during transfection, so there were

not enough cells that did express repeat-containing RNA for us to detect any differences.

2) Possible effects generated by exosome degrading structure RNA

When mutant DMPK transcripts are degraded by the nuclear exosome because of XRN2 inefficiency, helicase MTR4 from the TRAMP/NEXT complex may be required to unwind the CUG repeats structure (LaCava et al., 2005; Mitchell and Tollervey, 2003). Due to the complex secondary structure, this may cause a reduction in the availability of MTR4 which in turn causes the accumulation and export of normally unstable lncRNAs (prematurely terminated RNAs and upstream antisense RNAs; Ogami et al., 2017). This may have a global effect on cell metabolism.

3) Persistence of the 3' end of the DMPK 3' UTR beyond it's normal life span.

The 3' end of the human DMPK 3' UTR contains many RNA binding protein motifs according to RBPDB database (http://rbpdb.ccbr.utoronto.ca//). The persistence of the 3' end of the DMPK 3' UTR may pose a threat to cell metabolism by usurping these RNA-binding proteins that are essential for processing of other RNAs. For example, KRSP as a decay regulator, destabilizes mRNA AU-rich element such as Spry4 transcripts that translate to tumor suppressor protein (Bikkavilli et al., 2017). Proteins that may bind the 3' end of the DMPK 3' UTR in the nucleus according to RBPDB database are listed below in Table 8. A map of binding locations is depicted in Figure 22.

Figure 22: Map of RNA-binding protein sites on the 3' end of the human DMPK 3' UTR.

Table 8: RNA-binding proteins that may bind the 3' end of the DMPK 3' UTR

Protein (Label in appendix)	# of binding sites	Binding motif	Function	Reference
KSRP (purple)	8	GUCC	Regulation of RNA splicing and promotion of RNA decay	(Gherzi et al., 2004; Min et al., 1997)
A2BP1/RBFOX1 (yellow)	2	UGCAUG	RNA splicing	(Gao et al., 2015; Pedrotti et al., 2015)
	4	GCAUG		
RBM4 (green)	18	CGCG	Regulation of RNA splicing, negative regulation of translation	(Lin et al., 2017, 2007; Markus et al., 2016)
FUS/hnRNPP2 (pink)	8	GGUG	Regulation of transcription, RNA splicing and export	(Efimova et al., 2017)
SFRS9 (light blue)	4	AGGAC	Regulation of RNA splicing	(Screaton et al., 1995)
MBNL1 (brown)	19	UGCU	Regulation of RNA splicing, alternative polyadenylation	(Batra et al., 2014; Hino et al., 2007; Kino et al., 2009; Warf et al., 2009)

4.4.2 MBNL1 protein is required for inhibition of XRN2-mediated decay on mutant reporter mRNA

Our results have shown that sequestered MBNL1 proteins are required for inhibiting XRN2-mediated decay. However, it is unclear how the characteristic DMPK mRNA foci in DM1 are formed. XRN2-mediated decay does not create the foci as DMPK mRNA foci can be detected using oligos upstream of the repeats (Taneja et al., 1995). However, the requirement for MBNL1 protein is unclear. If foci exist after co-depletion of XRN2 and MBNL1 proteins, then MBNL1 protein is not needed for the formation of foci, and vice versa.

4.4.3 Towards understanding some preclinical treatments at the molecular level

Our findings may help explain how some preclinical treatments work to improve DM1 phenotypes. Some examples are listed here:

1) siRNA/ASO targeting mutant DMPK mRNA for decay may act by circumventing the 1st and/or 3rd rat- limiting step

It has been reported that targeting mutant DMPK mRNA for decay using siRNA or antisense oligonucleotide (ASO) can rescue some phenotypes seen in DM1 (Costales et al., 2016; Jauvin et al., 2017; Lee et al., 2012b; Wheeler et al., 2012). By bypassing the first rate-limiting step (Figure 21A), a decrease in abundance of the repeat-containing mRNA and nuclear foci formation were observed when using ASOs targeting the 5' end of the repeats (Jauvin et al., 2017; Wheeler et al., 2012). Interestingly, by circumventing the third rate-limiting step (Figure 21B), ASOs targeting the 3' end of the repeats was reported to have a stronger effect in knocking down mutant DMPK

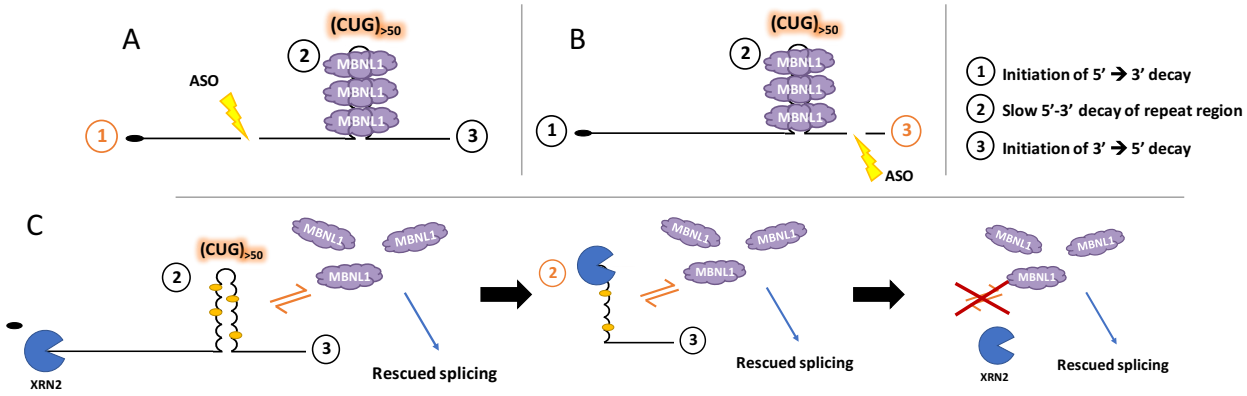

Figure 23: Diagram of drugs bypassing rate-limiting steps of mutant DMPK mRNA

transcripts and reducing the toxic foci (Jauvin et al., 2017; Wheeler et al., 2012). This is consistent with our study which suggests that the siRNA/ASO targeting the 3' end of the repeats may have a better success rate. However, further effort is needed to understand the relationship of the knockdown level and the exact location where siRNA/ASO targets on the mutant transcripts.

2) Small molecules competing with MBNL1 for binding to CUG repeats may be bypassing the 2nd rate-limiting step

Small molecules, for example Lomofungin (Hoskins et al., 2014), that compete with MBNL1 protein for binding to CUG repeats restore the function of MBNL1 protein which rescues RNA mis-splicing events (Hoskins et al., 2014; Wheeler et al., 2009). The removal of MBNL1 proteins could allow the mutant DMPK transcripts to be degraded more efficiently, as we saw with MBNL1 depletion, which circumvents the 2^{nd} rate limiting step (Figure 21&23C). This in turn prevents the re-association of MBNL1 proteins with the mutant DMPK mRNAs, which may further contribute to therapeutics. This is a theory that can be tested using our system by adding small molecules and assessing their effects on decay of 5' and 3' regions.

4.5 UPF1 protein is involved in the degradation of mutant DMPK mRNA

Our results have shown that the cycloheximide treatment causes the accumulation of the mutant reporter mRNA, and that the UPF1 protein depletion leads to increased stability of the CUG700 transcripts almost 3 fold. This is consistent with a previous finding that shows knocking down UPF1 in C. elegans causes an increase in toxic mRNA nuclear foci and exhibition of more severe motility deterioration (Garcia et al., 2014). Our results suggest that UPF1 protein is involved in the degradation of CUG700 transcripts, but it is not clear what specific role UPF1 protein may play. As UPF1 plays important roles in both the nucleus and the cytoplasm (Chawla et al., 2011; Kim et al., 2005b; Kurosaki and Maquat, 2016; Varsally and Brogna, 2012), three possible involvement of UPF1 in the degradation of repeat-containing mRNA are discussed below.

1) Nonsense-mediated decay?

UPF1 protein is involved in nonsense-mediated decay which targets mRNAs with a premature termination codon (Kurosaki and Maquat, 2016). Mutant DMPK mRNAs have extended distance between the stop codon and the poly(A) signal in mutant transcript caused by the CUG repeat expansion, which could be targeted by nonsense mediated decay (Amrani et al., 2004; Bühler et al., 2006). However, the actual distance between the stop codon and the poly(A) signal may be narrowed due to the secondary and tertiary structure of the mRNA. Additionally, there are only ~7% CUG700 transcripts in the cytoplasm as measured by cell fractionation in our study, it is doubtful that if the cytoplasmic nonsense-mediated decay is at play, it's abolition can create a ~3 fold stabilization of CUG700 transcripts.

2) Staufen1-mediated decay?

UPF1 protein is also involved in Staufen1-mediated decay (SMD; Gong et al., 2013), which is an mRNA degrdation process that is mediated by Staufen1 (STAU1) to regulate gene expression posttranscriptionally (Gong et al., 2009). STAU1 recogizes dsRNA structure formed either by intramolecular base pairing or intermolecular basepairing with STAU1-binding sites. UPF1 is recruited to the specifc mRNA 3' UTR by STAU1 to elicit mRNA decay (Kim et al., 2005b). It is not clear whether this process is purely cytoplasmic (Martel et al., 2006). Besides, STAU1 is increased in DM1 skeletal muscle and regulate RNA splicing in the nucleus (Ravel-Chapuis et al., 2012), which shows that STAU1 has nuclear functions. Though STAU1 is not found co-localizing with DMPK mRNA foci, it is controversial whether all mutant DMPK mRNAs are in foci or not

(Ho et al., 2005b; Pettersson et al., 2015). Therefore, it may be possible that the repeat-containing mRNAs are subjected to Staufen1-mediated decay.

3) Does UPF1 protein facilitate XRN2 for degradation of mutant transcripts?

It has been predicted bioinformatically that UPF1 protein may interact with DOM3Z protein in the nucleus in yeast (Varsally and Brogna, 2012). Human homologue of DOM3Z is decapping exoribonuclease (DXO1). Aside from its decapping activity for unmethylated (Jiao et al., 2013) and NAD^+ capped RNA, DOM3Z/DXO1 stimulates the 5' → 3' activity of XRN2 (Xiang et al., 2009). Though evidence of XRN2 and DXO1 interaction has not been reported in human (reviewed in Nagarajan et al., 2013), it is interesting to investigate if UPF1 protein interacts with DOM3Z/DXO1, and if DOM3Z/DXO1 facilitates the decay of mutant DMPK transcripts. As our results have indicated that UPF1 protein is required for the degradation of the repeat-containing mRNA, and that the CUG700 transcripts are predominantly subjected to XRN2-mediated pathway, UPF1 protein may be playing a direct role in facilitating XRN2 in the degradation of repeat-containing mRNA.

4.6 Conclusions

Through the experiments presented here, we have demonstrated several important findings. 1) Both normal and DMPK transcripts are predominantly nuclear and are degraded rapidly in different compartments. 2) The ribonucleoprotein structure formed by CUG repeats expansion and the sequestered MBNL1 proteins prevents the 5' → 3' exonuclease XRN2 from accessing the 3' end of the mutant reporter transcript, which may contribute to DM1 pathogenesis. 3) UPF1 is directly or indirectly involved in the degradation of mutant reporter transcripts.

Though the effect of mutant DMPK mRNA decay on the pathogenesis of the disease is not the only contributing factor, the studies presented here further our understanding of DM1 pathogenesis and may help gain insights into designing therapeutic targets.

REFERENCES

Abbruzzese, C., Costanzi Porrini, S., Mariani, B., Gould, F.K., Mcabney, J.P., Monckton, D.G., Ashizawa, T., and Giacanelli, M. (2002). Instability of a premutation allele in homozygous patients with myotonic dystrophy type 1. Ann. Neurol. *52*, 435–441.

van Agtmaal, E.L., André, L.M., Willemse, M., Cumming, S.A., van Kessel, I.D.G., van den Broek, W.J.A.A., Gourdon, G., Furling, D., Mouly, V., Monckton, D.G., et al. (2017). CRISPR/Cas9-Induced (CTG·CAG)n Repeat Instability in the Myotonic Dystrophy Type 1 Locus: Implications for Therapeutic Genome Editing. Mol. Ther. *25*, 24–43.

Alkalaeva, E.Z., Pisarev, A. V., Frolova, L.Y., Kisselev, L.L., and Pestova, T. V. (2006). In Vitro Reconstitution of Eukaryotic Translation Reveals Cooperativity between Release Factors eRF1 and eRF3. Cell *125*, 1125–1136.

Alwazzan, M., Newman, E., Hamshere, M.G., and Brook, J.D. (1999). Myotonic dystrophy is associated with a reduced level of RNA from the DMWD allele adjacent to the expanded repeat. Hum. Mol. Genet. *8*, 1491–1497.

Amack, J.D., and Mahadevan, M.S. (2001). The myotonic dystrophy expanded CUG repeat tract is necessary but not sufficient to disrupt C2C12 myoblast differentiation. Hum. Mol. Genet. *10*, 1879–1887.

Amack, J.D., Paguio, A.P., and Mahadevan, M.S. (1999). Cis and trans effects of the myotonic dystrophy (DM) mutation in a cell culture model. Hum. Mol. Genet. *8*, 1975–1984.

Amack, J.D., Reagan, S.R., and Mahadevan, M.S. (2002). Mutant DMPK 3'-UTR transcripts disrupt C2C12 myogenic differentiation by compromising MyoD. J. Cell Biol. *159*, 419–429.

Amberg, D.C., Goldstein, A.L., and Cole, C.N. (1992). Isolation and characterization of RAT1: an essential gene of Saccharomyces cerevisiae required for the efficient nucleocytoplasmic trafficking of mRNA. Genes Dev. *6*, 1173–1189.

Amrani, N., Ganesan, R., Kervestin, S., Mangus, D.A., Ghosh, S., and Jacobson, A. (2004). A faux 3′-UTR promotes aberrant termination and triggers nonsense- mediated mRNA decay. Nature *432*, 112–118.

Andersen, P.R., Domanski, M., Kristiansen, M.S., Storvall, H., Ntini, E., Verheggen, C., Schein, A., Bunkenborg, J., Poser, I., Hallais, M., et al. (2013). The human cap-binding complex is functionally connected to the nuclear RNA exosome. Nat. Struct. Mol. Biol. *20*, 1367–1376.

Angelbello, A.J., González, À.L., Rzuczek, S.G., and Disney, M.D. (2016). Development of pharmacophore models for small molecules targeting RNA: Application to the RNA repeat expansion in myotonic dystrophy type 1. Bioorg. Med. Chem. Lett. *26*, 5792–5796.

Araki, Y., Takahashi, S., Kobayashi, T., Kajiho, H., Hoshino, S., and Katada, T. (2001). Ski7p G protein interacts with the exosome and the Ski complex for 3'-to-5' mRNA decay in yeast. EMBO J. *20*, 4684–4693.

Ashley, C.T., and Warren, S.T. (1995). Trinucleotide Repeat Expansion and Human Disease. Annu. Rev. Genet. *29*, 703–728.

Aslanidis, C., Jansen, G., Amemiya, C., Shutler, G., Mahadevan, M., Tsilfidis, C., Chen, C., Alleman, J., Wormskamp, N.G.M., Vooijs, M., et al. (1992). Cloning of the essential myotonic dystrophy region and mapping of the putative defect. Nature *355*, 548–551.

Astrea, G., Battini, R., Lenzi, S., Frosini, S., Bonetti, S., Moretti, E., Perazza, S., Santorelli, F.M., and Pecini, C. (2016). Learning disabilities in neuromuscular disorders: a springboard for adult life. Acta Myol. Myopathies Cardiomyopathies Off. J. Mediterr. Soc. Myol. *35*, 90–95.

Bachi, A., Braun, I.C., Rodrigues, J.P., Panté, N., Ribbeck, K., von Kobbe, C., Kutay, U., Wilm, M., Görlich, D., Carmo-Fonseca, M., et al. (2000). The C-terminal domain of TAP interacts with the nuclear pore complex and promotes export of specific CTE-bearing RNA substrates. RNA *6*, 136–158.

Badis, G., Saveanu, C., Fromont-Racine, M., and Jacquier, A. (2004). Targeted mRNA Degradation by Deadenylation-Independent Decapping. Mol. Cell *15*, 5–15.

Bahar Halpern, K., Caspi, I., Lemze, D., Levy, M., Landen, S., Elinav, E., Ulitsky, I., and Itzkovitz, S. (2015). Nuclear Retention of mRNA in Mammalian Tissues. Cell Rep. *13*, 2653–2662.

Baldanzi, S., Ricci, G., Simoncini, C., Cosci O Di Coscio, M., and Siciliano, G. (2016). Hard ways towards adulthood: the transition phase in young people with myotonic dystrophy. Acta Myol. Myopathies Cardiomyopathies Off. J. Mediterr. Soc. Myol. *35*, 145–149.

Ballarino, M., Pagano, F., Girardi, E., Morlando, M., Cacchiarelli, D., Marchioni, M., Proudfoot, N.J., and Bozzoni, I. (2009). Coupled RNA Processing and Transcription of

Intergenic Primary MicroRNAs. Mol. Cell. Biol. *29*, 5632–5638.

Bansal, N., Houle, A., and Melnykovych, G. (1991). Apoptosis: mode of cell death induced in T cell leukemia lines by dexamethasone and other agents. FASEB J. *5*, 211–216.

Barbé, L., Lanni, S., López-Castel, A., Franck, S., Spits, C., Keymolen, K., Seneca, S., Tomé, S., Miron, I., Letourneau, J., et al. (2017). CpG Methylation, a Parent-of-Origin Effect for Maternal-Biased Transmission of Congenital Myotonic Dystrophy. Am. J. Hum. Genet. *100*, 488–505.

Batra, R., Charizanis, K., Manchanda, M., Mohan, A., Li, M., Finn, D.J., Goodwin, M., Zhang, C., Sobczak, K., Thornton, C.A., et al. (2014). Loss of MBNL Leads to Disruption of Developmentally Regulated Alternative Polyadenylation in RNA-Mediated Disease. Mol. Cell *56*, 311–322.

Begemann, G., Paricio, N., Artero, R., Kiss, I., Pérez-Alonso, M., and Mlodzik, M. (1997). muscleblind, a gene required for photoreceptor differentiation in Drosophila, encodes novel nuclear Cys3His-type zinc-finger-containing proteins. Development *124*, 4321–4331.

Bellini, M., Biagi, S., Stasi, C., Costa, F., Mumolo, M.G., Ricchiuti, A., and Marchi, S. (2006). Gastrointestinal manifestations in myotonic muscular dystrophy. World J. Gastroenterol. *12*, 1821–1828.

Benders, A.A., Groenen, P.J., Oerlemans, F.T., Veerkamp, J.H., and Wieringa, B. (1997). Myotonic dystrophy protein kinase is involved in the modulation of the Ca2+ homeostasis in skeletal muscle cells. J. Clin. Invest. *100*, 1440–1447.

Berul, C.I., Maguire, C.T., Aronovitz, M.J., Greenwood, J., Miller, C., Gehrmann, J., Housman, D., Mendelsohn, M.E., and Reddy, S. (1999). DMPK dosage alterations result in atrioventricular conduction abnormalities in a mouse myotonic dystrophy model. J. Clin. Invest. *103*, 1–7.

Bikkavilli, R.K., Zerayesus, S.A., Van Scoyk, M., Wilson, L., Wu, P.-Y., Baskaran, A., Tang, K., Raheem, S., Samuelson, B.A., Reddy, N.M., et al. (2017). K-homology splicing regulatory protein (KSRP) promotes post-transcriptional destabilization of Spry4 transcripts in non-small cell lung cancer. J. Biol. Chem. *292*, 7423–7434.

Birnboim, H.C., Mitchel, R.E., and Straus, N.A. (1973). Analysis of long pyrimidine polynucleotides in HeLa cell nuclear DNA: absence of polydeoxythymidylate. Proc. Natl. Acad. Sci. U. S. A. *70*, 2189–2192.

Birney, E., Stamatoyannopoulos, J.A., Dutta, A., Guigó, R., Gingeras, T.R., Margulies, E.H., Weng, Z., Snyder, M., Dermitzakis, E.T., Thurman, R.E., et al. (2007). Identification and analysis of functional elements in 1% of the human genome by the ENCODE pilot project. Nature *447*, 799–816.

Bland, C.S., Wang, E.T., Vu, A., David, M.P., Castle, J.C., Johnson, J.M., Burge, C.B., and Cooper, T.A. (2010). Global regulation of alternative splicing during myogenic differentiation. Nucleic Acids Res. *38*, 7651–7664.

Blau, H.M., Pavlath, G.K., Hardeman, E.C., Chiu, C.P., Silberstein, L., Webster, S.G., Miller, S.C., and Webster, C. (1985). Plasticity of the differentiated state. Science *230*, 758–766.

Bondy-Chorney, E., Crawford Parks, T.E., Ravel-Chapuis, A., Jasmin, B.J., and Côté, J.

(2016). Staufen1s role as a splicing factor and a disease modifier in Myotonic Dystrophy Type I. Rare Dis. (Austin, Tex.) *4*, e1225644.

Bonneau, F., Basquin, J., Ebert, J., Lorentzen, E., and Conti, E. (2009). The yeast exosome functions as a macromolecular cage to channel RNA substrates for degradation. Cell *139*, 547–559.

Botta, A., Rinaldi, F., Catalli, C., Vergani, L., Bonifazi, E., Romeo, V., Loro, E., Viola, A., Angelini, C., and Novelli, G. (2008). The CTG repeat expansion size correlates with the splicing defects observed in muscles from myotonic dystrophy type 1 patients. J. Med. Genet. *45*, 639–646.

Botta, A., Rossi, G., Marcaurelio, M., Fontana, L., D'Apice, M.R., Brancati, F., Massa, R., G Monckton, D., Sangiuolo, F., and Novelli, G. (2017). Identification and characterization of 5′ CCG interruptions in complex DMPK expanded alleles. Eur. J. Hum. Genet. *25*, 257–261.

Boucher, C.A., King, S.K., Carey, N., Krahe, R., Winchester, C.L., Rahman, S., Creavin, T., Meghji, P., Bailey, M.E., and Chartier, F.L. (1995). A novel homeodomain-encoding gene is associated with a large CpG island interrupted by the myotonic dystrophy unstable (CTG)n repeat. Hum. Mol. Genet. *4*, 1919–1925.

Brannan, K., Kim, H., Erickson, B., Glover-Cutter, K., Kim, S., Fong, N., Kiemele, L., Hansen, K., Davis, R., Lykke-Andersen, J., et al. (2012). mRNA decapping factors and the exonuclease Xrn2 function in widespread premature termination of RNA polymerase II transcription. Mol. Cell *46*, 311–324.

Bresson, S.M., and Conrad, N.K. (2013). The Human Nuclear Poly(A)-Binding Protein

Promotes RNA Hyperadenylation and Decay. PLoS Genet. *9*, e1003893.

Bresson, S.M., Hunter, O. V., Hunter, A.C., and Conrad, N.K. (2015). Canonical Poly(A) Polymerase Activity Promotes the Decay of a Wide Variety of Mammalian Nuclear RNAs. PLOS Genet. *11*, e1005610.

Brockhoff, M., Rion, N., Chojnowska, K., Wiktorowicz, T., Eickhorst, C., Erne, B., Frank, S., Angelini, C., Furling, D., Rüegg, M.A., et al. (2017). Targeting deregulated AMPK/mTORC1 pathways improves muscle function in myotonic dystrophy type I. J. Clin. Invest. *127*, 549–563.

Brook, J.D., McCurrach, M.E., Harley, H.G., Buckler, A.J., Church, D., Aburatani, H., Hunter, K., Stanton, V.P., Thirion, J.-P., Hudson, T., et al. (1992). Molecular basis of myotonic dystrophy: Expansion of a trinucleotide (CTG) repeat at the 3′ end of a transcript encoding a protein kinase family member. Cell *68*, 799–808.

Brouwer, J.R., Huguet, A., Nicole, A., Munnich, A., and Gourdon, G. (2013). Transcriptionally Repressive Chromatin Remodelling and CpG Methylation in the Presence of Expanded CTG-Repeats at the DM1 Locus. J. Nucleic Acids *2013*, 567435.

Bühler, M., Steiner, S., Mohn, F., Paillusson, A., and Mühlemann, O. (2006). EJC-independent degradation of nonsense immunoglobulin-μ mRNA depends on 3' UTR length. Nat. Struct. Mol. Biol. *13*, 462–464.

Burger, K., Mühl, B., Kellner, M., Rohrmoser, M., Gruber-Eber, A., Windhager, L., Friedel, C.C., Dölken, L., and Eick, D. (2013). 4-thiouridine inhibits rRNA synthesis and causes a nucleolar stress response. RNA Biol. *10*, 1623–1630.

Buxton, J., Shelbourne, P., Davies, J., Jones, C., Van Tongeren, T., Aslanidis, C., de Jong, P., Jansen, G., Anvret, M., and Riley, B. (1992). Detection of an unstable fragment of DNA specific to individuals with myotonic dystrophy. Nature *355*, 547–548.

Cabada, T., Iridoy, M., Jericó, I., Lecumberri, P., Seijas, R., Gargallo, A., and Gomez, M. (2017). Brain Involvement in Myotonic Dystrophy Type 1: A Morphometric and Diffusion Tensor Imaging Study with Neuropsychological Correlation. Arch. Clin. Neuropsychol. *11*, 1–12.

Caine, C., Kasherov, P., Silber, J., and Lalouette, A. (2014). Mef2 Interacts with the Notch Pathway during Adult Muscle Development in Drosophila melanogaster. PLoS One *9*, e108149.

Carango, P., Noble, J.E., Marks, H.G., and Funanage, V.L. (1993). Absence of Myotonic Dystrophy Protein Kinase (DMPK) mRNA as a Result of a Triplet Repeat Expansion in Myotonic Dystrophy. Genomics *18*, 340–348.

Carter, M.S., Doskow, J., Morris, P., Li, S., Nhim, R.P., Sandstedt, S., and Wilkinson, M.F. (1995). A regulatory mechanism that detects premature nonsense codons in T-cell receptor transcripts in vivo is reversed by protein synthesis inhibitors in vitro. J. Biol. Chem. *270*, 28995–29003.

Cerro-Herreros, E., Fernandez-Costa, J.M., Sabater-Arcis, M., Llamusi, B., and Artero, R. (2016). Derepressing muscleblind expression by miRNA sponges ameliorates myotonic dystrophy-like phenotypes in Drosophila. Sci. Rep. *6*, 36230.

Chakrabarti, A., and Maitra, U. (1991). Function of eukaryotic initiation factor 5 in the formation of an 80 S ribosomal polypeptide chain initiation complex. J. Biol. Chem. *266*,

14039–14045.

Chakrabarti, S., Jayachandran, U., Bonneau, F., Fiorini, F., Basquin, C., Domcke, S., Le Hir, H., and Conti, E. (2011). Molecular Mechanisms for the RNA-Dependent ATPase Activity of Upf1 and Its Regulation by Upf2. Mol. Cell *41*, 693–703.

Chakrabarti, S., Bonneau, F., Schüssler, S., Eppinger, E., and Conti, E. (2014). Phospho-dependent and phospho-independent interactions of the helicase UPF1 with the NMD factors SMG5-SMG7 and SMG6. Nucleic Acids Res. *42*, 9447–9460.

Chang, J.H., Xiang, S., Xiang, K., Manley, J.L., and Tong, L. (2011). Structural and biochemical studies of the 5'→3' exoribonuclease Xrn1. Nat. Struct. Mol. Biol. *18*, 270–276.

Chapman, E.G., Costantino, D.A., Rabe, J.L., Moon, S.L., Wilusz, J., Nix, J.C., and Kieft, J.S. (2014a). The Structural Basis of Pathogenic Subgenomic Flavivirus RNA (sfRNA) Production. Science (80-.). *344*.

Chapman, E.G., Moon, S.S.L., Wilusz, J., Kieft, J.J.S., Babendure, J., Adams, S., Tsien, R., Barclay, E., Baugh, C., Grate, D., et al. (2014b). RNA structures that resist degradation by Xrn1 produce a pathogenic Dengue virus RNA. Elife *3*, e01892.

Charizanis, K., Lee, K.-Y., Batra, R., Goodwin, M., Zhang, C., Yuan, Y., Shiue, L., Cline, M., Scotti, M.M., Xia, G., et al. (2012). Muscleblind-like 2-mediated alternative splicing in the developing brain and dysregulation in myotonic dystrophy. Neuron *75*, 437–450.

Charlet-B., N., Savkur, R.S., Singh, G., Philips, A. V., Grice, E.A., and Cooper, T.A. (2002). Loss of the Muscle-Specific Chloride Channel in Type 1 Myotonic Dystrophy

Due to Misregulated Alternative Splicing. Mol. Cell *10*, 45–53.

Chau, A., and Kalsotra, A. (2014). Developmental insights into the pathology and therapeutic strategies for DM1: Back to the basics. Dev. Dyn.

Chawla, R., Redon, S., Raftopoulou, C., Wischnewski, H., Gagos, S., and Azzalin, C.M. (2011). Human UPF1 interacts with TPP1 and telomerase and sustains telomere leading-strand replication. EMBO J. *30*, 4047–4058.

Chazal, P.-E., Daguenet, E., Wendling, C., Ulryck, N., Tomasetto, C., Sargueil, B., and Le Hir, H. (2013). EJC core component MLN51 interacts with eIF3 and activates translation. Proc. Natl. Acad. Sci. U. S. A. *110*, 5903–5908.

Cheadle, C., Fan, Ji., Cho-chung, Y.S., Werner, T., Ray, J., Do, L., Gorospe, M., and Becker, K.G. (2005). Stability Regulation of mRNA and the Control of Gene Expression. Ann. N. Y. Acad. Sci. *1058*, 196–204.

Chen, G., Masuda, A., Konishi, H., Ohkawara, B., Ito, M., Kinoshita, M., Kiyama, H., Matsuura, T., and Ohno, K. (2016). Phenylbutazone induces expression of MBNL1 and suppresses formation of MBNL1-CUG RNA foci in a mouse model of myotonic dystrophy. Sci. Rep. *6*, 25317.

Chen, J.L., Vanetten, D.M., Fountain, M.A., Yildirim, I., and Disney, M.D. (2017). Structure and dynamics of RNA repeat expansions that cause Huntington's Disease and myotonic dystrophy type 1.

Chen, N., Walsh, M.A., Liu, Y., Parker, R., and Song, H. (2005). Crystal Structures of Human DcpS in Ligand-free and m7GDP-bound forms Suggest a Dynamic Mechanism

for Scavenger mRNA Decapping. J. Mol. Biol. *347*, 707–718.

Chiu, Y.-L., Ho, C.K., Saha, N., Schwer, B., Shuman, S., and Rana, T.M. (2002). Tat Stimulates Cotranscriptional Capping of HIV mRNA. Mol. Cell *10*, 585–597.

Cho, H., Kim, K.M., Kim, Y.K., Lui, K., Chen, S., Isbell, D., Tso, P., Chen, S., Brann, D.W., Chen, S., et al. (2009). Human proline-rich nuclear receptor coregulatory protein 2 mediates an interaction between mRNA surveillance machinery and decapping complex. Mol. Cell *33*, 75–86.

Cho, H., Han, S., Choe, J., Park, S.G., Choi, S.S., and Kim, Y.K. (2013). SMG5-PNRC2 is functionally dominant compared with SMG5-SMG7 in mammalian nonsense-mediated mRNA decay. Nucleic Acids Res. *41*, 1319–1328.

Choe, J., Ahn, S.H., and Kim, Y.K. (2014). The mRNP remodeling mediated by UPF1 promotes rapid degradation of replication-dependent histone mRNA. Nucleic Acids Res. *42*, 9334–9349.

Cinesi, C., Aeschbach, L., Yang, B., and Dion, V. (2016). Contracting CAG/CTG repeats using the CRISPR-Cas9 nickase. Nat. Commun. *7*, 13272.

Connelly, S., and Manley, J.L. (1988). A functional mRNA polyadenylation signal is required for transcription termination by RNA polymerase II. Genes Dev. *2*, 440–452.

Coonrod, L.A., Nakamori, M., Wang, W., Carrell, S., Hilton, C.L., Bodner, M.J., Siboni, R.B., Docter, A.G., Haley, M.M., Thornton, C.A., et al. (2013). Reducing levels of toxic RNA with small molecules. ACS Chem. Biol. *8*, 2528–2537.

Copeland, P.R., and Wormington, M. (2001). The mechanism and regulation of

deadenylation: identification and characterization of Xenopus PARN. RNA *7*, 875–886.

Costales, M.G., Rzuczek, S.G., and Disney, M.D. (2016). Comparison of small molecules and oligonucleotides that target a toxic, non-coding RNA. Bioorg. Med. Chem. Lett. *26*, 2605–2609.

Cougot, N., Babajko, S., and Séraphin, B. (2004). Cytoplasmic foci are sites of mRNA decay in human cells. J. Cell Biol. *165*, 31–40.

Cronshaw, J.M., Krutchinsky, A.N., Zhang, W., Chait, B.T., and Matunis, M.J. (2002). Proteomic analysis of the mammalian nuclear pore complex. J. Cell Biol. *158*, 915–927.

Dahlqvist, J.R., Ørngreen, M.C., Witting, N., and Vissing, J. (2015). Endocrine function over time in patients with myotonic dystrophy type 1. Eur. J. Neurol. *22*, 116–122.

Dansithong, W., Paul, S., Comai, L., and Reddy, S. (2005). MBNL1 is the primary determinant of focus formation and aberrant insulin receptor splicing in DM1. J. Biol. Chem. *280*, 5773–5780.

Dansithong, W., Wolf, C.M., Sarkar, P., Paul, S., Chiang, A., Holt, I., Morris, G.E., Branco, D., Sherwood, M.C., Comai, L., et al. (2008). Cytoplasmic CUG RNA foci are insufficient to elicit key DM1 features. PLoS One *3*, e3968.

Das, B., Butler, J.S., and Sherman, F. (2003). Degradation of normal mRNA in the nucleus of Saccharomyces cerevisiae. Mol. Cell. Biol. *23*, 5502–5515.

Daughters, R.S., Tuttle, D.L., Gao, W., Ikeda, Y., Moseley, M.L., Ebner, T.J., Swanson, M.S., and Ranum, L.P.W. (2009). RNA Gain-of-Function in Spinocerebellar Ataxia Type 8. PLoS Genet. *5*, e1000600.

Davidson, L., Kerr, A., and West, S. (2012a). Co-transcriptional degradation of aberrant pre-mRNA by Xrn2. EMBO J. *31*, 2566–2578.

Davidson, L., Kerr, A., and West, S. (2012b). Co-transcriptional degradation of aberrant pre-mRNA by Xrn2. EMBO J. *31*, 2566–2578.

Davis, B.M., McCurrach, M.E., Taneja, K.L., Singer, R.H., and Housman, D.E. (1997). Expansion of a CUG trinucleotide repeat in the 3' untranslated region of myotonic dystrophy protein kinase transcripts results in nuclear retention of transcripts. Proc. Natl. Acad. Sci. U. S. A. *94*, 7388–7393.

Deniaud, A., Karuppasamy, M., Bock, T., Masiulis, S., Huard, K., Garzoni, F., Kerschgens, K., Hentze, M.W., Kulozik, A.E., Beck, M., et al. (2015). A network of SMG-8, SMG-9 and SMG-1 C-terminal insertion domain regulates UPF1 substrate recruitment and phosphorylation. Nucleic Acids Res. *43*, 7600–7611.

van Dijk, E., Cougot, N., Meyer, S., Babajko, S., Wahle, E., and Séraphin, B. (2002). Human Dcp2: a catalytically active mRNA decapping enzyme located in specific cytoplasmic structures. EMBO J. *21*, 6915–6924.

van Dijk, E.L., Chen, C.L., d'Aubenton-Carafa, Y., Gourvennec, S., Kwapisz, M., Roche, V., Bertrand, C., Silvain, M., Legoix-Né, P., Loeillet, S., et al. (2011). XUTs are a class of Xrn1-sensitive antisense regulatory non-coding RNA in yeast. Nature *475*, 114–117.

Dogan, C., De Antonio, M., Hamroun, D., Varet, H., Fabbro, M., Rougier, F., Amarof, K., Arne Bes, M.-C., Bedat-Millet, A.-L., Behin, A., et al. (2016). Gender as a Modifying Factor Influencing Myotonic Dystrophy Type 1 Phenotype Severity and Mortality: A Nationwide Multiple Databases Cross-Sectional Observational Study. PLoS One *11*,

e0148264.

Dölken, L., Ruzsics, Z., Rädle, B., Friedel, C.C., Zimmer, R., Mages, J., Hoffmann, R., Dickinson, P., Forster, T., Ghazal, P., et al. (2008). High-resolution gene expression profiling for simultaneous kinetic parameter analysis of RNA synthesis and decay. RNA *14*, 1959–1972.

Doma, M.K., and Parker, R. (2006). Endonucleolytic cleavage of eukaryotic mRNAs with stalls in translation elongation. Nature *440*, 561–564.

Douniol, M., Jacquette, A., Cohen, D., Bodeau, N., Rachidi, L., Angeard, N., Cuisset, J.-M., Vallée, L., Eymard, B., Plaza, M., et al. (2012). Psychiatric and cognitive phenotype of childhood myotonic dystrophy type 1. Dev. Med. Child Neurol. *54*, 905–911.

Dryland, P.A., Doherty, E., Love, J.M., and Love, D.R. (2013). Simple Repeat-Primed PCR Analysis of the *Myotonic Dystrophy Type 1* Gene in a Clinical Diagnostics Environment. J. Neurodegener. Dis. *2013*, 1–8.

Du, J., Campau, E., Soragni, E., Jespersen, C., and Gottesfeld, J.M. (2013). Length-dependent CTG·CAG triplet-repeat expansion in myotonic dystrophy patient-derived induced pluripotent stem cells. Hum. Mol. Genet. *22*, 5276–5287.

Eberle, A.B., Lykke-Andersen, S., M?hlemann, O., and Jensen, T.H. (2009). SMG6 promotes endonucleolytic cleavage of nonsense mRNA in human cells. Nat. Struct. Mol. Biol. *16*, 49–55.

Ebralidze, A., Wang, Y., Petkova, V., Ebralidse, K., and Junghans, R.P. (2004). RNA Leaching of Transcription Factors Disrupts Transcription in Myotonic Dystrophy.

Science (80-.). *303*.

Efimova, A.D., Ovchinnikov, R.K., Roman, A.Y., Maltsev, A. V., Grigoriev, V. V., Kovrazhkina, E.A., and Skvortsova, V.I. (2017). The FUS protein: Physiological functions and a role in amyotrophic lateral sclerosis. Mol. Biol. *51*, 341–351.

Fardaei, M., Larkin, K., Brook, J.D., and Hamshere, M.G. (2001). In vivo co-localisation of MBNL protein with DMPK expanded-repeat transcripts. Nucleic Acids Res. *29*, 2766–2771.

Fardaei, M., Rogers, M.T., Thorpe, H.M., Larkin, K., Hamshere, M.G., Harper, P.S., and Brook, J.D. (2002). Three proteins, MBNL, MBLL and MBXL, co-localize in vivo with nuclear foci of expanded-repeat transcripts in DM1 and DM2 cells. Hum. Mol. Genet. *11*, 805–814.

Finkbeiner, S. (2011). Huntington's Disease. Cold Spring Harb. Perspect. Biol. *3*.

Flaherty, S.M., Fortes, P., Izaurralde, E., Mattaj, I.W., and Gilmartin, G.M. (1997). Participation of the nuclear cap binding complex in pre-mRNA 3' processing. Proc. Natl. Acad. Sci. U. S. A. *94*, 11893–11898.

Fong, N., Brannan, K., Erickson, B., Kim, H., Cortazar, M.A., Sheridan, R.M., Nguyen, T., Karp, S., and Bentley, D.L. (2015). Effects of Transcription Elongation Rate and Xrn2 Exonuclease Activity on RNA Polymerase II Termination Suggest Widespread Kinetic Competition. Mol. Cell *60*, 256–267.

Freyermuth, F., Rau, F., Kokunai, Y., Linke, T., Sellier, C., Nakamori, M., Kino, Y., Arandel, L., Jollet, A., Thibault, C., et al. (2016). Splicing misregulation of SCN5A

contributes to cardiac-conduction delay and heart arrhythmia in myotonic dystrophy. Nat. Commun. *7*, 11067.

Frisch, R., Singleton, K.R., Moses, P.A., Gonzalez, I.L., Carango, P., Marks, H.G., and Funanage, V.L. (2001). Effect of Triplet Repeat Expansion on Chromatin Structure and Expression of DMPK and Neighboring Genes, SIX5 and DMWD, in Myotonic Dystrophy. Mol. Genet. Metab. *74*, 281–291.

Fritzsche, R., Karra, D., Bennett, K.L., Ang, F. yee, Heraud-Farlow, J.E., Tolino, M., Doyle, M., Bauer, K.E., Thomas, S., Planyavsky, M., et al. (2013). Interactome of Two Diverse RNA Granules Links mRNA Localization to Translational Repression in Neurons. Cell Rep. *5*, 1749–1762.

Fu, Y., Pizzuti, A., Fenwick, R., King, J., Rajnarayan, S., Dunne, P., Dubel, J., Nasser, G., Ashizawa, T., de Jong, P., et al. (1992). An unstable triplet repeat in a gene related to myotonic muscular dystrophy. Science (80-.). *255*.

Fu, Y.H., Friedman, D.L., Richards, S., Pearlman, J.A., Gibbs, R.A., Pizzuti, A., Ashizawa, T., Perryman, M.B., Scarlato, G., Fenwick, R.G., et al. (1993). Decreased expression of myotonin-protein kinase messenger RNA and protein in adult form of myotonic dystrophy. Science *260*, 235–238.

Fugier, C., Klein, A.F., Hammer, C., Vassilopoulos, S., Ivarsson, Y., Toussaint, A., Tosch, V., Vignaud, A., Ferry, A., Messaddeq, N., et al. (2011). Misregulated alternative splicing of BIN1 is associated with T tubule alterations and muscle weakness in myotonic dystrophy. Nat. Med. *17*, 720–725.

Furling, D., Doucet, G., Langlois, M.-A., Timchenko, L., Belanger, E., Cossette, L., and

Puymirat, J. (2003). Viral vector producing antisense RNA restores myotonic dystrophy myoblast functions. Gene Ther. *10*, 795–802.

Gao, C., Ren, S., Lee, J.-H., Qiu, J., Chapski, D.J., Rau, C.D., Zhou, Y., Abdellatif, M., Nakano, A., Vondriska, T.M., et al. (2015). RBFox1-mediated RNA splicing regulates cardiac hypertrophy and heart failure. J. Clin. Invest. *126*, 195–206.

Garcia, J.F., and Parker, R. (2015). MS2 coat proteins bound to yeast mRNAs block 5' to 3' degradation and trap mRNA decay products: implications for the localization of mRNAs by MS2-MCP system. RNA *21*, 1393–1395.

Garcia, S.M.D.A., Tabach, Y., Lourenço, G.F., Armakola, M., and Ruvkun, G. (2014). Identification of genes in toxicity pathways of trinucleotide-repeat RNA in C. elegans. Nat. Struct. Mol. Biol. *21*, 712–720.

Garcia-Lopez, A., Monferrer, L., Garcia-Alcover, I., Vicente-Crespo, M., Alvarez-Abril, M.C., and Artero, R.D. (2008). Genetic and chemical modifiers of a CUG toxicity model in Drosophila. PLoS One *3*, e1595.

Geisler, S., Lojek, L., Khalil, A.M., Baker, K.E., and Coller, J. (2012). Decapping of long noncoding RNAs regulates inducible genes. Mol. Cell *45*, 279–291.

des Georges, A., Hashem, Y., Unbehaun, A., Grassucci, R.A., Taylor, D., Hellen, C.U.T., Pestova, T. V, and Frank, J. (2014). Structure of the mammalian ribosomal pre-termination complex associated with eRF1•eRF3•GDPNP. Nucleic Acids Res. *42*, 3409–3418.

Gherzi, R., Lee, K.-Y., Briata, P., Wegm?ller, D., Moroni, C., Karin, M., and Chen, C.-Y.

(2004). A KH Domain RNA Binding Protein, KSRP, Promotes ARE-Directed mRNA Turnover by Recruiting the Degradation Machinery. Mol. Cell *14*, 571–583.

Girard, C., Will, C.L., Peng, J., Makarov, E.M., Kastner, B., Lemm, I., Urlaub, H., Hartmuth, K., and Lührmann, R. (2012). Post-transcriptional spliceosomes are retained in nuclear speckles until splicing completion. Nat. Commun. *3*, 994.

Giudice, J., Xia, Z., Wang, E.T., Scavuzzo, M. a, Ward, A.J., Kalsotra, A., Wang, W., Wehrens, X.H.T., Burge, C.B., Li, W., et al. (2014). Alternative splicing regulates vesicular trafficking genes in cardiomyocytes during postnatal heart development. Nat. Commun. *5*, 3603.

Gladman, J.T., Yadava, R.S., Mandal, M., Yu, Q., Kim, Y.K., and Mahadevan, M.S. (2015). NKX2-5, a modifier of skeletal muscle pathology due to RNA toxicity. Hum. Mol. Genet. *24*, 251–264.

Gokal, P.K., Cavanaugh, A.H., and Thompson, E.A. (1986). The effects of cycloheximide upon transcription of rRNA, 5 S RNA, and tRNA genes. J. Biol. Chem. *261*, 2536–2541.

Gong, C., Kim, Y.K., Woeller, C.F., Tang, Y., and Maquat, L.E. (2009). SMD and NMD are competitive pathways that contribute to myogenesis: effects on PAX3 and myogenin mRNAs. Genes Dev. *23*, 54–66.

Gong, C., Tang, Y., and Maquat, L.E. (2013). mRNA-mRNA duplexes that autoelicit Staufen1-mediated mRNA decay. Nat. Struct. Mol. Biol. *20*, 1214–1220.

Gourie-Devi, M., Chaudhuri, J.R., Vasanth, A., Saleem, Q., Mutsuddi, M., Gopinath, M.,

Sarkar, P.S., and Brahmachari, S.K. (1998). Correlation of clinical profile of myotonic dystrophy with CTG repeats in the myotonin protein kinase gene. Indian J. Med. Res. *107*, 187–196.

Grange, T., de Sa, C.M., Oddos, J., and Pictet, R. (1987). Human mRNA polyadenylate binding protein: evolutionary conservation of a nucleic acid binding motif. Nucleic Acids Res. *15*, 4771–4787.

Gregersen, L., Schueler, M., Munschauer, M., Mastrobuoni, G., Chen, W., Kempa, S., Dieterich, C., and Landthaler, M. (2014). MOV10 Is a 5' to 3' RNA Helicase Contributing to UPF1 mRNA Target Degradation by Translocation along 3' UTRs. Mol. Cell *54*, 573–585.

Groenen, P.J., Wansink, D.G., Coerwinkel, M., van den Broek, W., Jansen, G., and Wieringa, B. (2000). Constitutive and regulated modes of splicing produce six major myotonic dystrophy protein kinase (DMPK) isoforms with distinct properties. Hum. Mol. Genet. *9*, 605–616.

Gromadzka, A.M., Steckelberg, A.-L., Singh, K.K., Hofmann, K., and Gehring, N.H. (2016). A short conserved motif in ALYREF directs cap- and EJC-dependent assembly of export complexes on spliced mRNAs. Nucleic Acids Res. *44*, 2348–2361.

Grudzien-Nogalska, E., Jiao, X., Song, M.-G., Hart, R.P., and Kiledjian, M. (2016). Nudt3 is an mRNA decapping enzyme that modulates cell migration. RNA *22*, 773–781.

Gudde, A.E.E.G., González-Barriga, A., van den Broek, W.J.A.A., Wieringa, B., and Wansink, D.G. (2016). A low absolute number of expanded transcripts is involved in myotonic dystrophy type 1 manifestation in muscle. Hum. Mol. Genet.

Gudde, A.E.E.G., van Kessel, I.D.G., André, L.M., Wieringa, B., and Wansink, D.G. (2017a). Trinucleotide-repeat expanded and normal DMPK transcripts contain unusually long poly(A) tails despite differential nuclear residence. Biochim. Biophys. Acta - Gene Regul. Mech. *1860*, 740–749.

Gudde, A.E.E.G., van Heeringen, S.J., de Oude, A.I., van Kessel, I.D.G., Estabrook, J., Wang, E.T., Wieringa, B., and Wansink, D.G. (2017b). Antisense transcription of the myotonic dystrophy locus yields low-abundant RNAs with and without (CAG)n repeat. RNA Biol.

Haghighat Jahromi, A., Honda, M., Zimmerman, S.C., and Spies, M. (2013). Single-molecule study of the CUG repeat-MBNL1 interaction and its inhibition by small molecules. Nucleic Acids Res. *41*, 6687–6697.

Hamshere, M.G., and Brook, J.D. (1996). Myotonic dystrophy, knockouts, warts and all. Trends Genet. *12*, 332–334.

Hamshere, M.G., Newman, E.E., Alwazzan, M., Athwal, B.S., and Brook, J.D. (1997). Transcriptional abnormality in myotonic dystrophy affects DMPK but not neighboring genes. Proc. Natl. Acad. Sci. U. S. A. *94*, 7394–7399.

Harley, H.G., Brook, J.D., Rundle, S.A., Crow, S., Reardon, W., Buckler, A.J., Harper, P.S., Housman, D.E., and Shaw, D.J. (1992). Expansion of an unstable DNA region and phenotypic variation in myotonic dystrophy. Nature *355*, 545–546.

Harper, P.S., Harley, H.G., Reardon, W., and Shaw, D.J. (1992). Anticipation in myotonic dystrophy: new light on an old problem. Am. J. Hum. Genet. *51*, 10–16.

Hector, R.E., Nykamp, K.R., Dheur, S., Anderson, J.T., Non, P.J., Urbinati, C.R., Wilson, S.M., Minvielle-Sebastia, L., and Swanson, M.S. (2002). Dual requirement for yeast hnRNP Nab2p in mRNA poly(A) tail length control and nuclear export. EMBO J. *21*, 1800–1810.

Heinrich, S., Sidler, C.L., Azzalin, C.M., and Weis, K. (2017). Stem–loop RNA labeling can affect nuclear and cytoplasmic mRNA processing. RNA *23*, 134–141.

Hilleren, P., and Parker, R. (2001). Defects in the mRNA export factors Rat7p, Gle1p, Mex67p, and Rat8p cause hyperadenylation during 30-end formation of nascent transcripts. RNA *7*, 753–764.

Hilleren, P.J., and Parker, R. (2003). Cytoplasmic Degradation of Splice-Defective Pre-mRNAs and Intermediates. Mol. Cell *12*, 1453–1465.

Hilleren, P., McCarthy, T., Rosbash, M., Parker, R., and Jensen, T.H. (2001). Quality control of mRNA 3'-end processing is linked to the nuclear exosome. Nature *413*, 538–542.

Hino, S.-I., Kondo, S., Sekiya, H., Saito, A., Kanemoto, S., Murakami, T., Chihara, K., Aoki, Y., Nakamori, M., Takahashi, M.P., et al. (2007). Molecular mechanisms responsible for aberrant splicing of SERCA1 in myotonic dystrophy type 1. Hum. Mol. Genet. *16*, 2834–2843.

Le Hir, H., Izaurralde, E., Maquat, L.E., and Moore, M.J. (2000a). The spliceosome deposits multiple proteins 20-24 nucleotides upstream of mRNA exon-exon junctions. EMBO J. *19*, 6860–6869.

Le Hir, H., Moore, M.J., and Maquat, L.E. (2000b). Pre-mRNA splicing alters mRNP composition: evidence for stable association of proteins at exon-exon junctions. Genes Dev. *14*, 1098–1108.

Le Hir, H., Gatfield, D., Izaurralde, E., and Moore, M.J. (2001). The exon-exon junction complex provides a binding platform for factors involved in mRNA export and nonsense-mediated mRNA decay. EMBO J. *20*, 4987–4997.

Hirose, T., Virnicchi, G., Tanigawa, A., Naganuma, T., Li, R., Kimura, H., Yokoi, T., Nakagawa, S., Benard, M., Fox, A.H., et al. (2014). NEAT1 long noncoding RNA regulates transcription via protein sequestration within subnuclear bodies. Mol. Biol. Cell *25*, 169–183.

Ho, G., Cardamone, M., and Farrar, M. (2015). Congenital and childhood myotonic dystrophy: Current aspects of disease and future directions. World J. Clin. Pediatr. *4*, 66–80.

Ho, T.H., Charlet-B, N., Poulos, M.G., Singh, G., Swanson, M.S., and Cooper, T.A. (2004). Muscleblind proteins regulate alternative splicing. EMBO J. *23*, 3103–3112.

Ho, T.H., Bundman, D., Armstrong, D.L., and Cooper, T. a. (2005a). Transgenic mice expressing CUG-BP1 reproduce splicing mis-regulation observed in myotonic dystrophy. Hum. Mol. Genet. *14*, 1539–1547.

Ho, T.H., Savkur, R.S., Poulos, M.G., Mancini, M.A., Swanson, M.S., and Cooper, T.A. (2005b). Colocalization of muscleblind with RNA foci is separable from mis-regulation of alternative splicing in myotonic dystrophy. J. Cell Sci. *118*, 2923–2933.

Holt, I., Mittal, S., Furling, D., Butler-Browne, G.S., David Brook, J., and Morris, G.E. (2007). Defective mRNA in myotonic dystrophy accumulates at the periphery of nuclear splicing speckles. Genes to Cells *12*, 1035–1048.

van Hoof, A., Frischmeyer, P.A., Dietz, H.C., and Parker, R. (2002). Exosome-mediated recognition and degradation of mRNAs lacking a termination codon. Science *295*, 2262–2264.

Hoskins, J.W., Ofori, L.O., Chen, C.Z., Kumar, A., Sobczak, K., Nakamori, M., Southall, N., Patnaik, S., Marugan, J.J., Zheng, W., et al. (2014). Lomofungin and dilomofungin: inhibitors of MBNL1-CUG RNA binding with distinct cellular effects. Nucleic Acids Res. *42*, 6591–6602.

Houseley, J., LaCava, J., and Tollervey, D. (2006). RNA-quality control by the exosome. Nat. Rev. Mol. Cell Biol. *7*, 529–539.

Houseley, J.M., Wang, Z., Brock, G.J.R., Soloway, J., Artero, R., Perez-Alonso, M., O'Dell, K.M.C., and Monckton, D.G. (2005). Myotonic dystrophy associated expanded CUG repeat muscleblind positive ribonuclear foci are not toxic to Drosophila. Hum. Mol. Genet. *14*, 873–883.

Hsu, C.L., and Stevens, A. (1993). Yeast cells lacking 5'-->3' exoribonuclease 1 contain mRNA species that are poly(A) deficient and partially lack the 5' cap structure. Mol. Cell. Biol. *13*, 4826–4835.

Huang, Y., and Steitz, J.A. (2001). Splicing factors SRp20 and 9G8 promote the nucleocytoplasmic export of mRNA. Mol. Cell *7*, 899–905.

Huang, Y., Gattoni, R., Sté, J., and Steitz, J.A. (2003). SR Splicing Factors Serve as Adapter Proteins for TAP-Dependent mRNA Export. Mol. Cell *11*, 837–843.

Hunter, A., Tsilfidis, C., Mettler, G., Jacob, P., Mahadevan, M., Surh, L., and Korneluk, R. (1992). The correlation of age of onset with CTG trinucleotide repeat amplification in myotonic dystrophy. J. Med. Genet. *29*, 774–779.

Hutchinson, J.N., Ensminger, A.W., Clemson, C.M., Lynch, C.R., Lawrence, J.B., and Chess, A. (2007). A screen for nuclear transcripts identifies two linked noncoding RNAs associated with SC35 splicing domains. BMC Genomics *8*, 39.

Ikeda, S., He, A., Kong, S.W., Lu, J., Bejar, R., Bodyak, N., Lee, K.-H., Ma, Q., Kang, P.M., Golub, T.R., et al. (2009). MicroRNA-1 negatively regulates expression of the hypertrophy-associated calmodulin and Mef2a genes. Mol. Cell. Biol. *29*, 2193–2204.

Ikeuchi, T., Koide, R., Tanaka, H., Onodera, O., Igarashi, S., Takahashi, H., Kondo, R., Ishikawa, A., Tomoda, A., Miike, T., et al. (1995). Dentatorubral-pallidoluysian atrophy: clinical features are closely related to unstable expansions of trinucleotide (CAG) repeat. Ann. Neurol. *37*, 769–775.

Imataka, H., Gradi, A., and Sonenberg, N. (1998). A newly identified N-terminal amino acid sequence of human eIF4G binds poly(A)-binding protein and functions in poly(A)-dependent translation factor 4G/ poly(A)-binding protein/poly(A)-dependent translation/ translation initiation. EMBO J. *17*, 7480–7489.

Ingelfinger, D., Arndt-Jovin, D.J., Lührmann, R., and Achsel, T. (2002). The human LSm1-7 proteins colocalize with the mRNA-degrading enzymes Dcp1/2 and Xrnl in distinct cytoplasmic foci. RNA *8*, 1489–1501.

Isken, O., Kim, Y.K., Hosoda, N., Mayeur, G.L., Hershey, J.W.B., and Maquat, L.E. (2008). Upf1 Phosphorylation Triggers Translational Repression during Nonsense-Mediated mRNA Decay. Cell *133*, 314–327.

Jain, A., and Vale, R.D. (2017). RNA phase transitions in repeat expansion disorders. Nature *546*, 243–247.

Jansen, G., de Jong, P.J., Amemiya, C., Aslanidis, C., Shaw, D.J., Harley, H.G., Brook, J.D., Fenwick, R., Korneluk, R.G., Tsilfidis, C., et al. (1992). Physical and genetic characterization of the distal segment of the myotonic dystrophy area on 19q. Genomics *13*, 509–517.

Jansen, G., Groenen, P.J.T.A., Bächner, D., Jap, P.H.K., Coerwinkel, M., Oerlemans, F., van den Broek, W., Gohlsch, B., Pette, D., Plomp, J.J., et al. (1996). Abnormal myotonic dystrophy protein kinase levels produce only mild myopathy in mice. Nat. Genet. *13*, 316–324.

Januszyk, K., and Lima, C.D. (2014). The eukaryotic RNA exosome. Curr. Opin. Struct. Biol. *24*, 132–140.

Jauvin, D., Chrétien, J., Pandey, S.K., Martineau, L., Revillod, L., Bassez, G., Lachon, A., McLeod, A.R., Gourdon, G., Wheeler, T.M., et al. (2017). Targeting DMPK with Antisense Oligonucleotide Improves Muscle Strength in Myotonic Dystrophy Type 1 Mice. Mol. Ther. Nucleic Acids *7*, 465–474.

Jiang, H., Mankodi, A., Swanson, M.S., Moxley, R.T., and Thornton, C.A. (2004). Myotonic dystrophy type 1 is associated with nuclear foci of mutant RNA, sequestration of muscleblind proteins and deregulated alternative splicing in neurons. Hum. Mol.

Genet. *13*, 3079–3088.

Jiao, X., Chang, J.H., Kilic, T., Tong, L., and Kiledjian, M. (2013). A mammalian pre-mRNA 5' end capping quality control mechanism and an unexpected link of capping to pre-mRNA processing. Mol. Cell *50*, 104–115.

Johnson, C., Primorac, D., McKinstry, M., McNeil, J., Rowe, D., and Lawrence, J.B. (2000). Tracking COL1A1 RNA in osteogenesis imperfecta. splice-defective transcripts initiate transport from the gene but are retained within the SC35 domain. J. Cell Biol. *150*, 417–432.

Jones, C.I., Zabolotskaya, M.V., and Newbury, S.F. (2012a). The 5′ → 3′ exoribonuclease XRN1/Pacman and its functions in cellular processes and development. Wiley Interdiscip. Rev. RNA *3*, 455–468.

Jones, K., Wei, C., Iakova, P., Bugiardini, E., Schneider-Gold, C., Meola, G., Woodgett, J., Killian, J., Timchenko, N.A., and Timchenko, L.T. (2012b). GSK3β mediates muscle pathology in myotonic dystrophy. J. Clin. Invest. *122*, 4461–4472.

Jones, K., Wei, C., Schoser, B., Meola, G., Timchenko, N., and Timchenko, L. (2015). Reduction of toxic RNAs in myotonic dystrophies type 1 and type 2 by the RNA helicase p68/DDX5. Proc. Natl. Acad. Sci. U. S. A. *112*, 8041–8045.

Kalsotra, A., Xiao, X., Ward, A.J., Castle, J.C., Johnson, J.M., Burge, C.B., and Cooper, T.A. (2008). A postnatal switch of CELF and MBNL proteins reprograms alternative splicing in the developing heart. Proc. Natl. Acad. Sci. U. S. A. *105*, 20333–20338.

Kalsotra, A., Singh, R.K., Gurha, P., Ward, A.J., Creighton, C.J., and Cooper, T. a.

(2014). The Mef2 transcription network is disrupted in myotonic dystrophy heart tissue, dramatically altering miRNA and mRNA expression. Cell Rep. *6*, 336–345.

Kanadia, R.N., Johnstone, K.A., Mankodi, A., Lungu, C., Thornton, C.A., Esson, D., Timmers, A.M., Hauswirth, W.W., and Swanson, M.S. (2003). A Muscleblind Knockout Model for Myotonic Dystrophy. Science (80-.). *302*.

Kelly, S.M., Leung, S.W., Pak, C., Banerjee, A., Moberg, K.H., and Corbett, A.H. (2014). A conserved role for the zinc finger polyadenosine RNA binding protein, ZC3H14, in control of poly(A) tail length. RNA *20*, 681–688.

Ketley, A., Chen, C.Z., Li, X., Arya, S., Robinson, T.E., Granados-Riveron, J., Udosen, I., Morris, G.E., Holt, I., Furling, D., et al. (2014). High-content screening identifies small molecules that remove nuclear foci, affect MBNL distribution and CELF1 protein levels via a PKC-independent pathway in myotonic dystrophy cell lines. Hum. Mol. Genet. *23*, 1551–1562.

Kim, D.-H., Langlois, M.-A., Lee, K.-B., Riggs, A.D., Puymirat, J., and Rossi, J.J. (2005a). HnRNP H inhibits nuclear export of mRNA containing expanded CUG repeats and a distal branch point sequence. Nucleic Acids Res. *33*, 3866–3874.

Kim, Y.K., Furic, L., Desgroseillers, L., and Maquat, L.E. (2005b). Mammalian Staufen1 recruits Upf1 to specific mRNA 3'UTRs so as to elicit mRNA decay. Cell *120*, 195–208.

Kim, Y.K., Mandal, M., Yadava, R.S., Paillard, L., and Mahadevan, M.S. (2014). Evaluating the effects of CELF1 deficiency in a mouse model of RNA toxicity. Hum. Mol. Genet. *23*, 293–302.

Kim, Y.K., Yadava, R.S., Mandal, M., Mahadevan, K., Yu, Q., Leitges, M., and Mahadevan, M.S. (2016). Disease Phenotypes in a Mouse Model of RNA Toxicity Are Independent of Protein Kinase Cα and Protein Kinase Cβ. PLoS One *11*, e0163325.

Kimura, T., Nakamori, M., Lueck, J.D., Pouliquin, P., Aoike, F., Fujimura, H., Dirksen, R.T., Takahashi, M.P., Dulhunty, A.F., and Sakoda, S. (2005). Altered mRNA splicing of the skeletal muscle ryanodine receptor and sarcoplasmic/endoplasmic reticulum Ca2+-ATPase in myotonic dystrophy type 1. Hum. Mol. Genet. *14*, 2189–2200.

Kino, T., Hurt, D.E., Ichijo, T., Nader, N., and Chrousos, G.P. (2010). Noncoding RNA Gas5 Is a Growth Arrest- and Starvation-Associated Repressor of the Glucocorticoid Receptor. Sci. Signal. *3*, ra8-ra8.

Kino, Y., Washizu, C., Oma, Y., Onishi, H., Nezu, Y., Sasagawa, N., Nukina, N., and Ishiura, S. (2009). MBNL and CELF proteins regulate alternative splicing of the skeletal muscle chloride channel CLCN1. Nucleic Acids Res. *37*, 6477–6490.

Kino, Y., Washizu, C., Kurosawa, M., Oma, Y., Hattori, N., Ishiura, S., and Nukina, N. (2014). Nuclear localization of MBNL1: splicing-mediated autoregulation and repression of repeat-derived aberrant proteins. Hum. Mol. Genet.

Klesert, T.R., Cho, D.H., Clark, J.I., Maylie, J., Adelman, J., Snider, L., Yuen, E.C., Soriano, P., and Tapscott, S.J. (2000). Mice deficient in Six5 develop cataracts: implications for myotonic dystrophy. Nat. Genet. *25*, 105–109.

Koch, K.S., and Leffert, H.L. (1998). Giant Hairpins Formed by CUG Repeats in Myotonic Dystrophy Messenger RNAs Might Sterically Block RNA Export Through Nuclear Pores. J. Theor. Biol. *192*, 505–514.

Kong, H.E., Zhao, J., Xu, S., Jin, P., and Jin, Y. (2017). Fragile X-Associated Tremor/Ataxia Syndrome: From Molecular Pathogenesis to Development of Therapeutics. Front. Cell. Neurosci. *11*, 128.

Konzen, D., Moura de Souza, C.F., Saute, J.A.M., V, B., and G, T. (2017). A Cerebral Autosomal Dominant Arteriopathy With Subcortical Infarcts and Leukoencephalopathy Mimics on Brain Magnetic Resonance Imaging in Myotonic Dystrophy Type I. JAMA Neurol. *138*, 284–292.

Koob, M.D., Ranum, L.P.W., Moseley, M.L., Schut, L.J., Benzow, K.A., Bird, T.D., and Day, J.W. (1999). An untranslated CTG expansion causes a novel form of spinocerebellar ataxia (SCA8). Nat. Genet. *21*, 379–384.

Koshelev, M., Sarma, S., Price, R.E., Wehrens, X.H.T., and Cooper, T. a. (2010). Heart-specific overexpression of CUGBP1 reproduces functional and molecular abnormalities of myotonic dystrophy type 1. Hum. Mol. Genet. *19*, 1066–1075.

Kowolik, C.M., Liang, S., Yu, Y., and Yee, J.-K. (2004). Cre-mediated reversible immortalization of human renal proximal tubular epithelial cells. Oncogene *23*, 5950–5957.

Krahe, R., Ashizawa, T., Abbruzzese, C., Roeder, E., Carango, P., Giacanelli, M., Funanage, V.L., and Siciliano, M.J. (1995). Effect of Myotonic Dystrophy Trinucleotide Repeat Expansion on DMPK Transcription and Processing. Genomics *28*, 1–14.

Krol, J., Fiszer, A., Mykowska, A., Sobczak, K., de Mezer, M., and Krzyzosiak, W.J. (2007). Ribonuclease dicer cleaves triplet repeat hairpins into shorter repeats that silence specific targets. Mol. Cell *25*, 575–586.

Kühn, U., Buschmann, J., and Wahle, E. (2017). The nuclear poly(A) binding protein of mammals, but not of fission yeast, participates in mRNA polyadenylation. RNA *23*, 473–482.

Kurosaki, T., and Maquat, L.E. (2016). Nonsense-mediated mRNA decay in humans at a glance. J. Cell Sci. *129*, 461–467.

Kuyumcu-Martinez, N.M., Wang, G.-S., and Cooper, T.A. (2007). Increased Steady-State Levels of CUGBP1 in Myotonic Dystrophy 1 Are Due to PKC-Mediated Hyperphosphorylation. Mol. Cell *28*, 68–78.

de la Cruz, J., Kressler, D., and Linder, P. (1999). Unwinding RNA in Saccharomyces cerevisiae: DEAD-box proteins and related families. Trends Biochem. Sci. *24*, 192–198.

LaCava, J., Houseley, J., Saveanu, C., Petfalski, E., Thompson, E., Jacquier, A., and Tollervey, D. (2005). RNA degradation by the exosome is promoted by a nuclear polyadenylation complex. Cell *121*, 713–724.

Ladd, A.N., Charlet, N., and Cooper, T.A. (2001). The CELF family of RNA binding proteins is implicated in cell-specific and developmentally regulated alternative splicing. Mol. Cell. Biol. *21*, 1285–1296.

Langlois, M.-A., Lee, N.S., Rossi, J.J., and Puymirat, J. (2003a). Hammerhead ribozyme-mediated destruction of nuclear foci in myotonic dystrophy myoblasts. Mol. Ther. *7*, 670–680.

Langlois, M.-A., Furling, D., Boniface, C., and Puymirat, J. (2003b). Increased stability of mutant DMPK mRNA in congenital myotonic dystrophy. J. Biol. Chem.

Langlois, M.-A., Boniface, C., Wang, G., Alluin, J., Salvaterra, P.M., Puymirat, J., Rossi, J.J., and Lee, N.S. (2005). Cytoplasmic and nuclear retained DMPK mRNAs are targets for RNA interference in myotonic dystrophy cells. J. Biol. Chem. *280*, 16949–16954.

Laurent, F.-X.F.X., Sureau, A., Klein, A.F., Trouslard, F.F., Gasnier, E., Furling, D., and Marie, J.J. (2012). New function for the RNA helicase p68/DDX5 as a modifier of MBNL1 activity on expanded CUG repeats. Nucleic Acids Res. *40*, 3159–3171.

Lee, J.E., and Cooper, T.A. (2009). Pathogenic mechanisms of myotonic dystrophy. Biochem. Soc. Trans. *37*, 1281–1286.

Lee, G., Bratkowski, M.A., Ding, F., Ke, A., and Ha, T. (2012a). Elastic coupling between RNA degradation and unwinding by an exoribonuclease. Science (80-.). *336*, 1726–1729.

Lee, J.E., Lee, J.Y., Wilusz, J., Tian, B., and Wilusz, C.J. (2010). Systematic analysis of cis-elements in unstable mRNAs demonstrates that CUGBP1 is a key regulator of mRNA decay in muscle cells. PLoS One *5*, e11201.

Lee, J.E., Bennett, C.F., and Cooper, T.A. (2012b). RNase H-mediated degradation of toxic RNA in myotonic dystrophy type 1. Proc. Natl. Acad. Sci. U. S. A. *109*, 4221–4226.

Lee, S., Kopp, F., Chang, T.-C., Sataluri, A., Chen, B., Sivakumar, S., Yu, H., Xie, Y., and Mendell, J.T. (2016). Noncoding RNA NORAD Regulates Genomic Stability by Sequestering PUMILIO Proteins. Cell *164*, 69–80.

Lejeune, F., Li, X., and Maquat, L.E. (2003). Nonsense-mediated mRNA decay in mammalian cells involves decapping, deadenylating, and exonucleolytic activities. Mol.

Cell *12*, 675–687.

Li, Y., Song, M., and Kiledjian, M. (2011). Differential utilization of decapping enzymes in mammalian mRNA decay pathways. RNA *17*, 419–428.

Li, Y., Song, Y.-H., Liu, B., and Yu, X.-Y. (2017). The potential application and challenge of powerful CRISPR/Cas9 system in cardiovascular research. Int. J. Cardiol. *227*, 191–193.

Lin, J.-C., Lee, Y.-C., Liang, Y.-C., Fann, Y.C., Johnson, K.R., and Lin, Y.-J. (2017). The impact of the RBM4-initiated splicing cascade on modulating the carcinogenic signature of colorectal cancer cells. Sci. Rep. *7*, 44204.

Lin, J.C., Hsu, M., and Tarn, W.Y. (2007). Cell stress modulates the function of splicing regulatory protein RBM4 in translation control. Proc. Natl. Acad. Sci. *104*, 2235–2240.

Liquori, C.L., Ricker, K., Moseley, M.L., Jacobsen, J.F., Kress, W., Naylor, S.L., Day, J.W., and Ranum, L.P.W. (2001). Myotonic Dystrophy Type 2 Caused by a CCTG Expansion in Intron 1 of ZNF9. Science (80-.). *293*.

Liu, H., Rodgers, N.D., Jiao, X., and Kiledjian, M. (2002). The scavenger mRNA decapping enzyme DcpS is a member of the HIT family of pyrophosphatases. EMBO J. *21*, 4699–4708.

Liu, S.-W., Jiao, X., Liu, H., Gu, M., Lima, C.D., and Kiledjian, M. (2004). Functional analysis of mRNA scavenger decapping enzymes. RNA *10*, 1412–1422.

Ljungman, M., Zhang, F., Chen, F., Rainbow, A.J., and McKay, B.C. (1999). Inhibition of RNA polymerase II as a trigger for the p53 response. Oncogene *18*, 583–592.

Loh, B., Jonas, S., and Izaurralde, E. (2013). The SMG5-SMG7 heterodimer directly recruits the CCR4-NOT deadenylase complex to mRNAs containing nonsense codons via interaction with POP2. Genes Dev. *27*, 2125–2138.

López-Perrote, A., Castaño, R., Melero, R., Zamarro, T., Kurosawa, H., Ohnishi, T., Uchiyama, A., Aoyagi, K., Buchwald, G., Kataoka, N., et al. (2016). Human nonsense-mediated mRNA decay factor UPF2 interacts directly with eRF3 and the SURF complex. Nucleic Acids Res. *44*, 1909–1923.

Lubas, M., Damgaard, C.K., Tomecki, R., Cysewski, D., Jensen, T.H., and Dziembowski, A. (2013). Exonuclease hDIS3L2 specifies an exosome-independent 3'-5' degradation pathway of human cytoplasmic mRNA. EMBO J. *32*, 1855–1868.

Lucchiari, S., Pagliarani, S., Corti, S., Mancinelli, E., Servida, M., Fruguglietti, E., Sansone, V., Moggio, M., Bresolin, N., Comi, G.P., et al. (2008). Colocalization of ribonuclear inclusions with muscle blind like-proteins in a family with myotonic dystrophy type 2 associated with a short CCTG expansion.

Lukáš, Z., Falk, M., Feit, J., Souček, O., Falková, I., Štefančíková, L., Janoušová, E., Fajkusová, L., Zaorálková, J., and Hrabálková, R. (2012). Sequestration of MBNL1 in tissues of patients with myotonic dystrophy type 2. Neuromuscul. Disord. *22*, 604–616.

Luu, L.M., Nguyen, L., Peng, S., Lee, J., Lee, H.Y., Wong, C.-H., Hergenrother, P.J., Chan, H.Y.E., and Zimmerman, S.C. (2016). A Potent Inhibitor of Protein Sequestration by Expanded Triplet (CUG) Repeats that Shows Phenotypic Improvements in a Drosophila Model of Myotonic Dystrophy. ChemMedChem *11*, 1428–1435.

Lykke-Andersen, S., Chen, Y., Ardal, B.R., Lilje, B., Waage, J., Sandelin, A., and

Jensen, T.H. (2014). Human nonsense-mediated RNA decay initiates widely by endonucleolysis and targets snoRNA host genes. Genes Dev. *28*, 2498–2517.

Machyna, M., Neugebauer, K.M., and Staněk, D. (2015). Coilin: The first 25 years. RNA Biol. *12*, 590–596.

Maeda, M., Taft, C.S., Bush, E.W., Holder, E., Bailey, W.M., Neville, H., Perryman, M.B., and Bies, R.D. (1995). Identification, tissue-specific expression, and subcellular localization of the 80- and 71-kDa forms of myotonic dystrophy kinase protein. J. Biol. Chem. *270*, 20246–20249.

Mahadevan, M., Tsilfidis, C., Sabourin, L., Shutler, G., Amemiya, C., Jansen, G., Neville, C., Narang, M., Barcelo, J., O'Hoy, K., et al. (1992). Myotonic dystrophy mutation: an unstable CTG repeat in the 3' untranslated region of the gene. Science (80-.). *255*.

Mahadevan, M.S., Yadava, R.S., Yu, Q., Balijepalli, S., Frenzel-McCardell, C.D., Bourne, T.D., and Phillips, L.H. (2006). Reversible model of RNA toxicity and cardiac conduction defects in myotonic dystrophy. Nat. Genet. *38*, 1066–1070.

Malecki, M., Viegas, S.C., Carneiro, T., Golik, P., Dressaire, C., Ferreira, M.G., and Arraiano, C.M. (2013). The exoribonuclease Dis3L2 defines a novel eukaryotic RNA degradation pathway. EMBO J. *32*, 1842–1854.

Mandel, C.R., Kaneko, S., Zhang, H., Gebauer, D., Vethantham, V., Manley, J.L., and Tong, L. (2006). Polyadenylation factor CPSF-73 is the pre-mRNA 3'-end-processing endonuclease. Nature *444*, 953–956.

Mankodi, A., Logigian, E., Callahan, L., McClain, C., White, R., Henderson, D., Krym, M., and Thornton, C.A. (2000). Myotonic Dystrophy in Transgenic Mice Expressing an Expanded CUG Repeat. Science (80-.). *289*.

Mankodi, A., Urbinati, C.R., Yuan, Q.P., Moxley, R.T., Sansone, V., Krym, M., Henderson, D., Schalling, M., Swanson, M.S., and Thornton, C.A. (2001). Muscleblind localizes to nuclear foci of aberrant RNA in myotonic dystrophy types 1 and 2. Hum. Mol. Genet. *10*, 2165–2170.

Mankodi, A., Takahashi, M.P., Jiang, H., Beck, C.L., Bowers, W.J., Moxley, R.T., Cannon, S.C., and Thornton, C.A. (2002). Expanded CUG repeats trigger aberrant splicing of ClC-1 chloride channel pre-mRNA and hyperexcitability of skeletal muscle in myotonic dystrophy. Mol. Cell *10*, 35–44.

Mankodi, A., Teng-Umnuay, P., Krym, M., Henderson, D., Swanson, M., and Thornton, C.A. (2003). Ribonuclear inclusions in skeletal muscle in myotonic dystrophy types 1 and 2. Ann. Neurol. *54*, 760–768.

Marchini, C., Lonigro, R., Verriello, L., Pellizzari, L., Bergonzi, P., and Damante, G. (2000). Correlations between individual clinical manifestations and CTG repeat amplification in myotonic dystrophy. Clin. Genet. *57*, 74–82.

Margolis, R.L., O'Hearn, E., Rosenblatt, A., Willour, V., Holmes, S.E., Franz, M.L., Callahan, C., Hwang, H.S., Troncoso, J.C., and Ross, C.A. (2001). A disorder similar to Huntington's disease is associated with a novel CAG repeat expansion. Ann. Neurol. *50*, 373–380.

Markus, M.A., Yang, Y.H.J., and Morris, B.J. (2016). Transcriptome-wide targets of

alternative splicing by RBM4 and possible role in cancer. Genomics *107*, 138–144.

Martel, C., Macchi, P., Furic, L., Kiebler, M.A., and Desgroseillers, L. (2006). Staufen1 is imported into the nucleolus via a bipartite nuclear localization signal and several modulatory determinants. Biochem. J. *393*, 245–254.

Martinez, J., Ren, Y.G., Thuresson, A.C., Hellman, U., Astrom, J., and Virtanen, A. (2000). A 54-kDa fragment of the Poly(A)-specific ribonuclease is an oligomeric, processive, and cap-interacting Poly(A)-specific 3' exonuclease. J. Biol. Chem. *275*, 24222–24230.

Martînez, J., Ren, Y.G., Nilsson, P., Ehrenberg, M., and Virtanen, A. (2001). The mRNA cap structure stimulates rate of poly(A) removal and amplifies processivity of degradation. J. Biol. Chem. *276*, 27923–27929.

Mastroyiannopoulos, N.P., Feldman, M.L., Uney, J.B., Mahadevan, M.S., and Phylactou, L.A. (2005). Woodchuck post-transcriptional element induces nuclear export of myotonic dystrophy 3' untranslated region transcripts. EMBO Rep. *6*, 458–463.

Masuda, S., Das, R., Cheng, H., Hurt, E., Dorman, N., and Reed, R. (2005). Recruitment of the human TREX complex to mRNA during splicing. Genes Dev. *19*, 1512–1517.

Mateos-Aierdi, A.J., Goicoechea, M., Aiastui, A., Fernández-Torrón, R., Garcia-Puga, M., Matheu, A., and de Munain, A.L. (2015). Muscle wasting in myotonic dystrophies: a model of premature aging. Front. Aging Neurosci. *7*, 125.

Mathieu, J., and Prévost, C. (2012). Epidemiological surveillance of myotonic dystrophy

type 1: A 25-year population-based study. Neuromuscul. Disord. *22*, 974–979.

McKinsey, T.A., Zhang, C.L., and Olson, E.N. (2002). MEF2: a calcium-dependent regulator of cell division, differentiation and death. Trends Biochem. Sci. *27*, 40–47.

McLennan, A.G. (2006). The Nudix hydrolase superfamily. Cell. Mol. Life Sci. *63*, 123–143.

Meinel, D.M., Burkert-Kautzsch, C., Kieser, A., O'Duibhir, E., Siebert, M., Mayer, A., Cramer, P., S?ding, J., Holstege, F.C.P., and Str??er, K. (2013). Recruitment of TREX to the Transcription Machinery by Its Direct Binding to the Phospho-CTD of RNA Polymerase II. PLoS Genet. *9*, e1003914.

Melacini, P., Villanova, C., Menegazzo, E., Novelli, G., Danieli, G., Rizzoli, G., Fasoli, G., Angelini, C., Buja, G., Miorelli, M., et al. (1995). Correlation between cardiac involvement and CTG trinucleotide repeat length in myotonic dystrophy. J. Am. Coll. Cardiol. *25*, 239–245.

Meola, G. (2013). Clinical aspects, molecular pathomechanisms and management of myotonic dystrophies. Acta Myol. Myopathies Cardiomyopathies Off. J. Mediterr. Soc. Myol. *32*, 154–165.

Miki, T.S., and Großhans, H. (2013). The multifunctional RNase XRN2. Biochem. Soc. Trans. *41*.

Mila, M., Alvarez-Mora, M.I., Madrigal, I., and Rodriguez-Revenga, L. (2017). Fragile X syndrome: an overview and update of the FMR1 gene. Clin. Genet.

Miller, J.W., Urbinati, C.R., Teng-Umnuay, P., Stenberg, M.G., Byrne, B.J., Thornton,

C.A., and Swanson, M.S. (2000). Recruitment of human muscleblind proteins to (CUG)(n) expansions associated with myotonic dystrophy. EMBO J. *19*, 4439–4448.

Milligan, L., Torchet, C., Allmang, C., Shipman, T., and Tollervey, D. (2005). A nuclear surveillance pathway for mRNAs with defective polyadenylation. Mol. Cell. Biol. *25*, 9996–10004.

Milligan, L., Decourty, L., Saveanu, C., Rappsilber, J., Ceulemans, H., Jacquier, A., and Tollervey, D. (2008). A yeast exosome cofactor, Mpp6, functions in RNA surveillance and in the degradation of noncoding RNA transcripts. Mol. Cell. Biol. *28*, 5446–5457.

Min, H., Turck, C.W., Nikolic, J.M., and Black, D.L. (1997). A new regulatory protein, KSRP, mediates exon inclusion through an intronic splicing enhancer. Genes Dev. *11*, 1023–1036.

Mitchell, P., and Tollervey, D. (2003). An NMD Pathway in Yeast Involving Accelerated Deadenylation and Exosome-Mediated 3′→5′ Degradation. Mol. Cell *11*, 1405–1413.

Molenaar, C., Abdulle, A., Gena, A., Tanke, H.J., and Dirks, R.W. (2004). Poly(A)+ RNAs roam the cell nucleus and pass through speckle domains in transcriptionally active and inactive cells. J. Cell Biol. *165*, 191–202.

Mooers, B.H.M., Logue, J.S., and Berglund, J.A. (2005). The structural basis of myotonic dystrophy from the crystal structure of CUG repeats. Proc. Natl. Acad. Sci. U. S. A. *102*, 16626–16631.

Moon, S.L.S., Wilusz, J., Schoenberg, D., Maquat, L., Tycowski, K., Shu, M., Borah, S., Shi, M., Steitz, J., Dougherty, J., et al. (2013). Cytoplasmic Viruses: Rage against the

(Cellular RNA Decay) Machine. PLoS Pathog. *9*, e1003762.

Moon, S.L.S., Blackinton, J.G., Anderson, J.R.J., Dozier, M.K., Dodd, B.J.T., Keene, J.D., Wilusz, C.J.C., Bradrick, S.S.S., Wilusz, J., Stephanie L. Moon, Jeffrey G. Blackinton, John R. Anderson, Mary K. Dozier, Benjamin J. T. Dodd, Jack D. Keene, Carol J. Wilusz, Shelton S. Bradrick, J.W., et al. (2015). XRN1 Stalling in the 5' UTR of Hepatitis C Virus and Bovine Viral Diarrhea Virus Is Associated with Dysregulated Host mRNA Stability. PLOS Pathog. *11*, e1004708.

Morales, J.C., Richard, P., Patidar, P.L., Motea, E.A., Dang, T.T., Manley, J.L., and Boothman, D.A. (2016). XRN2 Links Transcription Termination to DNA Damage and Replication Stress. PLOS Genet. *12*, e1006107.

Morriss, G.R., and Cooper, T.A. (2017). Protein sequestration as a normal function of long noncoding RNAs and a pathogenic mechanism of RNAs containing nucleotide repeat expansions. Hum. Genet. *136*, 1247–1263.

Moseley, M.L., Zu, T., Ikeda, Y., Gao, W., Mosemiller, A.K., Daughters, R.S., Chen, G., Weatherspoon, M.R., Clark, H.B., Ebner, T.J., et al. (2006). Bidirectional expression of CUG and CAG expansion transcripts and intranuclear polyglutamine inclusions in spinocerebellar ataxia type 8. Nat. Genet. *38*, 758–769.

Moteki, S., and Price, D. (2002). Functional Coupling of Capping and Transcription of mRNA. Mol. Cell *10*, 599–609.

Muhlrad, D., and Parker, R. (2005). The yeast EDC1 mRNA undergoes deadenylation-independent decapping stimulated by Not2p, Not4p, and Not5p. EMBO J. *24*, 1033–1045.

Muhlrad, D., Decker, C.J., and Parker, R. (1994). Deadenylation of the unstable mRNA encoded by the yeast MFA2 gene leads to decapping followed by 5'-->3' digestion of the transcript. Genes Dev. *8*, 855–866.

Mukherjee, D., Gao, M., O'Connor, J.P., Raijmakers, R., Pruijn, G., Lutz, C.S., and Wilusz, J. (2002). The mammalian exosome mediates the efficient degradation of mRNAs that contain AU-rich elements. EMBO J. *21*, 165–174.

Mulders, S.A.M., van den Broek, W.J.A.A., Wheeler, T.M., Croes, H.J.E., van Kuik-Romeijn, P., de Kimpe, S.J., Furling, D., Platenburg, G.J., Gourdon, G., Thornton, C.A., et al. (2009). Triplet-repeat oligonucleotide-mediated reversal of RNA toxicity in myotonic dystrophy. Proc. Natl. Acad. Sci. U. S. A. *106*, 13915–13920.

Nagarajan, V.K., Jones, C.I., Newbury, S.F., and Green, P.J. (2013). XRN 5'→3' exoribonucleases: structure, mechanisms and functions. Biochim. Biophys. Acta *1829*, 590–603.

Nakamori, M., Kimura, T., Fujimura, H., Takahashi, M.P., and Sakoda, S. (2007). Altered mRNA splicing of dystrophin in type 1 myotonic dystrophy. Muscle Nerve *36*, 251–257.

Nakamori, M., Taylor, K., Mochizuki, H., Sobczak, K., and Takahashi, M.P. (2016). Oral administration of erythromycin decreases RNA toxicity in myotonic dystrophy. Ann. Clin. Transl. Neurol. *3*, 42–54.

Neff, A.T., Lee, J.Y., Wilusz, J., Tian, B., and Wilusz, C.J. (2012). Global analysis reveals multiple pathways for unique regulation of mRNA decay in induced pluripotent stem cells. Genome Res. *22*, 1457–1467.

Ni, J.Z., Grate, L., Donohue, J.P., Preston, C., Nobida, N., O'Brien, G., Shiue, L., Clark, T.A., Blume, J.E., Ares, M., et al. (2007). Ultraconserved elements are associated with homeostatic control of splicing regulators by alternative splicing and nonsense-mediated decay. Genes Dev. *21*, 708–718.

Nigro, G., Papa, A.A., and Politano, L. (2012). The heart and cardiac pacing in Steinert disease. Acta Myol. Myopathies Cardiomyopathies Off. J. Mediterr. Soc. Myol. *31*, 110–116.

Nott, A., Le Hir, H., and Moore, M.J. (2004). Splicing enhances translation in mammalian cells: an additional function of the exon junction complex. Genes Dev. *18*, 210–222.

Ogami, K., Richard, P., Chen, Y., Hoque, M., Li, W., Moresco, J.J., Yates, J.R., Tian, B., and Manley, J.L. (2017). An Mtr4/ZFC3H1 complex facilitates turnover of unstable nuclear RNAs to prevent their cytoplasmic transport and global translational repression. Genes Dev. *31*, 1257–1271.

Ohno, M., Sakamoto, H., and Shimura, Y. (1987). Preferential excision of the 5' proximal intron from mRNA precursors with two introns as mediated by the cap structure. Proc. Natl. Acad. Sci. U. S. A. *84*, 5187–5191.

Okada-Katsuhata, Y., Yamashita, A., Kutsuzawa, K., Izumi, N., Hirahara, F., and Ohno, S. (2012). N- and C-terminal Upf1 phosphorylations create binding platforms for SMG-6 and SMG-5:SMG-7 during NMD. Nucleic Acids Res. *40*, 1251–1266.

Orban, T.I., and Izaurralde, E. (2005). Decay of mRNAs targeted by RISC requires XRN1, the Ski complex, and the exosome. RNA *11*, 459–469.

Orengo, J.P., Chambon, P., Metzger, D., Mosier, D.R., Snipes, G.J., and Cooper, T.A. (2008). Expanded CTG repeats within the DMPK 3' UTR causes severe skeletal muscle wasting in an inducible mouse model for myotonic dystrophy. Proc. Natl. Acad. Sci. U. S. A. *105*, 2646–2651.

Oude Ophuis, R.J.A., Wijers, M., Bennink, M.B., van de Loo, F.A.J., Fransen, J.A.M., Wieringa, B., and Wansink, D.G. (2009). A Tail-Anchored Myotonic Dystrophy Protein Kinase Isoform Induces Perinuclear Clustering of Mitochondria, Autophagy, and Apoptosis. PLoS One *4*, e8024.

Pabis, M., Neufeld, N., Steiner, M.C., Bojic, T., Shav-Tal, Y., and Neugebauer, K.M. (2013). The nuclear cap-binding complex interacts with the U4/U6·U5 tri-snRNP and promotes spliceosome assembly in mammalian cells. RNA *19*, 1054–1063.

Palaniswamy, V., Moraes, K.C.M., Wilusz, C.J., and Wilusz, J. (2006). Nucleophosmin is selectively deposited on mRNA during polyadenylation. Nat. Struct. Mol. Biol. *13*, 429–435.

Palladino, A., D'Ambrosio, P., Papa, A.A., Petillo, R., Orsini, C., Scutifero, M., Nigro, G., and Politano, L. (2016). Management of cardiac involvement in muscular dystrophies: paediatric versus adult forms. Acta Myol. Myopathies Cardiomyopathies Off. J. Mediterr. Soc. Myol. *35*, 128–134.

Pandey, S.K., Wheeler, T.M., Justice, S.L., Kim, A., Younis, H.S., Gattis, D., Jauvin, D., Puymirat, J., Swayze, E.E., Freier, S.M., et al. (2015). Identification and characterization of modified antisense oligonucleotides targeting DMPK in mice and nonhuman primates for the treatment of myotonic dystrophy type 1. J. Pharmacol. Exp. Ther. *355*, 329–340.

Paul, S., Dansithong, W., Kim, D., Rossi, J., Webster, N.J.G., Comai, L., and Reddy, S. (2006). Interaction of muscleblind, CUG-BP1 and hnRNP H proteins in DM1-associated aberrant IR splicing. EMBO J. *25*, 4271–4283.

Pedrotti, S., Giudice, J., Dagnino-Acosta, A., Knoblauch, M., Singh, R.K., Hanna, A., Mo, Q., Hicks, J., Hamilton, S., and Cooper, T.A. (2015). The RNA-binding protein Rbfox1 regulates splicing required for skeletal muscle structure and function. Hum. Mol. Genet. *24*, 2360–2374.

Peng, W.-T., Robinson, M.D., Mnaimneh, S., Krogan, N.J., Cagney, G., Morris, Q., Davierwala, A.P., Grigull, J., Yang, X., Zhang, W., et al. (2003). A Panoramic View of Yeast Noncoding RNA Processing. Cell *113*, 919–933.

Peresleni, T.I., Mavletova, D.A., and Dvorkin, G.A. (1988). Effect of cycloheximide on transcription in eukaryotic cells. Biokhimiia *53*, 694–698.

Perfetti, A., Greco, S., Bugiardini, E., Cardani, R., Gaia, P., Gaetano, C., Meola, G., and Martelli, F. (2014). Plasma microRNAs as biomarkers for myotonic dystrophy type 1. Neuromuscul. Disord. *24*, 509–515.

Personius, K.E., Nautiyal, J., and Reddy, S. (2005). Myotonia and muscle contractile properties in mice withSIX5 deficiency. Muscle Nerve *31*, 503–505.

Pešović, J., Perić, S., Brkušanin, M., Brajušković, G., Rakočević-Stojanović, V., and Savić-Pavićević, D. (2017). Molecular genetic and clinical characterization of myotonic dystrophy type 1 patients carrying variant repeats within DMPK expansions. Neurogenetics.

Pestova, T. V., Lomakin, I.B., Lee, J.H., Choi, S.K., Dever, T.E., and Hellen, C.U.T. (2000). The joining of ribosomal subunits in eukaryotes requires eIF5B. Nature *403*, 332–335.

Pettersson, O.J., Aagaard, L., Andrejeva, D., Thomsen, R., Jensen, T.G., and Damgaard, C.K. (2014). DDX6 regulates sequestered nuclear CUG-expanded DMPK-mRNA in dystrophia myotonica type 1. Nucleic Acids Res. *42*, 7186–7200.

Pettersson, O.J., Aagaard, L., Jensen, T.G., and Damgaard, C.K. (2015). Molecular mechanisms in DM1 — a focus on foci. Nucleic Acids Res. *43*, 2433–2441.

Philips, A. V., Timchenko, L.T., and Cooper, T.A. (1998). Disruption of Splicing Regulated by a CUG-Binding Protein in Myotonic Dystrophy. Science (80-.). *280*.

te Poele, R.H., Okorokov, A.L., and Joel, S.P. (1999). RNA synthesis block by 5,6-dichloro-1-β-D-ribofuranosylbenzimidazole (DRB) triggers p53-dependent apoptosis in human colon carcinoma cells. Oncogene *18*, 5765–5772.

Pollock, C., and Huang, S. (2010). The perinucleolar compartment. Cold Spring Harb. Perspect. Biol. *2*, a000679.

Provost, P., Dishart, D., Doucet, J., Frendewey, D., Samuelsson, B., and Rådmark, O. (2002). Ribonuclease activity and RNA binding of recombinant human Dicer. EMBO J. *21*, 5864–5874.

Querido, E., Gallardo, F., Beaudoin, M., Ménard, C., and Chartrand, P. (2011). Stochastic and reversible aggregation of mRNA with expanded CUG-triplet repeats. J. Cell Sci. *124*, 1703–1714.

Rädle, B., Rutkowski, A.J., Ruzsics, Z., Friedel, C.C., Koszinowski, U.H., and Dölken, L. (2013). Metabolic labeling of newly transcribed RNA for high resolution gene expression profiling of RNA synthesis, processing and decay in cell culture. J. Vis. Exp.

Ranum, L.P.W., and Day, J.W. (2004). Myotonic dystrophy: RNA pathogenesis comes into focus. Am. J. Hum. Genet. *74*, 793–804.

Rau, F., Lainé, J., Ramanoudjame, L., Ferry, A., Arandel, L., Delalande, O., Jollet, A., Dingli, F., Lee, K.-Y., Peccate, C., et al. (2015). Abnormal splicing switch of DMD's penultimate exon compromises muscle fibre maintenance in myotonic dystrophy. Nat. Commun. *6*, 7205.

Ravel-Chapuis, A., Bélanger, G., Yadava, R.S., Mahadevan, M.S., DesGroseillers, L., Côté, J., and Jasmin, B.J. (2012). The RNA-binding protein Staufen1 is increased in DM1 skeletal muscle and promotes alternative pre-mRNA splicing. J. Cell Biol. *196*, 699–712.

Raymond, L.A., André, V.M., Cepeda, C., Gladding, C.M., Milnerwood, A.J., and Levine, M.S. (2011). Pathophysiology of Huntington's disease: time-dependent alterations in synaptic and receptor function. Neuroscience *198*, 252–273.

Reardon, W., MacMillan, J.C., Myring, J., Harley, H.G., Rundle, S.A., Beck, L., Harper, P.S., and Shaw, D.J. (1993). Cataract and myotonic dystrophy: the role of molecular diagnosis. Br. J. Ophthalmol. *77*, 579–583.

Reddy, S., Smith, D.B.J., Rich, M.M., Leferovich, J.M., Reilly, P., Davis, B.M., Tran, K., Rayburn, H., Bronson, R., Cros, D., et al. (1996). Mice lacking the myotonic dystrophy protein kinase develop a late onset progressive myopathy. Nat. Genet. *13*, 325–335.

Renwick, J.H., Bundey, S.E., Ferguson-Smith, M.A., and Izattt, M.M. (1971). Confirmation of Linkage of the Loci for Myotonic Dystrophy and ABH Secretion. J. Med. Genet. *8*.

Robb, G.B., Brown, K.M., Khurana, J., and Rana, T.M. (2005). Specific and potent RNAi in the nucleus of human cells. Nat. Struct. Mol. Biol. *12*, 133–137.

Rollnik, J.D., Heinz, U., and Lenz, O. (2013). Myotonic dystrophy type 1 presenting with stroke-like episodes: a case report. BMC Res. Notes *6*, 243.

Rout, M.P., Aitchison, J.D., Suprapto, A., Hjertaas, K., Zhao, Y., and Chait, B.T. (2000). The yeast nuclear pore complex: composition, architecture, and transport mechanism. J. Cell Biol. *148*, 635–651.

Rudnicki, D.D., Holmes, S.E., Lin, M.W., Thornton, C.A., Ross, C.A., and Margolis, R.L. (2007). Huntington's disease-like 2 is associated with CUG repeat-containing RNA foci. Ann. Neurol. *61*, 272–282.

Russo, J., Heck, A.M., Wilusz, J., and Wilusz, C.J. (2017). Metabolic labeling and recovery of nascent RNA to accurately quantify mRNA stability. Methods *120*, 39–48.

Rzuczek, S.G., Southern, M.R., and Disney, M.D. (2015). Studying a Drug-like, RNA-Focused Small Molecule Library Identifies Compounds That Inhibit RNA Toxicity in Myotonic Dystrophy. ACS Chem. Biol. *10*, 2706–2715.

Sabouri, L.A., Mahadevan, M.S., Narang, M., Lee, D.S.C., Surh, L.C., and Korneluk, R.G. (1993). Effect of the myotonic dystrophy (DM) mutation on mRNA levels of the DM gene. Nat. Genet. *4*, 233–238.

Sachs, A.B., and Deardorff, J.A. (1992). Translation initiation requires the PAB-dependent poly(A) ribonuclease in yeast. Cell *70*, 961–973.

Sagawa, F., Ibrahim, H., Morrison, A.L., Wilusz, C.J., and Wilusz, J. (2011). Nucleophosmin deposition during mRNA 3′ end processing influences poly(A) tail length. EMBO J. *30*, 3994–4005.

Salas-Marco, J., and Bedwell, D.M. (2004). GTP hydrolysis by eRF3 facilitates stop codon decoding during eukaryotic translation termination. Mol. Cell. Biol. *24*, 7769–7778.

Sanpei, K., Takano, H., Igarashi, S., Sato, T., Oyake, M., Sasaki, H., Wakisaka, A., Tashiro, K., Ishida, Y., Ikeuchi, T., et al. (1996). Identification of the spinocerebellar ataxia type 2 gene using a direct identification of repeat expansion and cloning technique, DIRECT. Nat. Genet. *14*, 277–284.

Sansó, M., Levin, R.S., Lipp, J.J., Wang, V.Y.-F., Greifenberg, A.K., Quezada, E.M., Ali, A., Ghosh, A., Larochelle, S., Rana, T.M., et al. (2016). P-TEFb regulation of transcription termination factor Xrn2 revealed by a chemical genetic screen for Cdk9 substrates. Genes Dev. *30*, 117–131.

Santoro, M., Masciullo, M., Pietrobono, R., Conte, G., Modoni, A., Bianchi, M.L.E., Rizzo, V., Pomponi, M.G., Tasca, G., Neri, G., et al. (2013). Molecular, clinical, and muscle studies in myotonic dystrophy type 1 (DM1) associated with novel variant CCG expansions. J. Neurol. *260*, 1245–1257.

Sarkar, P.S., Appukuttan, B., Han, J., Ito, Y., Ai, C., Tsai, W., Chai, Y., Stout, J.T., and Reddy, S. (2000). Heterozygous loss of Six5 in mice is sufficient to cause ocular

cataracts. Nat. Genet. *25*, 110–114.

Savkur, R.S., Philips, A. V., and Cooper, T.A. (2001). Aberrant regulation of insulin receptor alternative splicing is associated with insulin resistance in myotonic dystrophy. Nat. Genet. Publ. Online 27 August 2001; | doi10.1038/ng704 *29*, 40.

Schilders, G., Raijmakers, R., Raats, J.M.H., and Pruijn, G.J.M. (2005). MPP6 is an exosome-associated RNA-binding protein involved in 5.8S rRNA maturation. Nucleic Acids Res. *33*, 6795–6804.

Schneider, C., Kudla, G., Wlotzka, W., Tuck, A., and Tollervey, D. (2012). Transcriptome-wide Analysis of Exosome Targets. Mol. Cell *48*, 422–433.

Schneider-Poetsch, T., Ju, J., Eyler, D.E., Dang, Y., Bhat, S., Merrick, W.C., Green, R., Shen, B., and Liu, J.O. (2010). Inhibition of eukaryotic translation elongation by cycloheximide and lactimidomycin. Nat. Chem. Biol. *6*, 209–217.

Schoser, B., and Timchenko, L. (2010). Myotonic dystrophies 1 and 2: complex diseases with complex mechanisms. Curr. Genomics *11*, 77–90.

Screaton, G.R., Cáceres, J.F., Mayeda, A., Bell, M. V, Plebanski, M., Jackson, D.G., Bell, J.I., and Krainer, A.R. (1995). Identification and characterization of three members of the human SR family of pre-mRNA splicing factors. EMBO J. *14*, 4336–4349.

Searfoss, A., Dever, T.E., and Wickner, R. (2001). Linking the 3’ poly(A) tail to the subunit joining step of translation initiation: relations of Pab1p, eukaryotic translation initiation factor 5b (Fun12p), and Ski2p-Slh1p. Mol. Cell. Biol. *21*, 4900–4908.

Seznec, H., Agbulut, O., Sergeant, N., Savouret, C., Ghestem, A., Tabti, N., Willer, J.C.,

Ourth, L., Duros, C., Brisson, E., et al. (2001). Mice transgenic for the human myotonic dystrophy region with expanded CTG repeats display muscular and brain abnormalities. Hum. Mol. Genet. *10*, 2717–2726.

Sharova, L. V, Sharov, A.A., Nedorezov, T., Piao, Y., Shaik, N., and Ko, M.S.H. (2009). Database for mRNA half-life of 19 977 genes obtained by DNA microarray analysis of pluripotent and differentiating mouse embryonic stem cells. DNA Res. *16*, 45–58.

Sheets, M.D., and Wickens, M. (1989). Two phases in the addition of a poly(A) tail. Genes Dev. *3*, 1401–1412.

Shelbourne, P., and Johnson, K. (1992). Myotonic dystrophy: Another case of too many repeats? Hum. Mutat. *1*, 183–189.

Shutler, G., Korneluk, R.G., Tsilfidis, C., Mahadevan, M., Bailly, J., Smeets, H., Jansen, G., Wieringa, B., Lohman, F., Aslanidis, C., et al. (1992). Physical mapping and cloning of the proximal segment of the myotonic dystrophy gene region. Genomics *13*, 518–525.

Siboni, R.B.B., Nakamori, M., Wagner, S.D.D., Struck, A.J.J., Coonrod, L.A.A., Harriott, S.A.A., Cass, D.M.M., Tanner, M.K.K., and Berglund, J.A.A. (2015). Actinomycin D Specifically Reduces Expanded CUG Repeat RNA in Myotonic Dystrophy Models. Cell Rep. *13*, 2386–2394.

Singh, S., Zhang, A., Dlouhy, S., and Bai, S. (2014). Detection of large expansions in myotonic dystrophy type 1 using triplet primed PCR. Front. Genet. *5*, 94.

Slomovic, S., Laufer, D., Geiger, D., and Schuster, G. (2006). Polyadenylation of

ribosomal RNA in human cells. Nucleic Acids Res. *34*, 2966–2975.

Smith, K.P., Byron, M., Johnson, C., Xing, Y., and Lawrence, J.B. (2007). Defining early steps in mRNA transport: mutant mRNA in myotonic dystrophy type I is blocked at entry into SC-35 domains. J. Cell Biol. *178*, 951–964.

Sobczak, K., Wheeler, T.M., Wang, W., and Thornton, C.A. (2013). RNA interference targeting CUG repeats in a mouse model of myotonic dystrophy. Mol. Ther. *21*, 380–387.

Solnestam, B., Stranneheim, H., Hällman, J., Käller, M., Lundberg, E., Lundeberg, J., and Akan, P. (2012). Comparison of total and cytoplasmic mRNA reveals global regulation by nuclear retention and miRNAs. BMC Genomics *13*, 574.

Song, M.-G., Li, Y., and Kiledjian, M. (2010). Multiple mRNA decapping enzymes in mammalian cells. Mol. Cell *40*, 423–432.

Stallings, R.L., Olson, E., Strauss, A.W., Thompson, L.H., Bachinski, L.L., and Siciliano, M.J. (1988). Human Creatine Kinase Genes on Chromosomes 15 and 19, and Proximity of the Gene for the Muscle Form to the Genes for Apolipoprotein C2 and Excision Repair. Am. J. Hum. Genet *43*, 144–151.

Steinert, H. (1909). Über das klinische und anatomische Bild des Muskelschwunds der Myotoniker. Dtsch Z Nervenheilkd 58–104.

Stoimenov, I., Schultz, N., Gottipati, P., and Helleday, T. (2011). Transcription Inhibition by DRB Potentiates Recombinational Repair of UV Lesions in Mammalian Cells. PLoS One *6*, e19492.

Storbeck, C.J., Drmanic, S., Daniel, K., Waring, J.D., Jirik, F.R., Parry, D.J., Ahmed, N., Sabourin, L.A., Ikeda, J.-E., and Korneluk, R.G. (2004). Inhibition of myogenesis in transgenic mice expressing the human DMPK 3'-UTR. Hum. Mol. Genet. *13*, 589–600.

Sureau, A., Gattoni, R., Dooghe, Y., Stévenin, J., and Soret, J. (2001). SC35 autoregulates its expression by promoting splicing events that destabilize its mRNAs. EMBO J. *20*, 1785–1796.

Szczepinska, T., Kalisiak, K., Tomecki, R., Labno, A., Borowski, L.S., Kulinski, T., Adamska, D., Kosinska, J., and Dziembowski, A. (2015). DIS3 shapes the RNA polymerase II transcriptome in humans by degrading a variety of unwanted transcripts. Genome Res.

Takahashi, S., Miyamoto, A., Oki, J., and Okuno, A. CTG trinucleotide repeat length and clinical expression in a family with myotonic dystrophy. Brain Dev. *18*, 127–130.

Taneja, K.L., McCurrach, M., Schalling, M., Housman, D., and Singer, R.H. (1995). Foci of trinucleotide repeat transcripts in nuclei of myotonic dystrophy cells and tissues. J. Cell Biol. *128*, 995–1002.

Tang, Y., Wang, H., Wei, B., Guo, Y., Gu, L., Yang, Z., Zhang, Q., Wu, Y., Yuan, Q., Zhao, G., et al. (2015). CUG-BP1 regulates RyR1 ASI alternative splicing in skeletal muscle atrophy. Sci. Rep. *5*, 16083.

Tarun, S.Z., and Sachs, A.B. (1996). Association of the yeast poly(A) tail binding protein with translation initiation factor eIF-4G. EMBO J. *15*, 7168–7177.

Taylor, M.J., and Peculis, B.A. (2008). Evolutionary conservation supports ancient origin

for Nudt16, a nuclear-localized, RNA-binding, RNA-decapping enzyme. Nucleic Acids Res. *36*, 6021–6034.

Tharun, S., He, W., Mayes, A.E., Lennertz, P., Beggs, J.D., and Parker, R. (2000). Yeast Sm-like proteins function in mRNA decapping and decay. Nature *404*, 515–518.

Thornton, C.A., Wang, E., and Carrell, E.M. (2017). Myotonic dystrophy: approach to therapy. Curr. Opin. Genet. Dev. *44*, 135–140.

Tian, B., White, R.J., Xia, T., Welle, S., Turner, D.H., Mathews, M.B., and Thornton, C.A. (2000). Expanded CUG repeat RNAs form hairpins that activate the double-stranded RNA-dependent protein kinase PKR. RNA *6*, 79–87.

Tichon, A., Gil, N., Lubelsky, Y., Havkin Solomon, T., Lemze, D., Itzkovitz, S., Stern-Ginossar, N., and Ulitsky, I. (2016). A conserved abundant cytoplasmic long noncoding RNA modulates repression by Pumilio proteins in human cells. Nat. Commun. *7*, 12209.

Timchenko, L.T., Timchenko, N.A., Caskey, C.T., and Roberts, R. (1996a). Novel Proteins with Binding Specificity for DNA CTG Repeats And RNA Cug Repeats: Implications for Myotonic Dystrophy. Hum. Mol. Genet. *5*, 115–121.

Timchenko, L.T., Miller, J.W., Timchenko, N.A., DeVore, D.R., Datar, K. V, Lin, L., Roberts, R., Caskey, C.T., and Swanson, M.S. (1996b). Identification of a (CUG)n triplet repeat RNA-binding protein and its expression in myotonic dystrophy. Nucleic Acids Res. *24*, 4407–4414.

Timchenko, N.A., Cai, Z.J., Welm, A.L., Reddy, S., Ashizawa, T., and Timchenko, L.T. (2001). RNA CUG repeats sequester CUGBP1 and alter protein levels and activity of

CUGBP1. J. Biol. Chem. *276*, 7820–7826.

Timchenko, N.A., Patel, R., Iakova, P., Cai, Z.-J.Z.-J., Quan, L., and Timchenko, L.T. (2004). Overexpression of CUG triplet repeat-binding protein, CUGBP1, in mice inhibits myogenesis. J. Biol. Chem. *279*, 13129–13139.

Tiscornia, G., and Mahadevan, M.S. (2000). Myotonic Dystrophy: The Role of the CUG Triplet Repeats in Splicing of a Novel DMPK Exon and Altered Cytoplasmic DMPK mRNA Isoform Ratios. Mol. Cell *5*, 959–967.

Tollervey, D. (2004). Molecular biology: Termination by torpedo. Nature *432*, 456–457.

Tomecki, R., Kristiansen, M.S., Lykke-Andersen, S., Chlebowski, A., Larsen, K.M., Szczesny, R.J., Drazkowska, K., Pastula, A., Andersen, J.S., Stepien, P.P., et al. (2010). The human core exosome interacts with differentially localized processive RNases: hDIS3 and hDIS3L. EMBO J. *29*, 2342–2357.

Trachsel, H., Erni, B., Schreier, H., and Staehelw-F, T. (1977). Initiation of Mammalian Protein Synthesis II. The Assembly of the Initiation Complex with Purified Initiation Factors. J. Mol. Biol *116*, 755–767.

Uchida, N., Hoshino, S.-I., Imataka, H., Sonenberg, N., and Katada, T. (2002). A novel role of the mammalian GSPT/eRF3 associating with poly(A)-binding protein in Cap/Poly(A)-dependent translation. J. Biol. Chem. *277*, 50286–50292.

Udd, B., and Krahe, R. (2012). The myotonic dystrophies: molecular, clinical, and therapeutic challenges. Lancet Neurol. *11*, 891–905.

Urbanek, M., Nawrocka, A., and Krzyzosiak, W. (2015). Small RNA Detection by in Situ

Hybridization Methods. Int. J. Mol. Sci. *16*, 13259–13286.

Usuki, F., Ishiura, S., Saitoh, N., Sasagawa, N., Sorimachi, H., Kuzume, H., Maruyama, K., Terao, T., and Suzuki, K. (1997). Expanded CTG repeats in myotonin protein kinase suppresses myogenic differentiation. Neuroreport *8*, 3749–3753.

Usuki, F., Takahashi, N., Sasagawa, N., and Ishiura, S. (2000). Differential signaling pathways following oxidative stress in mutant myotonin protein kinase cDNA-transfected C2C12 cell lines. Biochem. Biophys. Res. Commun. *267*, 739–743.

Varsally, W., and Brogna, S. (2012). UPF1 involvement in nuclear functions. Biochem. Soc. Trans. *40*, 778–783.

Verkerk, A.J., Pieretti, M., Sutcliffe, J.S., Fu, Y.H., Kuhl, D.P., Pizzuti, A., Reiner, O., Richards, S., Victoria, M.F., and Zhang, F.P. (1991). Identification of a gene (FMR-1) containing a CGG repeat coincident with a breakpoint cluster region exhibiting length variation in fragile X syndrome. Cell *65*, 905–914.

Wahle, E. (1991). A novel poly(A)-binding protein acts as a specificity factor in the second phase of messenger RNA polyadenylation. Cell *66*, 759–768.

Wang, M., and Pestov, D.G. (2011). 5’-end surveillance by Xrn2 acts as a shared mechanism for mammalian pre-rRNA maturation and decay. Nucleic Acids Res. *39*, 1811–1822.

Wang, Z., and Kiledjian, M. (2001). Functional Link between the Mammalian Exosome and mRNA Decapping. Cell *107*, 751–762.

Wang, D., Furuichi, Y., and Shatkin, A.J. (1982). Covalent guanylyl intermediate formed

by HeLa cell mRNA capping enzyme. Mol. Cell. Biol. *2*, 993–1001.

Wang, G.-S., Kearney, D.L., De Biasi, M., Taffet, G., and Cooper, T.A. (2007). Elevation of RNA-binding protein CUGBP1 is an early event in an inducible heart-specific mouse model of myotonic dystrophy. J. Clin. Invest. *117*, 2802–2811.

Wang, G.S., Kuyumcu-Martinez, M.N., Sarma, S., Mathur, N., Wehrens, X.H.T., and Cooper, T. a. (2009). PKC inhibition ameliorates the cardiac phenotype in a mouse model of myotonic dystrophy type 1. J. Clin. Invest. *119*, 3797–3806.

Wang, J., Pegoraro, E., Menegazzo, E., Gennarelli, M., Hoop, R.C., Angelini, C., and Hoffman, E.P. (1995). Myotonic dystrophy: evidence for a possible dominant-negative RNA mutation. Hum. Mol. Genet. *4*, 599–606.

Wang, Y.H., Amirhaeri, S., Kang, S., Wells, R.D., and Griffith, J.D. (1994). Preferential nucleosome assembly at DNA triplet repeats from the myotonic dystrophy gene. Science *265*, 669–671.

Wang, Z., Jiao, X., Carr-Schmid, A., and Kiledjian, M. (2002). The hDcp2 protein is a mammalian mRNA decapping enzyme. Proc. Natl. Acad. Sci. *99*, 12663–12668.

Ward, A.J., Rimer, M., Killian, J.M., Dowling, J.J., and Cooper, T.A. (2010). CUGBP1 overexpression in mouse skeletal muscle reproduces features of myotonic dystrophy type 1. Hum. Mol. Genet. *19*, 3614–3622.

Warf, M.B., and Berglund, J.A. (2007). MBNL binds similar RNA structures in the CUG repeats of myotonic dystrophy and its pre-mRNA substrate cardiac troponin T. RNA *13*, 2238–2251.

Warf, M.B., Diegel, J. V, von Hippel, P.H., and Berglund, J.A. (2009). The protein factors MBNL1 and U2AF65 bind alternative RNA structures to regulate splicing. Proc. Natl. Acad. Sci. U. S. A. *106*, 9203–9208.

Warner, J.P., Barron, L.H., Goudie, D., Kelly, K., Dow, D., Fitzpatrick, D.R., and Brock, D.J. (1996). A general method for the detection of large CAG repeat expansions by fluorescent PCR. J. Med. Genet. *33*, 1022–1026.

Wasmuth, E. V, and Lima, C.D. (2012). Exo- and endoribonucleolytic activities of yeast cytoplasmic and nuclear RNA exosomes are dependent on the noncatalytic core and central channel. Mol. Cell *48*, 133–144.

Watanabe, K., Miyagawa, R., Tomikawa, C., Mizuno, R., Takahashi, A., Hori, H., and Ijiri, K. (2013). Degradation of initiator tRNA Met by Xrn1/2 via its accumulation in the nucleus of heat-treated HeLa cells. Nucleic Acids Res. *41*, 4671–4685.

Weil, D., Boutain, S., Audibert, A., and Dautry, F. (2000). Mature mRNAs accumulated in the nucleus are neither the molecules in transit to the cytoplasm nor constitute a stockpile for gene expression. RNA *6*, 962–975.

Weischenfeldt, J., Damgaard, I., Bryder, D., Theilgaard-Monch, K., Thoren, L.A., Nielsen, F.C., Jacobsen, S.E.W., Nerlov, C., and Porse, B.T. (2008). NMD is essential for hematopoietic stem and progenitor cells and for eliminating by-products of programmed DNA rearrangements. Genes Dev. *22*, 1381–1396.

Wells, S.E., Hillner, P.E., Vale, R.D., and Sachs, A.B. (1998). Circularization of mRNA by eukaryotic translation initiation factors. Mol. Cell *2*, 135–140.

West, S., Gromak, N., and Proudfoot, N.J. (2004). Human 5′ → 3′ exonuclease Xrn2 promotes transcription termination at co-transcriptional cleavage sites. Nature *432*, 522–525.

Wheeler, T.M., Sobczak, K., Lueck, J.D., Osborne, R.J., Lin, X., Dirksen, R.T., and Thornton, C.A. (2009). Reversal of RNA dominance by displacement of protein sequestered on triplet repeat RNA. Science *325*, 336–339.

Wheeler, T.M., Leger, A.J., Pandey, S.K., MacLeod, A.R., Nakamori, M., Cheng, S.H., Wentworth, B.M., Bennett, C.F., and Thornton, C.A. (2012). Targeting nuclear RNA for in vivo correction of myotonic dystrophy. Nature *488*, 111–115.

Wilburn, B., Rudnicki, D.D., Zhao, J., Weitz, T.M., Cheng, Y., Gu, X., Greiner, E., Park, C.S., Wang, N., Sopher, B.L., et al. (2011). An antisense CAG repeat transcript at JPH3 locus mediates expanded polyglutamine protein toxicity in Huntington's disease-like 2 mice. Neuron *70*, 427–440.

Wilkinson, M.F., and MacLeod, C.L. (1988). Complex regulation of the T cell receptor alpha gene: three different modes of triggering induction. Eur. J. Immunol. *18*, 873–879.

Williams, M.J., Eriksson, A., Shaik, M., Voisin, S., Yamskova, O., Paulsson, J., Thombare, K., Fredriksson, R., and Schiöth, H.B. (2015). The Obesity-Linked Gene Nudt3 Drosophila Homolog Aps Is Associated With Insulin Signaling. Mol. Endocrinol. *29*, 1303–1319.

Winstall, E., Sadowski, M., Kuhn, U., Wahle, E., and Sachs, A.B. (2000). The Saccharomyces cerevisiae RNA-binding protein Rbp29 functions in cytoplasmic mRNA metabolism. J. Biol. Chem. *275*, 21817–21826.

Wishart, J.A., Hayes, A., Wardleworth, L., Zhang, N., and Oliver, S.G. (2005). Doxycycline, the drug used to control the tet-regulatable promoter system, has no effect on global gene expression in Saccharomyces cerevisiae. Yeast *22*, 565–569.

Wojtkowiak-Szlachcic, A., Taylor, K., Stepniak-Konieczna, E., Sznajder, L.J., Mykowska, A., Sroka, J., Thornton, C.A., and Sobczak, K. (2015). Short antisense-locked nucleic acids (all-LNAs) correct alternative splicing abnormalities in myotonic dystrophy. Nucleic Acids Res. *43*, 3318–3331.

Wolin, S.L., Sim, S., and Chen, X. (2012). Nuclear noncoding RNA surveillance: is the end in sight? Trends Genet. *28*, 306–313.

Wong, N.C., Schwartz, H.L., Santos, A., and Oppenheimer, J.H. (1987). Cycloheximide inhibits S-14 gene transcription and abolishes DNase I hypersensitive S-14 sites in the livers of euthyroid but not hypothyroid rats. Mol. Endocrinol. *1*, 459–464.

Wormington, M., Searfoss, A.M., Hurney, C.A., Sachs, A., Birkenhäger, R., McCarthy, J., and Osborne, H. (1996). Overexpression of poly(A) binding protein prevents maturation-specific deadenylation and translational inactivation in Xenopus oocytes. EMBO J. *15*, 900–909.

Wu, D., Muhlrad, D., Bowler, M.W., Jiang, S., Liu, Z., Parker, R., and Song, H. (2014). Lsm2 and Lsm3 bridge the interaction of the Lsm1-7 complex with Pat1 for decapping activation. Cell Res. *24*, 233–246.

Xiang, S., Cooper-Morgan, A., Jiao, X., Kiledjian, M., Manley, J.L., and Tong, L. (2009). Structure and function of the 5′→3′ exoribonuclease Rat1 and its activating partner Rai1. Nature *458*, 784–788.

Yadava, R.S., Frenzel-McCardell, C.D., Yu, Q., Srinivasan, V., Tucker, A.L., Puymirat, J., Thornton, C.A., Prall, O.W., Harvey, R.P., and Mahadevan, M.S. (2008). RNA toxicity in myotonic muscular dystrophy induces NKX2-5 expression. Nat. Genet. *40*, 61–68.

Yaffe, D., and Saxel, O. (1997). Serial passaging and differentiation of myogenic cells isolated from dystrophic mouse muscle. Nature *270*, 725–727.

Yamada, M., Shimohata, M., Sato, T., Tsuji, S., and Takahashi, H. (2006). Polyglutamine disease: Recent advances in the neuropathology of dentatorubral-pallidoluysian atrophy. Neuropathology *26*, 346–351.

Yamashita, A., Chang, T.-C., Yamashita, Y., Zhu, W., Zhong, Z., Chen, C.-Y.A., and Shyu, A.-B. (2005). Concerted action of poly(A) nucleases and decapping enzyme in mammalian mRNA turnover. Nat. Struct. Mol. Biol. *12*, 1054–1063.

Yang, E., van Nimwegen, E., Zavolan, M., Rajewsky, N., Schroeder, M., Magnasco, M., and Darnell, J.E. (2003). Decay rates of human mRNAs: correlation with functional characteristics and sequence attributes. Genome Res. *13*, 1863–1872.

Yanovsky-Dagan, S., Avitzour, M., Altarescu, G., Renbaum, P., Eldar-Geva, T., Schonberger, O., Mitrani-Rosenbaum, S., Levy-Lahad, E., Birnbaum, R.Y., Gepstein, L., et al. (2015). Uncovering the Role of Hypermethylation by CTG Expansion in Myotonic Dystrophy Type 1 Using Mutant Human Embryonic Stem Cells. Stem Cell Reports *5*, 221–231.

Yeilding, N.M., Procopio, W.N., Rehman, M.T., and Lee, W.M. (1998). c-myc mRNA is down-regulated during myogenic differentiation by accelerated decay that depends on translation of regulatory coding elements. J. Biol. Chem. *273*, 15749–15757.

Yoo, W.-K., Park, Y.G., Choi, Y.C., and Kim, S.M. (2017). Cortical Thickness and White Matter Integrity are Associated with CTG Expansion Size in Myotonic Dystrophy Type I. Yonsei Med. J. *58*, 807.

Yuan, Y., Compton, S.A., Sobczak, K., Stenberg, M.G., Thornton, C.A., Griffith, J.D., and Swanson, M.S. (2007). Muscleblind-like 1 interacts with RNA hairpins in splicing target and pathogenic RNAs. Nucleic Acids Res. *35*, 5474–5486.

Yue, F., Cheng, Y., Breschi, A., Vierstra, J., Wu, W., Ryba, T., Sandstrom, R., Ma, Z., Davis, C., Pope, B.D., et al. (2014). A comparative encyclopedia of DNA elements in the mouse genome. Nature *515*, 355–364.

Zarkower, D., Stephenson, P., Sheets, M., and Wickens, M. (1986). The AAUAAA Sequence Is Required both for Cleavage and for Polyadenylation of Simian Virus 40 Pre-mRNA In Vitro. Mol. Cell. Biol. *6*, 2317–2323.

Zhang, B., Gunawardane, L., Niazi, F., Jahanbani, F., Chen, X., and Valadkhan, S. (2014). A novel RNA motif mediates the strict nuclear localization of a long noncoding RNA. Mol. Cell. Biol. *34*, 2318–2329.

Zhang, H., Kolb, F.A., Brondani, V., Billy, E., and Filipowicz, W. (2002). Human Dicer preferentially cleaves dsRNAs at their termini without a requirement for ATP. EMBO J. *21*, 5875–5885.

Zhang, S., Welch, E.M., Hogan, K., Brown, A.H., Peltz, S.W., and Jacobson, A. (1997). Polysome-associated mRNAs are substrates for the nonsense-mediated mRNA decay pathway in Saccharomyces cerevisiae. RNA *3*, 234–244.

Zu, T., Gibbens, B., Doty, N.S., Gomes-Pereira, M., Huguet, A., Stone, M.D., Margolis, J., Peterson, M., Markowski, T.W., Ingram, M.A.C., et al. (2011). Non-ATG-initiated translation directed by microsatellite expansions. Proc. Natl. Acad. Sci. U. S. A. *108*, 260–265.

Zünd, D., Gruber, A.R., Zavolan, M., and Mühlemann, O. (2013). Translation-dependent displacement of UPF1 from coding sequences causes its enrichment in 3′ UTRs.

APPENDIX

Appendix A1: XRN2 and MBNL1 co-immunofluorescence microscopy in CUG700 cells. XRN2 protein was labeled with secondary antibody conjugated with Alexa fluor 647 (red), MBNL1 was labeled with secondary antibody conjugated with Alexa fluor 594 (green), the DNA was stained with DAPI demonstrating the nucleus.